

Reliability Assessment for Loadbearing Concrete Masonry Walls Subjected to Gravity and Lateral Loads

by

Odin Guzman Sanchez

A thesis submitted in partial fulfillment of the requirements for the degree of

Doctor of Philosophy

in

STRUCTURAL ENGINEERING

Department of Civil and Environmental Engineering
University of Alberta

© Odin Guzman Sanchez, 2023

ABSTRACT

The current Canadian standard for masonry structures design (CSA S304-14) is based on a Limit-State Design (LSD) philosophy, incorporating masonry-specific material strength reduction factors initially calibrated in the 1980s. These factors were last updated in 2014, prompted by changes in the Canadian standard for reinforced concrete structures (CSA A23.3-14). However, a rigorous, masonry-specific reliability analysis was not performed to support the strength reduction factors used in S304-14. Therefore, there are safety and economic uncertainties in the performance of masonry elements designed in accordance with the strength reduction factors in the 2014 (reaffirmed in 2019) version of the Canadian masonry standard.

In this thesis, a reliability analysis for reinforced, concrete masonry walls (RMWs) under axial compression and out-of-plane uniform load is presented, along with the development of a limit state function that incorporates second-order effects. The analysis is performed using currently available probability information on loads and strength of reinforced concrete masonry walls, realistic loading conditions, and the Monte Carlo method to calculate reliability indices.

The aim of this analysis is to evaluate the structural safety and performance of RMWs under the specified loading conditions.

An innovative part of the analysis is that it takes into account realistic loads and second-order effects, both aspects that seem to be scant in the limit state function formulations found in the literature.

A range of different slender walls are analysed in this study, varying their slenderness ratio, cross-section properties and load relationships. The results show that the reliability indices (β) increase as the slenderness factor increases, while for walls with low slenderness, the reliability indices remain similar and constant over different eccentricities.

DEDICATION

*To my parents, Elizabeth and Avertano:
Thank you for instilling in me a deep appreciation for studying.*

*To my family, Elena, Yazid, and Marely:
Thank you for keeping my dreams alive.*

*To all my brethren, friends, and colleagues.
Thank you for your continuous support and encouragement.*

*To the Most High,
“Non nobis Domine, non nobis, sed Nomini Tuo da gloriam”*

ACKNOWLEDGEMENT

The completion of this thesis was made possible thanks to the invaluable assistance of friends, colleagues, and professors in the Structural Engineering program at the University of Alberta. First and foremost, I am deeply grateful to my research supervisor, Dr. Carlos “Lobo” Cruz-Noguez, whose unwavering guidance and support were indispensable in making this project and my journey at UofA a reality. I also extend my heartfelt appreciation to Dr. Yong Li, my co-supervisor, for their valuable contributions. I would like to extend my gratitude to the other members of the committee for their gracious support.

I am immensely thankful to Mexico's National Commission of Science and Technology (CONACYT), Mirko Ambrozic Graduate Scholarship, Mitacs, and the University of Alberta for generously providing the funding that enabled me to conduct my research.

Finally, I would like to thank my entire family for always encouraging me to continue working towards my dreams and to my parents for being the role models I needed in life for hard work, dedication, and perseverance. I am especially grateful for the patience shown by Elena, Yazid, and Marely, who have witnessed this entire journey and expressed their unconditional love and support throughout.

TABLE OF CONTENTS

ABSTRACT.....	ii
DEDICATION.....	iii
ACKNOWLEDGEMENT.....	iv
LIST OF TABLES	vii
LIST OF FIGURES.....	viii
LIST OF SYMBOLS AND ABBREVIATIONS	x
1. INTRODUCTION	1
1.2. Organization of the Thesis	8
2. LITERATURE REVIEW	9
2.2.1. Non-Slender Structural Elements.....	12
2.2.2. Slender Structural Elements	17
3. METHODOLOGY	23
3.1. Flexural Capacity of a Reinforced-Concrete Masonry Section	23
3.2. Reliability Analysis Problem	32
3.3. Random Variables for Masonry Materials and Loads	42
4. NUMERICAL ANALYSIS AND RESULTS.....	48
4.1. Compressive Strength, Workmanship, and Rate of Loading	48
4.2. Steel Reinforcement	49
4.3. Slenderness	50
4.4. Eccentricity.....	50
4.5. Loads.....	51
4.6. Results and Discussion.....	52
4.6.1. Effect of the slenderness on the reliability ratio (β).....	62

4.6.1. Effect of the loads on the reliability ratio (β).....	62
5. CONCLUSIONS AND RECOMMENDATIONS	64
5.1. <i>Summary</i>	64
5.2. <i>Conclusions</i>	65
5.3. <i>Recommendations and Future Research</i>	66
REFERENCES.....	67
Appendix A.....	71
Appendix B	73
Appendix C.....	89

LIST OF TABLES

Table 2-1 Target Reliabilities Indices (βT) from CSA S408 (2011) for 30-year (50-year)	10
Table 2-2 Target Reliabilities Indices (βT) from JCSS (2001a) for 1-year (50-year) reference period and ultimate limit states	11
Table 2-3 Annual target Reliabilities (βT) for economic optimization (AS5104-2017)	20
Table 3-1 Statistical Information for Material and Geometry	43
Table 3-2 Workmanship Factor (Turkstra et al. 1989)	44
Table 3-3 Statistical Information for loads	45
Table 4-1 Compressive Strength Adapted from Table 4 (CSA S304-14)	49

LIST OF FIGURES

Fig. 1-1 Wall Under Lateral and Axial Loads	5
Fig. 2-1 Mathematical Model of a Column Under Axial Load and Equal Eccentricities and associated P-M interaction diagram.....	13
Fig. 2-2 Limit-State Functions defined by Tychy et al. (1962).....	14
Fig. 2-3 Summary of the Literature Review	22
Fig. 3-1 Stress, Strain, and Resultant Forces at Ultimate Moment Capacity	24
Fig. 3-2 Stress-Strain Relationship for Masonry	25
Fig. 3-3 Stress-Strain Relationship for Reinforcement Steel.....	26
Fig. 3-4 P-M Interaction Diagram	27
Fig. 3-5 Instability-Related Failure Modes.....	27
Fig. 3-6 Total Factored Moment (M_{ft}).....	28
Fig. 3-7 Illustration of the total moment calculation for walls with $kht > 30$	31
Fig. 3-8 Monte Carlo Method.....	34
Fig. 3-9 Proposed Limit-State Functions (Tychy et al.,1962).....	35
Fig. 3-10 Limit-State for Non-Slender Walls with the Fixed Eccentricity Approach.....	37
Fig. 3-11 Slender Column under Axial Load with Equal Eccentricities	38
Fig. 3-12 Representation of the Limit-State for Slender Walls.....	39
Fig. 3-13 Limit State Simulations for Slender Elements.....	42
Fig. 4-1 Examples of Typical Eccentricities in Buildings.....	51
Fig. 4-2 Cross-Section Properties	52
Fig. 4-3 Reliability Indices for a Wall with $ht = 10.5$ ($L/D = 1.0, W = 1.2$ kPa)	53
Fig. 4-4 Reliability Indices for different slenderness ratios ($L/D = 1.0, W = 1.2$ kPa)	55

Fig. 4-5 Monte Carlo Simulations for $W02$	56
Fig. 4-6 Reliability Indices for a Wall with $ht = 10.5$ ($L/D = 1.5, W = 1 \text{ kPa}$)	58
Fig. 4-7 Reliability Indices for different slenderness ratios ($L/D = 1.5, W = 1 \text{ kPa}$).....	59
Fig. 4-8 Reliability Indices for a Wall with $ht = 10.5$ ($L/D = 1.5, W = 1.5 \text{ kPa}$)	60
Fig. 4-9 Reliability Indices for different slenderness ratios ($L/D = 1.5, W = 1.5 \text{ kPa}$)	61

LIST OF SYMBOLS AND ABBREVIATIONS

a	Depth of the equivalent rectangular stress block
A_s	Area of Tensile Steel
$A_{s,min}$	Minimum Area of Tensile Steel
A_g	Gross Cross-Sectional Area of Masonry
ACI	American Concrete Institute
ASD	Allowable Stress Design
apt	Arbitrary point-in-time
b	Width of the Masonry Wall
BIA	Brick Institute of America
C	Masonry Compression Force
c	Distance from extreme compression fibre to the neutral axis
C_m	The ratio of End Moments on a Member
CMU	Concrete Masonry Unit
C.O.V.	Coefficient of Variation
CSA	Canadian Masonry Association
d	Distance from extreme compression fibre to centroid of tension reinforcement
d	Random variable for the location of the steel reinforcement
d_n	Nominal location of the steel reinforcement
DL	Dead Load
D	Random variable for Dead Load
e_i	Initial Eccentricity
e_1	Smaller Virtual Eccentricity

e_2	Larger Virtual Eccentricity
E_m	Modulus of Elasticity of Masonry
E_s	Modulus of Elasticity of Steel
$(EI)_{eff}$	Effective Stiffness of the Wall
f'_m	Compressive Strength of Masonry
f_m	Random Variable for the Compressive Strength of Masonry
f_{mn}	Nominal Compressive Strength of Masonry
FOSM	First-Order Second-Moment Reliability Method
FOSM	First-Order Second-Moment Reliability Method
f_y	Yield Strength of Reinforcing Steel
f_y	Random Variable for the Yield Strength of Reinforcing Steel
f_{yn}	Nominal Yield Strength of Reinforcing Steel
f_s	Stress in Reinforcing Steel
$G(\mathbf{X})$	Limit State Function
h	Height of the Wall
HSC	High-Strength Concrete
k	Effective Length Coefficient
I_o	Moment of Inertia of the Effective Cross-Section
I_{cr}	Transformed Moment of Inertia of the Cracked Section
LL	Live Load
L	Random Variable for Live Load
LSD	Limit-State Design
JCSS	Joint Committee on Structural Safety
M	Nominal Bending Moment

M_1	Smaller Factored End Moment at the Wall
M_2	Larger Factored End Moment at the Wall
M_f	Factored Bending Moment
M_{f1}	Primary Factored Moment
M_r	Bending Moment Resistant
M_{ft}	Amplified Factored Total Moment
M_{ftot}	Factored Total Moment
M^*_1	Probable Primary Moment
M^*_t	Probable Total Moment
M^*_n	Probable Resistant Moment
MMF	Moment Magnifier Factor
NBCC	National Building Code of Canada
OOP	Out-Of-Plane
P	Nominal Axial Load
P_f	Factored Axial Load
P_{fw}	Factored Axial Load due to Self-weight of the wall
P_r	Axial Load Resistant
P_{cr}	Critical Axial Compressive Load
$P_{failure}$	Probability of Failure
$P^T_{failure}$	True Probability of Failure
P^*	Probable Axial Load
R	Random Variable for the Resistant
R_d	Design Resistant

R_n	Nominal Resistant
RC	Reinforced Concrete
RCDF	Mexico City Code
S	Random Variable for the Load Effect
S	Random Variable for the Snow Load
S_d	Design Load Effect
S_n	Nominal Load Effect
S_{max}	Maximum Value of the Load
t	Thickness of the Wall
t	Random Variable for the Thickness of the Cross-Section
t_n	Nominal Thickness of the Wall
T_s	Tension Force in the Reinforcing Steel
W	Wind Load
W	Random Variable for Wind Load
w	Lateral Uniform Load
w_f	Lateral Factor Uniform Load
X	Vector containing all basic random variables
β	Reliability Index
β_1	Ratio to depth of rectangular compression block to depth to the neutral axis
β_d	Ratio of factored dead load moment to total factored moment
β_T	Target Reliability Index
Δ_0	First-Order Deflection
Δ_1	Second-Order Effects Deflection

Δ_m	Total Lateral Deflection
Δ_f	Lateral Deflection
$\delta_{P_{failure}}$	Coefficient of Variation of the Probability of Failure
ε	Strain in Masonry
ε_{mu}	Ultimate Compressive Strain in Masonry
ε_s	Strain in Reinforcing Steel
ε_y	Yield Strain
ϕ_c	Reduction Factor for the Compressive Strength of Concrete
ϕ_{er}	Stiffness Reduction Factor for Masonry
ϕ_k	Stiffness Reduction Factor for Concrete
ϕ_m	Reduction Factor for the Compressive Strength of Masonry
ϕ_y	Reduction Factor for the Yield Strength of Reinforcing Steel
γ_D	Factor for Dead Load
γ_L	Factor for Live Load
γ_W	Factor for Wind Load
γ_S	Factor for Snow Load
γ_E	Factor for Earthquake Load
σ	Stress of Masonry
ρ_w	Workmanship Factor
ρ_r	Rate of Loading
ρ	Reinforcement Ratio
ρ_b	Balance Ratio

1. INTRODUCTION

The allowable stress design (ASD) was the initial design philosophy for masonry structures in Canada, starting with the 1965 version of the National Building Code of Canada (NBCC 1965), in the form of elementary rules for the design of plain and reinforced masonry. In ASD, the loads represent the maximum probable load to occur during a period of time, which is the life expectancy of the structure. The computed stresses in the members resulting from the application of these loads are limited to a certain allowable value, chosen based on engineering judgement and experience. The ratio of the allowable stress to the computed member stress represents the overall factor of safety. The main advantage of the ASD method is its simplicity of use in design. A disadvantage is that a fixed set of allowable stresses does not guarantee a consistent level of safety for all structural elements and types of loads.

The limit-state design (LSD) philosophy was introduced in the Canadian masonry standard in 1994 (S304.1-94). In the LSD criteria, the design of a structural member is satisfactory if the factored design resistance (nominal resistance reduced by the material resistant reduction factors) is greater than or equal to the factored load effects (nominal loads amplified by the load factors). In contrast to the ASD method, the LSD method provides greater consistency in the design due to its recommendations on factors depending on the material used for the structure and the type of load. Specifically, the material resistance reduction factors for the design of reinforced masonry walls include ϕ_m , which is a reduction factor for the compressive strength of masonry (f'_m), and ϕ_s , which is a reduction factor for the yield strength (f_y) of the reinforcing steel. The material strength reduction factors account for the variability of material properties and dimensions of structural elements.

The load factors depend on the type of load, including γ_D as the factor for dead load, γ_L as the factor for live load, γ_S as the factor for snow load, γ_W as the factor for wind load and γ_E as the factor for earthquake load. These factors account for the variability of loading and the probability of having loads from different sources simultaneously when the load combination is considered.

The LSD criteria implemented in the masonry design standard S304.1-94 were based on reliability studies performed by Turkstra et al. (1978; 1980; 1982; 1983; 1984; 1989) where experimental

data, statistical information, and design equations known at the time were used for the calibration and estimation of the design factors and safety levels of the standard. The masonry-specific changes to the strength reduction factors in the masonry standard CSA S304-14 were proposed by Laird et al. (2005), who was inspired on reliability studies conducted for the reinforced concrete design standard CSA A23.3-04. The material resistance factor for masonry (ϕ_m) was increased from 0.55 to 0.60, mirroring an increment of the material factor for concrete (ϕ_c) which went from 0.60 to 0.65 in CSA A23.3-04. Another change proposed by Laird et al. (2005) was made to the resistance factor for the effective stiffness of reinforced masonry walls and columns (ϕ_{er}), which was increased from 0.65 to 0.75, the same as the stiffness reduction factor (ϕ_k) in slender reinforced concrete columns. This factor accounts for the variability in unintended geometric imperfections in slender elements. It is noted, however, that the main limitation in these changes was that no detailed masonry-specific reliability analysis was conducted to support the increase of factors ϕ_m and ϕ_k .

The design equations for reinforced masonry have been significantly influenced by reinforced concrete. However, despite employing similar principles, the uncertainties in design and construction for these two materials differ.

Previous reliability studies on masonry walls under out-of-plane loads are scarce. Most of the existing work has been performed in reinforced-concrete (RC) columns subjected to simplified loads, with just a few studies including second-order effects. Second-order effects on slender elements refers to the additional deformations and stresses that occur due to the combined effects of axial load and bending. In design, second-order effects are important to consider in slender elements to ensure their structural safety and integrity.

In this study, a reliability analysis of masonry walls with varying slenderness ratios under axial compression, and out-of-plane uniform loads will be conducted in the context of the Canadian masonry code (CSA S304-14). The objectives of the study are: i) to conduct a literature review to provide a comprehensive history and rationale behind the current (CSA S304-14) guidelines for out-of-plane (OOP) masonry walls, ii) to develop a limit states function which considers slenderness and lateral loads effects in masonry walls, and iii) to assess the reliability levels in the current Canadian masonry code (CSA S304-14) for slender walls.

A more accurate limit state function accounting for lateral loads and second-order effects is proposed to assess the safety levels of the code. Available statistical information for the random variables of the loads (dead, live, wind and snow loads) and properties of the walls (thickness, location of reinforcement bars, compressive strength and the yield stress of the reinforcement) is used. For load combinations which consider more than one time-varying source of load, the Turkstra's rule is used to combine them. The Monte Carlo method is used to simulate the loads, resistance of the walls, and to calculate the probability of failure.

The results of the study are expected to find a direct relationship between the structural reliability levels and the slenderness ratio of the walls. The reliability indices for slender elements are expected to be greater to the target reliability indices recommended by safety standards, CSA S408 (2011) and the Joint Committee on Structural Safety (JCSS 2001a).

1.1. Problem Statement, Objectives and Scope

1.1.1. Problem Statement

The values of the strength reduction factors in the Canadian masonry code from 1994 (CSA S304-94) were first calibrated with reliability studies performed by Turkstra et al. in the 1980s. Design equations and statistical information for the loads and resistance of that time were used. Twenty years later, the material reduction factors included in the current code, CSA S304-14 (2014), were chosen based on studies performed on reinforced concrete, without any dedicated detail reliability analyses conducted for masonry. Therefore, there is uncertainty about the safety and economy that the current code provides.

Most reliability studies investigating elements subjected to axial loads and out-of-plane bending have focused on reinforced-concrete elements, such as columns, and those that have addressed masonry walls are very scarce. In these investigations, the preferred approach has been to define limit states functions that are based on very simple loading conditions – typically, an eccentric axial load applied to the member. For such a system, the bending moments are assumed to increase proportionally with the axial load (the so-called “fixed eccentricity” approach). While these limit states may be appropriate for interior columns in a building, which are not usually subjected to lateral loads between the supports, the need to account for the presence of a uniform lateral load is

warranted in the case of a loadbearing exterior wall designed to resist out-of-plane actions (“OOP walls”). OOP walls typically bear an axial load from the roof and/or the upper floors, which is often applied eccentrically due to the connections at the upper edge of the wall, as well as being subjected to lateral load due to wind pressure or inertial forces due to seismic actions. In such a case, the out-of-plane bending moment at the midspan of the wall, assuming pinned-pinned boundary conditions, will be the sum of the moment generated by the initial eccentricity of the axial load, the moment generated by the lateral load, and the second-order effects. Therefore, the bending moment is not directly proportional to the axial load, and therefore, the “fixed eccentricity” approach is not suitable for the study of an exterior wall. The nonlinear relationship of axial load and bending moment in exterior walls is compounded due to the increase in second-order effects as the slenderness ratio of the wall increases; the preferred approach for considering second-order effects has been to use a moment-magnifier approach to either reduce the cross-section strength of the wall or to amplify the moment that is applied to the member.

Another limitation is that in the few studies (Turkstra et al. 1983, Mosavi et al. 2017), that explicitly included lateral loads, such as wind, the considered load combinations included only one time-varying load such as dead (DL) plus live load (LL) or dead (DL) plus wind load (W), and not all combinations as required by the latest NBCC (2020) have been explored. This is a serious limitation in the assessment of the safety of structural elements.

When assessing the reliability of a structural member (e.g., a column or a beam), the analysis requires the statistical consideration of the resistance and load variables over certain predetermined ranges chosen by the analyst. Sometimes, this results in combinations of strength parameters that are unrealistic or unfeasible to build. For instance, in the case of a masonry wall, the range of possible reinforcement ratios is restricted by the number of bars that can be placed on the cells of the block, which depends on the size of the bars and maximum/minimum reinforcement limits allowed by the code and the fixed geometry of a typical concrete masonry unit (CMU). Consequently, values of reliability obtained for arbitrary reinforcement ratios, for instance, are not indicative of the true reliability of the system, and only realistic reinforcement schemes should be analyzed.

The system that is investigated for reliability analysis in this research is an exterior wall under realistic loading conditions based on the current NBCC (2020) standard. The wall has been loaded

under axial load (P) with an initial eccentricity at the top (e_i) and is also subjected to a lateral uniform load (w) due to wind (Fig. 1-1). This is a common loading condition for masonry walls in warehouses, school gymnasiums, and retail facilities in North America. The axial load includes a time-varying load (a live load) in addition to the permanent load (dead load), and a lateral pressure (wind), which is assumed uniform. And this combination is not frequently used for reliability analysis, even when is specified by the standard (NBCC 2020).

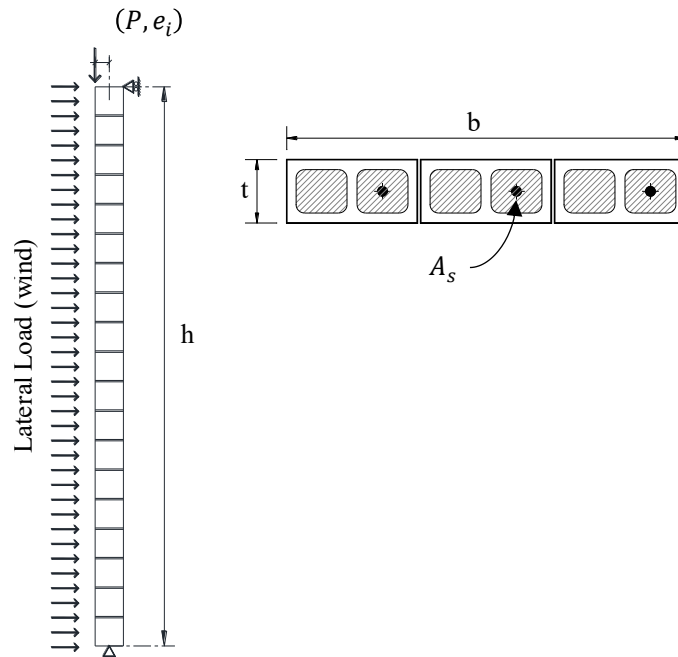


Fig. 1-1 Wall Under Lateral and Axial Loads

The limit states developed for this study for masonry slender tall walls aims to incorporate a more realistic loading condition to what was assumed in previous analyses regarding masonry walls (Ellingwood et al. 1985 and Moosavi et al. 2017). This will be achieved by allowing statistical variation in both the axial loads and moments, using a discrete approach to select load combinations that are typically observed in masonry walls. The walls investigated will have a practical range of slenderness ratios that will correspond to both multi-storey construction and tall walls such as those found in warehouses and industrial facilities.

To summarize, a rational study to assess the reliability of concrete block masonry walls is required to evaluate the safety and economy of the current Canadian masonry design standard (CSA S304).

Such a study includes updated statistical information for loads, material, strength, workmanship factor, and realistic loading conditions.

1.1.2. Objectives

The main goal of this research is to assess the reliability levels of the Canadian masonry standard for the design of masonry walls under realistic load conditions. This assessment will specifically focus on walls with various slenderness ratios, subjected to axial compression, and out-of-plane uniform loads. The evaluation will be conducted within the framework of the Canadian masonry standard (CSA S304).

The following research tasks are set to achieve the main goal of this work.

1. Literature review to provide a comprehensive history and rationale behind the current CSA S304 guidelines for OOP masonry walls.

Specific aim 1.1: Conduct a literature review on structural reliability studies conducted on concrete and masonry elements under axial loads and bending moments, with an emphasis on those related to the development of the Canadian masonry guidelines.

Specific aim 1.2: Identify the most significant random variables used in previous reliability analyses.

Specific aim 1.3: Review and assess the limit states functions used in the literature for slender and non-slender, reinforced concrete and masonry columns and walls.

2. Development of a limit state function for non-slender and slender masonry walls.

Specific aim 2.1: Develop a limit state function for masonry walls that allows the statistical variation of both loads and moments to be considered.

Specific aim 2.2: Develop a detailed procedure to work with the proposed limit state functions and calculate the reliability indices of masonry walls with different slenderness ratios under OOP loads.

Specific aim 2.3: Identify relevant loads for investigation, including both permanent and time-varying loads, such as combinations of dead load plus live load plus wind load, where live and wind load are time-varying.

Specific aim 2.4: Define practical ranges of variables related to the strength of a masonry wall, including concrete block thicknesses and location of the steel reinforcement bars.

3. Assessment of the reliability levels in the current Canadian masonry code (CSA S304-14) for slender walls.

Specific aim 3.1: Calculate the reliability indices for masonry walls of different slenderness ratios, reinforcement ratios, and compressive strength.

Specific aim 3.2: Compare the target reliability indices (β_T) from the safety standards CSA S408 (2011) and JCSS (2001a) with the reliability indices calculated in this research.

1.1.3. Scope

This research is focused on evaluating the safety levels of OOP masonry walls designed as per CSA S304-14. The reliability or accuracy of the code clauses themselves is not being investigated. The methods used in this study allow for the study of material failure in the walls due to flexure and instability failure due to the combination of axial loads and bending moments. This investigation does not account for out-of-plane shear failure mechanisms, such as diagonal tension or sliding shear. Although uncommon in masonry walls of practical heights (> 2.5m high), which are flexure-dominated due to the large spans, the possibility of out-of-plane shear failures should always be investigated, especially for shorter walls with small axial loads (e.g., parapets) subjected to significant lateral loads.

The only type of lateral load considered in this study is the wind load. However, the methods developed in this research are applicable to other lateral loads that can be modeled as a static uniform pressure over the height of the wall.

The boundary conditions of the walls are assumed to be pinned-pinned both at the base and at the top. This corresponds to the assumption that the rotational stiffness provided by the foundation of the wall is small compared to the flexural stiffness of the wall itself, caused by degradation of the wall-foundation interface under cyclic loads, and it is also representative of typical wall-roof connections in industrial buildings. With no restraints, connections, or loads applied between the base and the top, the walls are assumed to bend in single curvature.

Only reinforced concrete block, fully grouted, masonry walls will be studied in this research; however, the same method can be expanded to partially grouted walls.

1.2. Organization of the Thesis

This thesis is organized into five chapters. In Chapter 1, the introduction, problem statement, objectives, and scope are presented. In Chapter 2, the literature review is presented in two parts. The first part is related to reliability studies proposed for non-slender concrete columns and how they were used as a base for non-slender masonry walls. The second part is focused on studies on slender concrete columns, their limitations, and how the limit state functions proposed could be used as a base for slender masonry walls. In Chapter 3, the methodology of this work is explained in detail. First, a review on how the design capacity of a masonry wall following the Canadian design standard CSA S304-14 is presented. The different categories of slender walls are also discussed in this chapter. Finally, the reliability method used in this study to calculate the reliability indices is explained. All the statistical properties required to perform a reliability analysis are shown in this chapter. In Chapter 4, the results for the proposed walls are shown. The levels of safety that resulted from the analysis are discussed. In Chapter 5, a summary of this work, the conclusions, and the future work are presented.

2. LITERATURE REVIEW

The literature survey that follows is divided into two parts. The first part focuses on the reliability studies that were used in the development of the Canadian masonry code (S304-14). The second part includes a review of studies related to the development of reliability limit states for elements subjected to flexure and axial loads.

2.1. Development of the Reliability Provision for Walls in CSA S304

A limit state can be defined as a condition of a structure failing to fulfill its intended design purpose. For example, a structure's ultimate strength limit state can be mathematically described by a limit state function, i.e., the difference between the load effect (S) and the resistance (R) for a structural element or system. The derivation of the load and resistance factors for the design of masonry in the S304.1-94, which was the first standard for masonry design with the LSD method, was performed based on a series of reliability studies conducted by Turkstra et al. (1978; 1980; 1982; 1983; 1984; 1989). Turkstra and his collaborators developed different limit states for masonry members.

Turkstra and Daly (1978) reviewed the reliability methods available at the time, which typically were simplified methods that used linear equations and methods, aiming to apply them to elements subjected to combined flexure and axial load. They evaluated the methods through numerical examples, studying walls made with different material such as concrete, steel, and masonry. For masonry, they studied a non-slender masonry wall under axial load applied concentrically and eccentrically. The calculation of the reliability index in their study considered two limit states: one for the axial load capacity, and another for the moment capacity. Turkstra and Daly concluded that for situations where the load side of the limit state function can be reduced to a single variable (for example, when a total load effect is defined as the sum of the different sources of load, such as dead load, live load, wind load, etc.), the problem can be represented only by the load random variable (S) at the time of the reliability calculation. A similar situation could be observed with the resistance. For example, the resistance moment, which includes different random variables (such as the sections properties or material properties), could be represented only by the random

variable (R). Working with these two variables, Cornell (1969) and Rosenblueth-Esteva (1972) developed robust methodologies that were based on the mean and variance of random variables.

Turkstra and Ojinaga (1980) discussed the code development challenges in developing a masonry code using a consistent limit states design (LSD) philosophy. Recommendations were given for factors pertaining to the strength of the masonry materials and the treatment of the uncertainties in the workmanship, inspection, and structural analysis processes. A preliminary safety index analysis for plain (unreinforced) masonry walls was presented to assess construction practices at the time. Plain, non-slender masonry walls were analyzed under combinations of ratios of nominal dead to live loads from 0.0 to 2.0 and under an eccentric axial load, with reliability indices varying from 3.5 to 3.8 for walls deflecting in single curvature and 5.1 to 5.3 for walls deflecting in double curvature.

As a reference, the calculated indices β are typically compared to target reliability indices (β_T) proposed by regional and national code committees. Allowable values of β_T depend on different variables and situations, such as the type of failure, the expected cost of failure, the cost of increasing the safety level, and the existing safety level. Table 2.1 shows recommended target reliabilities in the guidelines for the development of limit states design in Canada (CSA S408-11), and Table 2.2 shows the recommended values by the Joint Committee on Structural Safety (JCSS 2001a). This comparison shows that, at the time of Turkstra and Ojinaga’s study, the safety levels for masonry were relatively high.

Table 2-1 Target Reliabilities Indices (β_T) from CSA S408 (2011) for 30-year (50-year)

Safety Class	Type of Failure	
	Gradual	Sudden
Not Serious	2.5 (2.3)	3.0 (2.8)
Serious (normal buildings)	3.5 (3.4)	4.0 (3.9)
Very Serious*	4.0 (3.9)	4.5 (4.4)

*It is assumed that for very serious consequences there is better quality control

Table 2-2 Target Reliabilities Indices (β_T) from JCSS (2001a) for 1-year (50-year) reference period and ultimate limit states

Relative cost for enhancing the structural reliability	Failure Consequences		
	Minor ^a	Average ^b	Major ^c
Large	3.1 (1.7)	3.3 (2.0)	3.7 (2.6)
Medium	3.7 (2.6)	4.2 (3.2) ^d	4.4 (3.5)
Small	4.2 (3.2)	4.4 (3.5)	4.7 (3.8)

^ae.g. agricultural buildings

^be.g. office buildings, residential buildings or industrial buildings

^ce.g. bridges, stadiums or high-rise buildings

^dRecommendation for regular cases

For illustrative purposes, the probability of failure (P_f) for various values of the reliability index (β) is provided as follows: $\beta = 3$ corresponds to $P_f = 1.3 \times 10^{-4}$, $\beta = 3.5$ corresponds to $P_f = 2.3 \times 10^{-4}$, and $\beta = 4$ corresponds to $P_f = 3.2 \times 10^{-5}$. As it can be observed, this increment is not linear.

Turkstra and Ojinaga (1981) studied the ultimate limit state for reinforced masonry compression members subjected to concentric and eccentric axial loads. Stress-strain constitutive relationships were defined for masonry and steel, and the resistance of the members was calculated through an axial load-moment interaction curve (*P-M diagram*). This study showed the reduction in strength due to slenderness in a masonry element subjected to flexure and axial load.

Turstra et al. (1983) summarized the evolution of the limit states design procedures for masonry based on rational mechanics and a comprehensive safety index analysis. This study was focused on the behaviour of plain and reinforced masonry walls subjected to minor axis bending. The analysis was for walls subjected to axial load, eccentricities at both ends, and transversal load due to wind or earthquake. The workmanship factor was highlighted because available test data indicated that the compressive masonry strength was highly dependent on construction practices, mason qualifications, and inspection during construction. Three levels of workmanship factors were proposed: rigorous work inspection, moderate work inspection, and uninspected construction. A set of strength reduction factors ϕ_m (0.60, 0.80) for masonry compressive strength and ϕ_s (0.50, 0.80) for steel tensile strength were proposed based on the level of workmanship (lower values of ϕ correspond to lower levels of inspection).

Tursktra (1989) analyzed some aspects of the limit state design for plain and reinforced masonry, and proposed values for the material strength reduction factors for masonry compressive strength $\phi_m(0.5, 0.8)$ and for steel yield strength $\phi_s(0.5, 0.8)$. A wall with a slenderness ratio of 15 and a nominal dead to live load ratio of 1.0 was used in the analysis. For a regularly inspected, reinforced concrete block masonry wall, reliability indices varying from 3.0 to 5.0 were calculated.

Laird et al. (2005) presented changes of the CSA S304-2004, where the resistance factor for masonry compressive strength (ϕ_m) changed from 0.55 to 0.60, and the resistance factor for member stiffness (ϕ_{er}) changed from 0.65 to 0.75. These changes were motivated by the changes established in the CSA A23.3-97 standard for reinforced concrete while recognizing a need for comprehensive reliability analysis for masonry walls. However, no masonry-specific reliability analysis was conducted to justify these values.

Mosavi et al. (2014) evaluated the reliability levels of concrete masonry under axial compression under the Canadian Standard CSA S304 in its 1994 and 2004 versions. The First Order Reliability Method (FORM) was used to calculate the reliability indices under live-to-dead and snow-to-dead load ratio relationships. They concluded that neither the masonry resistant factor of 0.6 adopted in the current Canadian masonry design standard (S304-04) nor the previous value of 0.55 in the (S304-94) achieved an acceptable reliability level for masonry construction.

2.2. Reliability Limit States for Non-Slender and Slender Elements

2.2.1. Non-Slender Structural Elements

The definition of reliability limit states for elements subjected to combinations of axial load and out of plane flexural loading has traditionally been different depending on the significance of the second-order effects. For non-slender (short) elements, in which the additional moments due to the deflections are not significant, the limit states are usually defined based on the cross-section failure, with the help of P-M interaction diagrams, in which the loads corresponding to the factored moment and axial load (given by a point in the diagram) are related to the strength (the P-M curve) through relationships based on the behaviour in the member. Note that in a wall under eccentric factored axial load P_f , and equal moments at the top and bottom equal to $M_f = P_f e_i$, where e_i is the initial eccentricity all the probable combinations of axial load and moment will fall into a

straight line with slope equal to $e_i = M_f/P_f$ and equal to the resistance as $e_i = M_r/P_r$ in the P-M interaction diagram.

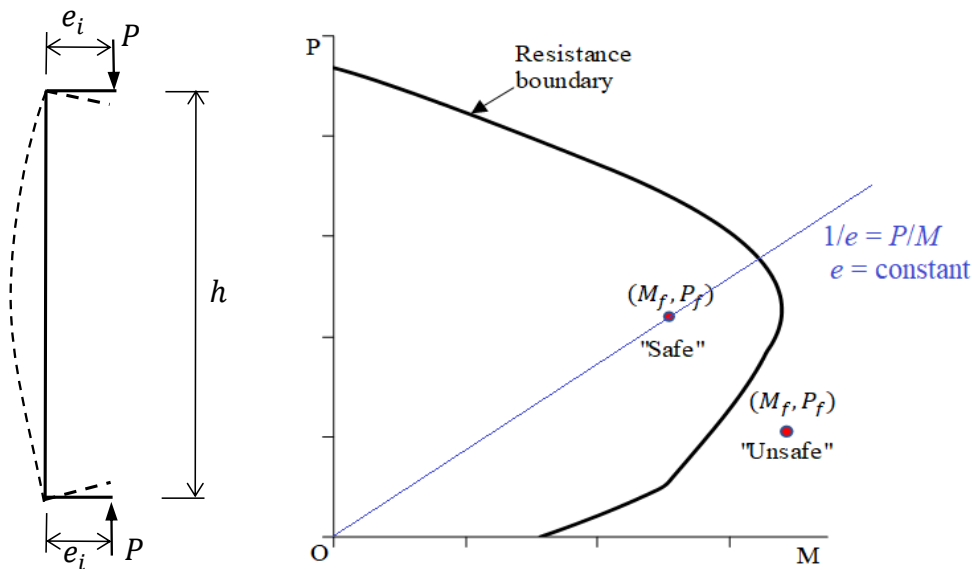


Fig. 2-1 Mathematical Model of a Column Under Axial Load and Equal Eccentricities and associated P-M interaction diagram

For slender members, the problem is more complex, as the second-order effects can be seen as an amplification to the factored moment M_f , or a reduction to the strength of the cross-section, with increasing influence as the loads increase. In the very simple example explained in Fig. 2.2-1, the line that represents the behaviour of the initial eccentricity $e_i = M_f/P_f$ is not a straight line, and the assumption of the uniform increment between P and M is not valid ($e_i = M_f/P_f \neq M_r/P_r$).

Since the limit states developed for masonry elements have traditionally been based on those used for reinforced concrete (RC), milestone RC studies are discussed in this section as well.

In 1962, Tychy and Vorlicek evaluated the safety levels of RC eccentrically loaded columns. The concept of ultimate strength and factor of safety was new at that time. They pointed out that the safety levels depended on how the limit state function was defined.

Tychy and Vorlicek defined three possible limit state functions to calculate the reliability levels in a non-slender column under three loading scenarios (e.g., fixed axial load, fixed moment, or fixed eccentricity). Point L represents the load effects, and the “distance” from point L to the interaction

curve can be seen as the reserve of strength possessed by the column due to different design and construction uncertainties. Point L is calculated using the statistical properties of the loads and the interaction curve is calculated using the statistical properties of the cross-section.

The limit-state represented by line LA is known as “fixed moment.” For this function, the axial load is assumed to be the only load parameter that is permitted to vary according to a suitable probability distribution while the moment remains constant. Line LB , representing a “fixed eccentricity,” illustrates the case in which both variables, the axial load and the bending moment, are assumed to increase in the same proportion. This is the case for a short column subjected to an eccentric axial load, in which the eccentricity is kept constant, but the axial load is allowed to vary. Finally, Line LC , called the “fixed axial load” function, represents a situation in which the moment is allowed to vary but the axial load stays constant.

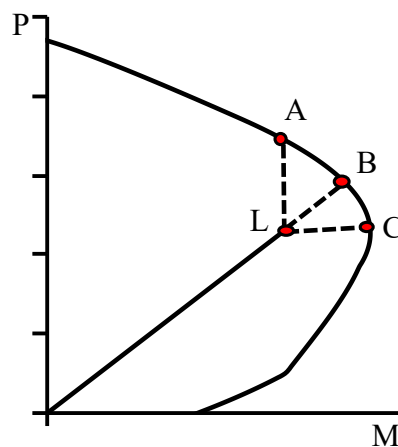


Fig. 2-2 Limit-State Functions defined by Tychy et al. (1962)

As a result of this analysis, Tychy et al. (1962) recommended a fixed eccentricity limit state, which assumes that the axial load and bending moment change in the same proportion, for the analysis of eccentrically loaded columns, introducing the approach of a limit state function instead of a single, empirical safety factor for design.

Ellingwood (1977) agreed that the resistance of a RC beam-column and its margin of safety may be defined in several ways as it was pointed out by Tychy et al. (1962), finding that the fixed eccentricity approach was the most widely used in columns under axial load and bending moment.

Ellingwood, however, suggested that for cases where the moment increases rapidly, the fixed axial load approach is more appropriate.

Grant et al. (1978) studied the distribution properties of reinforced concrete rectangular tied short columns using Monte Carlo simulations. The fixed eccentricity limit state was used. They found that the variability of the concrete strength was the major contributing factor for the cross-section strength in the compression failure region, and the variability of the steel strength was the major contributing factor to the strength in the tension failure region.

Israel et al. (1987) proposed strength resistance factors for concrete ($\phi_m = 0.60$) and steel ($\phi_s = 0.90$) to account for the uncertainty in the resistance variables in the design of RC elements designed with the American code (ACI 318 – 83). The First-order Second-Moment (FOSM) reliability analysis method, combined with the fixed eccentricity limit state were used to calculate the reliability indices. FOSM is a method that makes use of only first and second statistical moments (i.e. mean and standard deviation) of the random variables, requiring a linearized form of the limit state function at the mean values of the random variables.

Ruiz (1993) studied the reliability of short columns under the effect of dead load plus live load. In this work, the reliability of the ACI 318-89 was compared to the Mexican code (NTC-87). The reliability index (β) was calculated via the Monte Carlo simulation technique and the fixed eccentricity limit state was used. The results showed that the NTC-87 had greater reliability indices than those at ACI 318. An explanation of the findings was that the Mexican code provided higher protection against uncertainties associated with concrete properties, loads and quality control.

Diniz and Frangopol (1998) presented the reliability analysis of high-strength concrete (HSC) columns designed according to the ACI 318-1995. The reliabilities of both short and slender columns were assessed using a hybrid probabilistic approach. In this method, column strength statistics were obtained via Monte Carlo simulation and the reliability indices were computed through the first-order reliability method (FORM). The fixed eccentricity limit state was used to perform the reliability analysis on short columns. The analyzed model consisted of a column bent in single curvature by equal moments acting at both ends under the effect of dead plus live load. The calculated reliability indices were in a range from approximately 3.0 to 4.5. The results

demonstrated that the reliability of short HSC columns is lower than the corresponding normal-strength concrete columns.

Szerszen et al. (2005) studied RC columns eccentrically loaded, incorporating the most recently available statistical data for the constituent materials. The fixed eccentricity limit state was used to perform the structural reliability analysis. The equations for the limit state were developed based on equilibrium, strain compatibility, and stress-strain relationships for the constituent materials. The statistical parameters of the resistance were calculated using Monte Carlo simulations. The columns were loaded under the effect of dead and live load, combined according to the ACI 318-2005. The Cornell reliability index (Cornell, 1969) for normal distributions of the random variables was used to calculate the reliability indices. RC strength reduction factors were proposed depending on the tensile strain in steel and the reinforcement ratio.

For masonry walls, Ellingwood et al. (1985) showed how a probability-based criteria could be developed for the limit states of brick and concrete masonry walls under the combination of axial compression and out-of-plane flexure. Dead plus live axial loads were used in the analysis. With the objective of evaluating the safety of current design practices in walls built with brick and concrete masonry, with varying amounts of reinforcement, the reliability index (β) was calculated using the FOSM method. The fixed eccentricity limit state was used. The walls were assumed supervised, and the workmanship factor was not considered in the analysis. The reliability values were calculated following the design recommendations for two codes, the American Concrete Institute (ACI 531-1979) and the Brick Institute of America (BIA-1969). The values of the reliability indices (β) varied over the range of the initial eccentricity from pure compression to pure flexure. The reliability indices as per the ACI were from 3.8 to 9.5 depending on the amount of steel and the load eccentricity. As per the BIA-1969, the values ranged from 2.9 to 8.20. Significant reliability inconsistency was observed for these design codes.

Stewart et al. (2002) developed a method to calculate the structural reliability of typical unreinforced masonry walls subjected to out-of-plane bending. The limit state considered first-cracking, the possible redistribution of stresses, possible additional cracking and continuing until collapse occurs. Due to the complexity of the limit state, the Monte Carlo simulation was used to evaluate the reliability indices. It was found that the reliability indices vary from 3.1 to 6.5,

showing the large effect that workmanship and material have on structural reliability. The Australian Masonry Standard (AS3700-1998) was used in this analysis.

Moosavi et al. (2017) conducted a reliability study on non-slender masonry walls following the Canadian code recommendations (CSA S304-14) for the design and the load combinations according to the NBCC-15. Combinations of dead plus live load, dead plus snow and dead plus wind load were considered in the study and recent statistical information for the loads was considered (Bartlett et al. 2003). The fixed eccentricity limit state was used in the analysis. To estimate the reliability levels, a proposed value for the workmanship factor with a mean of 0.85, and a coefficient of variation of 0.15 was considered based on Turkstra's previous work. The First Order Reliability Method (FORM) was used to calculate the reliability indices. Moosavi et al. (2017) found that reliability levels for the design of masonry members are smaller than those for concrete members when the load is caused by the combination dead plus snow load, where the lowest reliability index was 2.82.

Chi et al. (2019) developed a reliability model and method to evaluate the structural reliability of reinforced masonry walls subjected to seismic force. The model incorporates the effect of model error, axial force and compressive strength for grouted concrete block masonry walls. The reliability evaluation was in accordance with the Chinese standard GB 50003 (2011). The shear load effect and shear resistance of the wall were used to define a limit state function, in which the load effect was calculated according to GB 50011 (2010) and the resistance to GB 50003 (2011). A design equation for the structural resistance from the standard was taken as a limit state function, and the first-order second-moment (FOSM) method was used to calculate the reliability indices. Three different wall models were studied under five levels of axial load and five types of probability distributions for the model error. The reliability indices (β) varied from 1.9 to 6.7. It was found that the axial load has a positive influence on the reliability index (i.e., it increases it) of walls under horizontal seismic load.

2.2.2. Slender Structural Elements

From the above discussion, it is evident that these simple limit states (such as those based on the fixed eccentricity approach), although convenient for straightforward computations, are not able to capture common loading conditions for exterior walls, in which the load, moment, and location

of the load have variations. In addition, any wall will be subjected to second-order effects that influence the amount of moment they experience.

Mirza and MacGregor (1989) studied the variability of the ultimate strength of rectangular reinforced concrete slender columns bending in single curvature. The Monte Carlo method was used to simulate the variability of the ultimate strength. The columns studied were pinned-pinned, with equal load eccentricities acting at both ends. Various combinations of the cross-sectional size, the specified concrete strength, the longitudinal steel ratio, the slenderness ratio, and the eccentricity ratio were used to study the effects of these variables on the probability distribution properties of the slender column strength. The results indicated that the ratio of the longitudinal steel, the slenderness, and the end eccentricity have a significant influence on the probability distribution properties of the slender column strength. The variability of the concrete strength was a major contributor to the slender column strength variability in the region of low eccentricity ratios, whereas the variability in the steel strength made a major contribution to the slender column strength variability when the end eccentricity ratios are high.

Ruiz and Aguilar (1994) evaluated reliability indices associated with short and slender columns. The design was in accordance with the ACI 318-89 and the Mexico City code (RCDF-87). The columns were under axial load and equal eccentricities at both ends, deflecting in single curvature. The axial compression was due to dead plus live load. The moment magnifier method was used to calculate the design resistance for the slender columns. This method consists of amplifying the applied moments using a parameter that is derived from an elastic analysis of the deformed shape of the wall under axial load, capturing the first- and second-order effects (MacGregor et al. 1970). Detailed information about the moment-magnifier in S304 is presented in Chapter 3. The Monte Carlo simulation technique was used to simulate the random variables, and the reliability index was calculated through the Rosenblueth-Esteva method (1971), which considers lognormal distributions for the resultant random variables. The results revealed that the load and slenderness ratios, longitudinal steel, and end eccentricity ratio are significant parameters in the reliability evaluation. The reliability indices for slender columns are greater than the ones calculated for short columns at least 12%. The reliability levels of the Mexican code were greater than those found in the U.S. code.

Diniz and Frangopol (1998) calculated the reliability of slender high-strength concrete (HSC) columns. The analyzed column bent in single curvature, and it was under dead plus live eccentrically axial loads, with three slenderness ratios of 0, 22 and 50. In this study, the slenderness effects were accounted for by comparing the initial loads acting in the column (not the magnified moment) and the slender column strength (smaller than the cross-section strength). The initial loads were taken as those that match the column design strength after moment magnification; this method was proposed by the same authors in a paper published in 1997. Similar to the case of short columns, a hybrid probabilistic approach was used, where column strength statistics were obtained via Monte Carlo simulation and the reliability indices are computed through the first-order reliability method (FORM). The calculated reliability indices ranged from 2.3 to 4.5.

In masonry, Ellingwood et al. (1985) calculated reliability indices for slender walls deflected in single curvature under dead and live axial load. The studied slenderness ratios (effective height to thickness of the block (h/t)) were from 5 to 35. The walls were designed according to the Brick Institute of America Standard (BIA-1969) and the ACI 531-79. The moment magnifier method was used to account for the second order effects by amplifying the loads. The reliability index (β) was calculated by the first-order, second-moment (FOSM) method, and the fixed eccentricity was used for the limit state. It was shown that the walls increased their reliability index as the slenderness ratio increased. The reported reliability indices ranged from 8 to 12, depending on the load eccentricity and amount of steel reinforcement.

Stewart and Masia (2019) studied the reliability of unreinforced masonry walls under out-of-plane bending. A spatial variability was observed due to variations in the quality of the workmanship, weather during construction, and materials from location to location. A stochastic computational model which combines the Finite Element Method and Monte Carlo simulation was developed to study the variability of material properties. The structural reliability analysis considered the random variability of model error, flexural bond strength, brick thickness, brick self-weight, and wind load. Two predictive models were used, the design model based on the Australian design code (AS3700) and a finite element model. The results' reliability indices were compared to the target reliabilities recommended by AS5104-2017 (adapted from JCSS 2001) and shown in Table 2.3. The models were considered Class 3 with a target reliability of 4.2. The results

supported increasing the capacity reduction factor for flexure from 0.60 to 0.65, which represents an 8% increase in design capacity.

Table 2-3 Annual target Reliabilities (β_T) for economic optimization (AS5104-2017)

Relative Cost of Safety Measures	Consequences of Failure		
	Class 2 (Minor)	Class 3 (Moderate)	Class 4 (Large)
Large	3.1	3.3	3.7
Medium	3.7	4.2	4.4
Small	4.2	4.4	4.7

The load statistical information used in this research is taken from Bartlett et al. (2003). The current load factors in the design combinations recommended by the National Building Code of Canada (NBCC-2015) were calibrated based on the work presented in this paper. This work summarized and presented statistical parameters of the different types of loads, such as dead, live, snow, and wind load.

The literature review is summarized in Fig. 2.2-3.

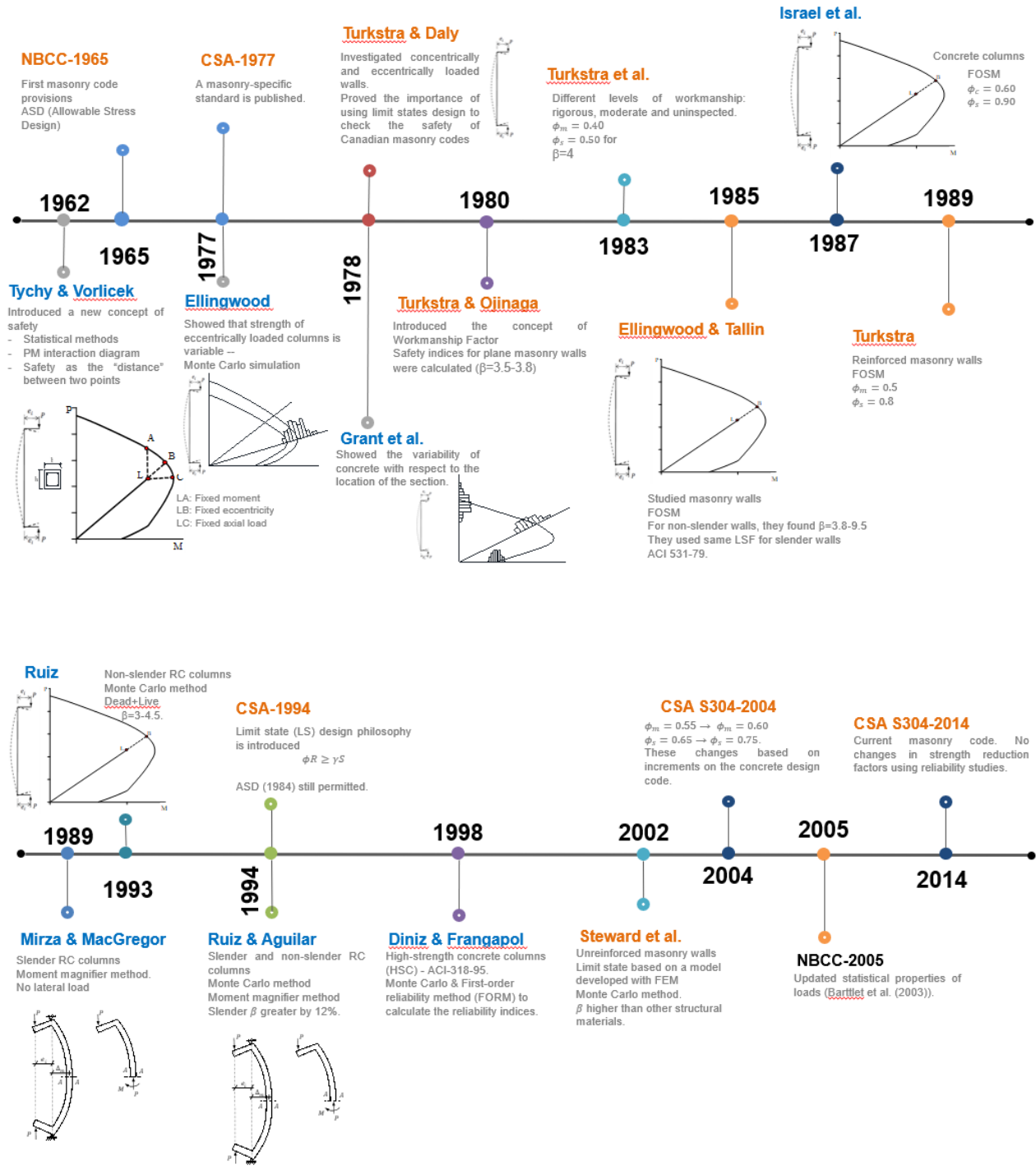


Fig. 2-3 Summary of the Literature Review (continued in next page)

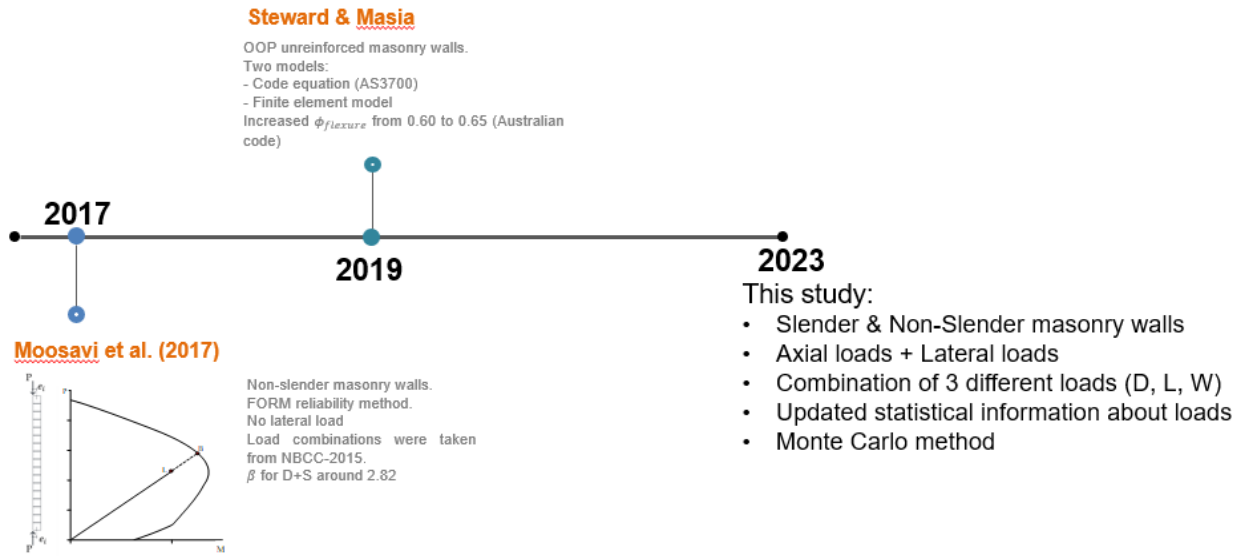


Fig. 2-3 Summary of the Literature Review

3. METHODOLOGY

The organization of this section is as follows:

First, a background on the design of masonry walls, including slenderness effects according to CSA S304-14, is presented. This is done through the development of a P-M interaction diagram.

The slenderness provisions in the Canadian masonry standard are presented, and the additional limitations when the slenderness is over 30 are discussed. Then, the limit state function used to estimate the reliability levels on non-slender elements is described, and its limitations are reviewed. The limit state functions for slender elements are also discussed, and the function proposed in this research to calculate reliability levels on slender walls is presented.

After the development of the limit state function, the methodology for the probabilistic approach to compute the reliability indices of slender walls is explained. Finally, the statistical information of the random variables considered in this study to perform a reliability analysis for the strength and loads are shown.

3.1. Flexural Capacity of a Reinforced-Concrete Masonry Section

To provide background for the development of the limit state function, relevant design provisions in S304-14 will be summarized in this section. The strength of a wall cross-section against a combination of bending moment and axial force can be derived based on equilibrium, strain compatibility and stress-strain relationships for its constituent materials (Fig. 3-1). The standard ultimate compressive strain in masonry is ε_{mu} (Fig. 3-1a), where the masonry is assumed to crush in compression beyond that limit. The stress distribution at ultimate for masonry is curvilinear (Fig. 3-1b) and can be represented with an equivalent rectangular stress with $\beta_1 = 0.80$ (Fig. 3-1c). The stress-strain relationship for the reinforcing steel is assumed to be elastic ($f_s = E_s \varepsilon_s$) for $|\varepsilon_s| \leq \varepsilon_y$, and perfectly plastic ($f_s = f_y$) for $|\varepsilon_s| > \varepsilon_y$, where f_y is the yield strength of the steel, ε_y is the yield strain, and E_s is the steel modulus of elasticity. In Fig. 3-1, for a cross-section of the wall, C is the masonry compression force, T_s is the steel tension force, and P_f is the factored compressive axial load assumed to be applied in the center of the wall cross-section.

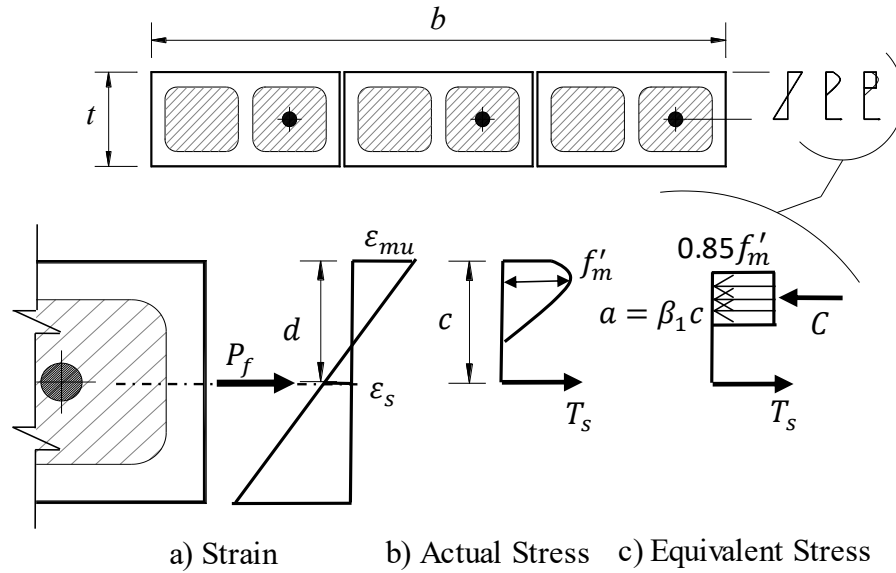


Fig. 3-1 Stress, Strain, and Resultant Forces at Ultimate Moment Capacity

Equilibrium of axial forces and moments (Fig. 3-1c) is given by the following equations:

$$P_f = C - T_s \quad (3-1)$$

$$C = \phi_m 0.85 f'_m b \beta_1 c \quad (3-2)$$

$$T_s = \phi_s A_s f_y \quad (3-3)$$

$$M_r = C \left(d - \frac{a}{2} \right) \quad (3-4)$$

where M_r is the maximum (factored) design resistance moment, calculated with material reduction factors of $\phi_m = 0.6$ and $\phi_s = 0.85$ according to CSA S304-14. The nominal resistance moment (M_n) is obtained with strength reduction factors taken as 1.0 and a nominal axial load (P) acting in the section.

Stress-Strain Relationship of Masonry

In this study, a modified version of the model proposed by Priestley and Elder (1983) was used. The model assumes the maximum stress of the masonry to occur at a strain of 0.002 (Drysdale

and Hamid, 2005). The behaviour consists of three portions: a parabolic rising curve, a linear falling branch, and a final horizontal plateau, and it is represented by the Eq. 3-5. Compression stress increases with strain and arrives at a maximum right after initiation of a failure mode. The stress-strain curve takes a zero slope around maximum stress and falls rapidly as the failure mode dominates and the curve flattens afterwards.

$$\sigma = \begin{cases} f'_m \left[\frac{2\varepsilon}{0.002} - \left(\frac{\varepsilon}{0.002} \right)^2 \right], & \varepsilon < 0.002 \\ f'_m [1 - Z(\varepsilon - 0.002)], & 0.002 < \varepsilon < \varepsilon_{0.2u} \\ 0.2f'_m, & \varepsilon_{0.2u} < \varepsilon \end{cases} \quad (3-5)$$

where

$$Z = \frac{0.5}{\left(\frac{3 + 0.29f'_m}{145f'_m - 1000} \right) - 0.002} \quad (3-6)$$

Z is a parameter that controls the slope of the linear falling branch ($0.002 < \varepsilon < \varepsilon_{0.2u}$), and $\varepsilon_{0.2u}$ is the strain where the constant stress initiates. The stress-strain behaviour of masonry is shown in Fig. 3-2.

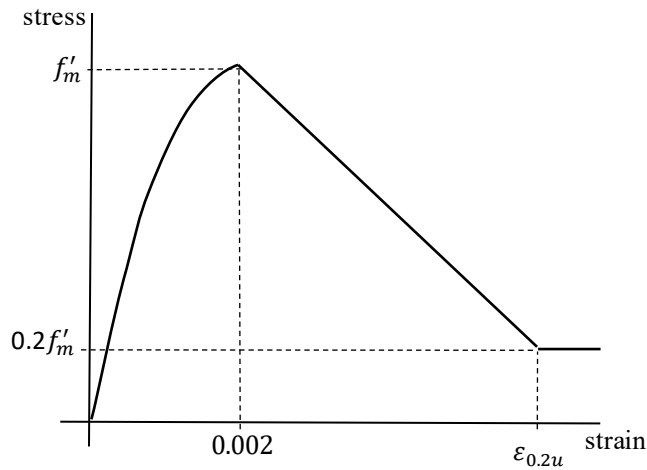


Fig. 3-2 Stress-Strain Relationship for Masonry

Stress-Strain Relationship of Steel

In this study, the stress-strain relationship for steel reinforcement is assumed to be elastic-perfectly plastic and it is a model commonly used in the literature. This behaviour is represented by the Eq. 3-7 and Fig. 3-3.

$$\sigma_s = \begin{cases} E_s \varepsilon_s, & \varepsilon_s < \varepsilon_y \\ f_y, & \varepsilon_s \geq \varepsilon_y \end{cases} \quad (3-7)$$

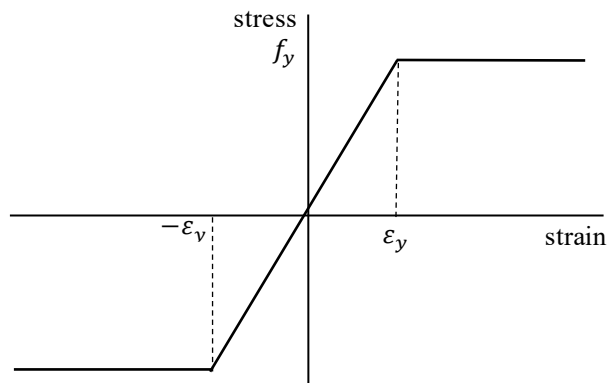


Fig. 3-3 Stress-Strain Relationship for Reinforcement Steel

Interaction between Axial Load and Bending Moments

The resistance of a wall cross-section under combinations of axial load and bending moment can be illustrated via a P-M interaction diagram (Fig. 3-4). The continuous line in Fig. 3-4 represents the ultimate cross-section resistance of the wall, while the dashed line represents its factored or design resistance. Factored load points that are inside the resistance boundary represent “safe” and points outside the resistance boundary are “unsafe”. In a wall, an optimal design, considered in this study, is to choose the wall properties and materials in such a way that the factored axial load (P_f) and moment (M_f), resulting from the worst-case load combination, fall exactly at the designed resistance boundary in Fig. 3-4.

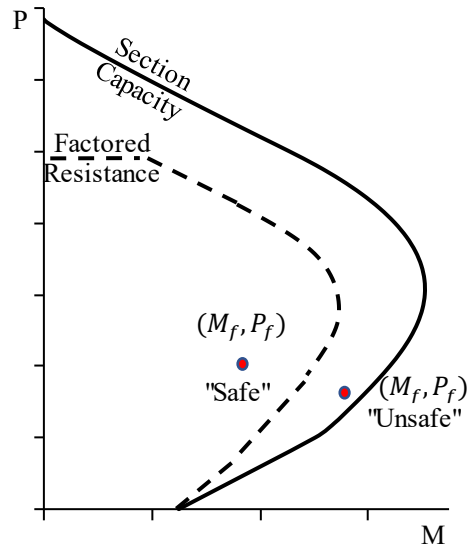


Fig. 3-4 P-M Interaction Diagram

Slenderness Effects

As the height of a vertical structural element increases beyond a certain limit, its axial-moment capacity tends to decrease due to slenderness effects. A slender masonry wall may fail due to instability or the combination of instability and material failure (Fig. 3-5).

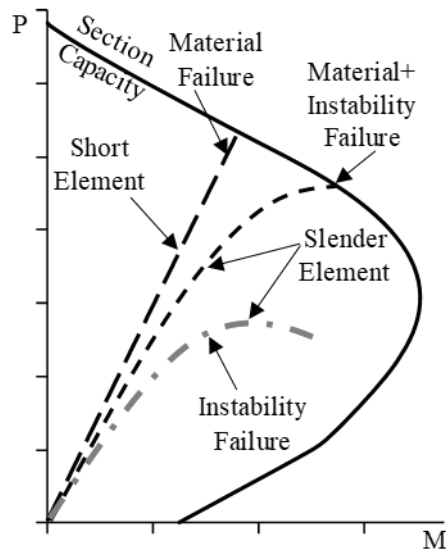


Fig. 3-5 Instability-Related Failure Modes

Slender masonry walls must resist a factored axial load (P_f) plus the amplified factored total moment (M_{ft}), defined as the sum of the primary moment (M_{f1}) plus a secondary moment arising from the combined effect of the axial load and the out-of-plane deflections, i.e., the second-order moment. In Fig. 3-4, the horizontal gap between the primary factored moment (M_{f1}) and the total factored moment (M_{ft}) represents the magnification due to second order effects for a given initial eccentricity and axial load. From a design perspective, Fig. 3-6 shows that the magnified total factored moment (M_{ft}) should be equal to or less than the factored section capacity.

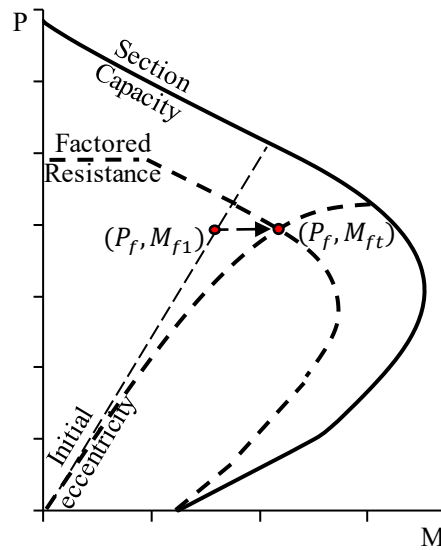


Fig. 3-6 Total Factored Moment (M_{ft})

The moment-magnifier method, codified in CSA S304-14 and in many other material standards, is popular among designers since it offers a non-iterative procedure to calculate second-order moments. The moment magnifier factor (MMF) in S304-14 is given by

$$MMF = \left(\frac{C_m}{1 - \frac{P_f}{P_{cr}}} \right) \quad (3-8)$$

where C_m is the factor that relates the actual moment diagram to an equivalent moment diagram, using the end moments at the wall M_1 and M_2 , being M_1 the lesser and M_2 the greater of the two

moments. M_2 is positive, while M_1 is positive if the member is bent in single curvature or negative if bent in a double curvature.

$$C_m = 0.6 + 0.4 \frac{M_1}{M_2} \geq 0.4 \quad (3-9)$$

Another recommendation is given by the masonry standard (S304-14) when there are lateral loads in the member, the ratio of M_1/M_2 is also taken as 1.

The critical buckling load (P_{cr}) in Eq. 3-5 is calculated as

$$P_{cr} = \frac{\pi^2 \phi_{er} (EI)_{eff}}{(1 + 0.5\beta_d)(kh)^2} \quad (3-10)$$

where the factor β_d accounts for the effect of creep, a long term deformation under sustained stress. β_d is calculated in S304-14 as the ratio of the factored dead load moment to factored total moment. The height of the wall is denoted by h , and k is the effective height factor which depends on the end conditions of the wall. The factor ϕ_{er} accounts for the effects of variability of materials on buckling and deflection ($\phi_{er} = 0.75$) as discussed earlier.

The effective stiffness $(EI)_{eff}$ is given by

$$(EI)_{eff} = E_m \left[0.25I_o - (0.25I_o - I_{cr}) \left(\frac{(e - e_k)}{2e_k} \right) \right] \quad (3-11)$$

$(EI)_{eff}$ should be greater than $E_m I_{cr}$ and less than $0.25E_m I_o$. E_m is the modulus of elasticity of masonry, I_o is the moment of inertia of the effective cross-section, I_{cr} is the transformed moment of inertia of the cracked section, $e = M_{f1}/P_f$ is the virtual eccentricity, $e_k = S_e/A_e$ is the kern eccentricity for the effective cross-sectional area A_e , and S_e is the section modulus of the effective cross-section.

The total factored moment (M_{ft}) is thus expressed as

$$M_{ft} = M_{f1} \times MMF = M_{f1} \left(\frac{C_m}{1 - \frac{P_f}{P_{cr}}} \right) \quad (3-12)$$

Figure 3b shows that the combination of factored axial load, P_f , and the amplified total moment M_{ft} , must fall inside of the P-M interaction curve according to the design criteria.

Wall Categories in the Canadian Code for Masonry Structures

Slenderness in S304-14 is expressed in terms of height-to-thickness ratio (kh/t) with the end conditions considered. The end conditions in the walls of this study are assumed to be pinned-pinned ($k = 1$), which is a typical assumption in the design of loadbearing, flexural masonry walls.

There are three categories of walls in S304-14:

1. The effects of slenderness can be neglected when the ratio of effective height to thickness is

$$h/t < 10 - 3.5(e_1/e_2) \quad (3-13)$$

with e_1 and e_2 representing the smaller and larger virtual eccentricities occurring at the top or bottom of the wall. Virtual eccentricity is the eccentricity of the axial load at a section calculated by dividing the total moment at the section by the axial load at the section.

2. For walls with a slenderness ratio of $h/t \leq 30$, the second order effects are to be accounted for through the moment magnifier method using Eq. 3-12.

3. For walls with slenderness ratio of $h/t > 30$, the second-order effects are considered through an equation to calculate the total factored moment at mid-height of the wall (Eq. 3-14). For these walls, flexural behaviour with significant deformation is anticipated, and ductility needs to be ensured. The equation terms are illustrated in Fig. 3-5, using wind as a lateral load for illustration purposes.

$$M_{ft} = \frac{w_f h^2}{8} + P_f(e_i/2) + (P_{fw} + P_f)\Delta_f \quad (3-14)$$

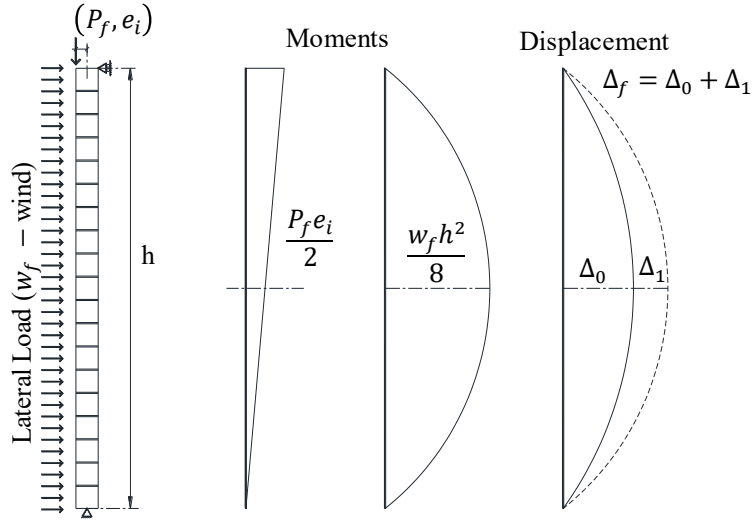


Fig. 3-7 Illustration of the total moment calculation for walls with $kh/t > 30$

In Eq. 3-14, w_f is the factored uniform lateral wind load on the wall, h is the height of the wall, P_f is the factored axial load from tributary roof or floor area, e_i is the initial eccentricity of P_f , P_{fw} is the factored weight of wall tributary to and above the design section, Δ_f is the lateral deflection of wall at mid-height under factored lateral and axial loads, Δ_0 is the first-order deflection, and Δ_1 is the deflection due to second-order effects.

Expressing Eq. 3-14 in terms of the moment magnifier, we can write an expression for the total factored moment for walls with slenderness over 30:

$$M_{ftot} = \frac{w_f h^2}{8} + P_f (e_i/2) + (P_{fw} + P_f) \Delta_0 \left(\frac{1}{1 + \frac{P_f + P_{fw}}{P_{cr}}} \right) \quad (3-15)$$

with

$$\Delta_0 = \frac{5w_f h^4}{384(EI)_{eff}} + \frac{P_f e h^2}{16(EI)_{eff}} \quad (3-16)$$

Additionally, for walls with $h/t > 30$, additional requirements must be considered. Masonry units with $t \geq 140$ mm must be used, with no raked joints; eccentric pin end conditions at each end

of the member, inducing symmetrical single curvature, are to be assumed; the factored axial load (P_f), shall not exceed $0.1\phi_m f'_m A_e$, where A_e the effective cross-sectional area of the wall; and finally, a ductile behaviour must be ensured, by making

$$\frac{c}{d} \leq \frac{600}{600 + f_y} \quad (3-17)$$

in this equation f_y is in MPa .

3.2. Reliability Analysis Problem

Limit-state Function

A limit state function represents a boundary between desired and undesired performance of a structure. The safety levels against structural failure or collapse are associated with the Ultimate Limit State (ULS). The general expression for a limit state function $G(\mathbf{X})$ to perform a reliability analysis can be formulated in the safety margin format as shown in Eq. 3-18,

$$G(\mathbf{X}) = R(\mathbf{X}) - S(\mathbf{X}) \quad (3-18)$$

where R and S are the random variables that represent the resistance and the load effect, respectively, and \mathbf{X} represents the vector containing all basic random variables. The basic random variables considered in this paper are:

- Geometry-related: the thickness of the cross-section (t) and the location of the steel reinforcement in the block cell (d).
- Material-related: masonry compressive strength (f_m), reinforcement yield stress (f_y), and workmanship factor (ρ_w).
- Load-related: dead load (D), live load (L), wind load (W), snow load (S), and the rate of loading (ρ_r).

A structure is considered safe when $G(\mathbf{X}) > 0$ in Eq. 3-15, while $G(\mathbf{X}) \leq 0$ denotes failure. The reliability of a structural element can be expressed as the complementary probability of the probability of failure ($P_{failure}$), which is indicated by Eq. 3-19

$$P_{failure} = P(R(\mathbf{X}) - S(\mathbf{X}) < 0) = P(G(\mathbf{X}) < 0) \quad (3-19)$$

or in terms of the reliability index (β) by Eq. 3-20

$$\beta = -\Phi^{-1}(P_{failure}) \quad (3-20)$$

where Φ^{-1} is the inverse standard normal cumulative distribution function and β is the reliability index. If β increases, the probability of failure decreases. Therefore, β can be considered a measure of the reliability of a structural member.

There are different methods to calculate the reliability index (β). The Monte Carlo method is popular due to its simplicity and accuracy. Using this method, Eq. 3-15 could be solved as follows:

- a. Using the statistical properties of the basic random variables \mathbf{X} , randomly generate or simulate “N” values for each of the random variables according to the probability models for basic random variables.
- b. Evaluate the limit state function ($G(\mathbf{X}) = R(\mathbf{X}) - S(\mathbf{X})$) at all N samples.
- c. Estimate the probability of failure as

$$P_{failure} = \frac{\text{number of occurrences in which } G(\mathbf{X}) < 0}{\text{total number of simulations}} \quad (3-21)$$

- d. Calculate the reliability index ($\beta = -\Phi^{-1}(P_{failure})$)

The Monte Carlo method can be illustrated by Fig. 3-8.

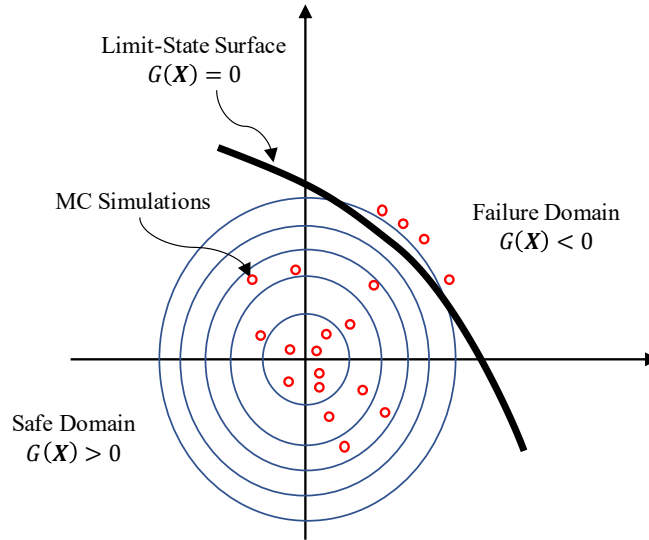


Fig. 3-8 Monte Carlo Method

In the Crude Monte Carlo method, the accuracy increases as the number of estimations increases. One way to evaluate the accuracy of the number of simulations is to calculate the coefficient of variation (COV) of the probability of failure ($P_{failure}$), a smaller value of this coefficient is desirable (Ayyub and Haldar, 1984).

$$COV(P_{failure}) = \delta_{P_{failure}} \approx \frac{\sqrt{\frac{(1 - P_{failure})P_{failure}}{N}}}{P_{failure}} \quad (3-22)$$

when $\delta_{P_{failure}}$ approaches to zero as N approaches to infinity.

Shooman (1968) presented an alternate methodology to study the error related to the number of simulations. This approach is focused on the examination of the 95% interval of the estimated probability of failure, Eq. 3-23

$$P \left[-2 \sqrt{\frac{(1 - p_f^T)p_f^T}{N}} < \frac{N_f}{N} - p_f^T < 2 \sqrt{\frac{(1 - p_f^T)p_f^T}{N}} \right] = 0.95 \quad (3-23)$$

where N_f is the number of occurrences in which $G(\mathbf{X}) < 0$, and p_f^T is the true probability of failure. The percentage error can be defined as

$$\varepsilon\% = \frac{\frac{N_f}{N} - p_f^T}{p_f^T} \times 100\% \quad (3-24)$$

Combining Eq. 3-23 and 3-24

$$\varepsilon\% = \sqrt{\frac{(1 - p_f^T)}{N \times p_f^T}} \times 200\% \quad (3-25)$$

In this research, the Eq. 3-25 was used iteratively to estimate the number of simulations, in all the cases the target error was $\varepsilon\% < 5\%$.

In this reliability analysis, the calculated reliability indices (β) are compared to target reliability indices (β_T) proposed by regional and national code committees, CSA S408 (2011) and the Joint Committee on Structural Safety (JCSS 2001a).

As pointed out in the literature review, Tychy and Vorlicek (1962) found that the safety levels depended on the definition of the limit state function. Fig. 3-9 (repeated from Fig. 2.2-2) shows three possible limit states: lines LA , LB , and LC are known as “fixed moment”, “fixed eccentricity,” and “fixed axial load” functions, respectively.

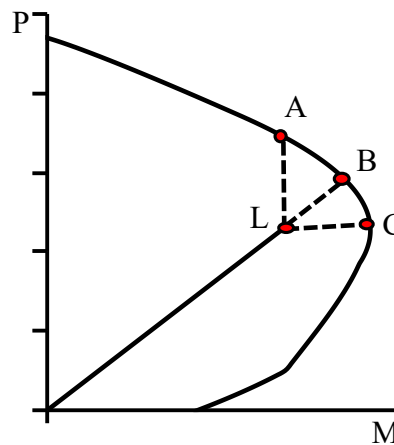


Fig. 3-9 Proposed Limit-State Functions (Tychy et al.,1962)

Limit-state function for non-slender elements

For the analysis of non-slender structural elements under eccentric axial load, different limit state functions have been proposed. Usually, simple load conditions are assumed such that the “fixed eccentricity” approach is applicable. The structural element experiences a constant moment along its height that is proportional to the axial load (P) by a quantity equal to the eccentricity (e_i). Although seldom found in practice, this loading type offers a straightforward way to illustrate the development of the limit state function for structural elements subjected to axial loads and out-of-plane moment. This is the case of the analyses conducted in non-slender reinforced concrete columns (Tychy and Vorlicek 1962, Ellingwood 1977, Ruiz and Aguilar 1994, Diniz and Frangopol 1998, Szerszen et al. 2005) and non-slender masonry walls (Ellingwood and Tallin 1985, Moosavi et al. 2017).

When used within the framework of a P-M interaction diagram, the fixed eccentricity limit state can be directly related to the “distance” between the load effect (S) and the resistance (R), these points are shown in Fig. 3-10a. The calculation of the distance between the points is aided by the fact that in the fixed-eccentricity approach, the loads and resistance can only move along a straight line, given by the initial eccentricity e_i . Thus, the value of the reliability index can be readily calculated using a reliability method, as the distance between the coordinates ($S(\mathbf{X})$) and the predicted intersection between the eccentricity line and the P-M interaction diagram ($R(\mathbf{X})$), as seen in Fig. 3-10b.

In Fig. 3-10a, R represents the nominal resistance (or ultimate strength) boundary calculated using the properties of the cross-section without reduction factors ($\phi_m = \phi_s = 1$), and R_d is a point in the factored resistance boundary of the cross-section calculated with reduction factors ($\phi_m = 0.60, \phi_s = 0.85$). S_d represents the factored load effect, and the nominal load S_n can be obtained from S_d and the load factors of the applicable building code. In this study, an optimal design consists of designing a structural member to exactly resist the applied loads; namely, the design resistance (R_d) is considered equal to the applied load (S_d).

In Eq. 3-15 the probabilistic load $S(\mathbf{X})$ and probabilistic resistance $R(\mathbf{X})$ are measured as the Euclidian distance in terms of axial load and out-of-plane bending moment for non-slender

masonry walls. $S(\mathbf{X})$ is calculated using the nominal load S_n and the statistical properties of the sources of loads (dead, live, wind and snow load given in Table 3-2). In the same way, $R(\mathbf{X})$ is calculated using R and the statistical properties of the materials and geometry of the cross-section. Fig. 3-7b shows the points used in the limit state function corresponding to the fixed eccentricity approach that could be applicable in non-slender elements.

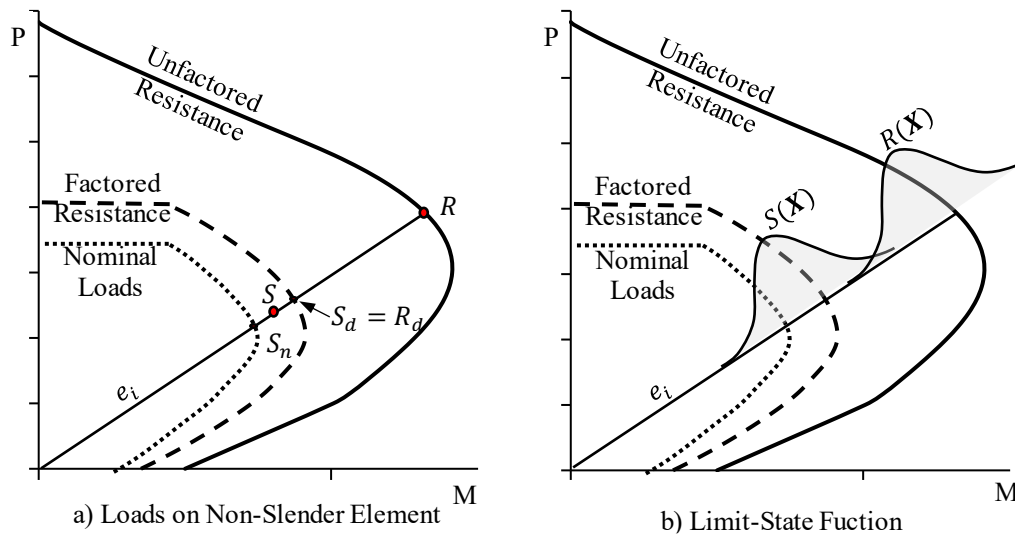


Fig. 3-10 Limit-State for Non-Slender Walls with the Fixed Eccentricity Approach

Limit-state function for slender elements

This section provides a brief overview of the development of the limit state function for slender RC concrete columns and proposes a limit state for slender masonry walls. The limit state in Fig. 3-7b would not be applicable for elements with lateral load and slender elements under compression because the load point (M_{ft}, P_f) would not move along the straight line given by the initial eccentricity e_i , due to second-order effects. The second order effects would be further exacerbated when the element is subjected to lateral loads, such as in the case of an exterior wall. For slender elements under axial load and out-of-plane bending in addition to the variabilities inherent in the material properties, member geometry, and sources of loads, the second order effects should be taken into account. MacGregor and Mirza (1989) proposed one approach to calculate the variability of the ultimate strength, in terms of axial load and bending moment, of rectangular cast-in-place reinforced concrete slender columns bent in single curvature. This

method was based on the estimation of the column's lateral deflection and second-order moment, which was added to the primary moment to calculate the total amplified moment (Fig. 3-11).

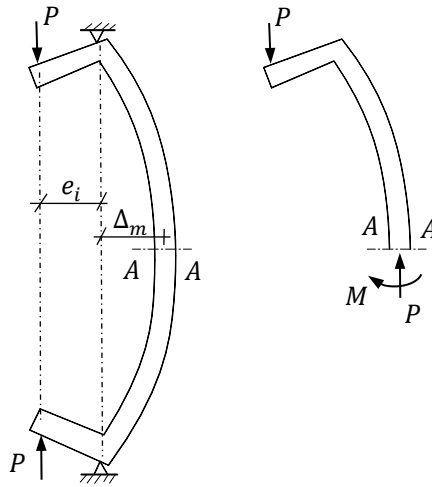


Fig. 3-11 Slender Column under Axial Load with Equal Eccentricities

The maximum moment in a slender element with equal eccentricities is assumed to occur at mid-height. The deflection Δ_m can be calculated iteratively, and the moment is calculated with Eq. 3-26

$$M = P(e_i + \Delta_m) \quad (3-26)$$

where P is the axial load, and e_i is the initial eccentricity.

Ruiz and Aguilar (1994) used the moment magnifier method to calculate the total moment due to second order effects in RC slender columns. In this approach, the design resistance (R_d) is made equal to the design load (S_d) which is the amplified moment for a given axial load and initial eccentricity. Ruiz and Aguilar showed that the use of the moment-magnifier was a simple, yet robust approach to account for second-order effects.

The results from McGregor and Mirza (1989) and Ruiz and Aguilar (1994) showed that including second-order effects in a reliability analysis is achievable. In the current study, this is done by using the fixed axial load approach (line LC in Fig. 3-9) as a basis, with one modification. In the previous approach (line LC), the axial load was considered as constant and deterministic. In this

study, the statistical properties of the sources of load (i.e., dead, live, snow, and wind) are taken into consideration to estimate the probabilistic axial load.

In the approach proposed in the current study, the design should comply with the code requirements as follows. The primary or initial factored moment (M_{f1}) is amplified using the moment magnifier method to calculate the magnified or total factored moment (M_{ft}) due to the slenderness effect. Given a combination of factored axial load, uniform distributed lateral load (w_f), and initial eccentricity (e_i) at the top, the maximum factored primary moment at the midspan of the wall is given by

$$M_{f1} = \frac{w_f h^2}{8} + \frac{P_f e_i}{2} \quad (3-27)$$

The total factored moment (M_{ft}) is calculated using the primary moment from Eq. 3-20 and the moment magnifier method (Eqs. 3-12 or 3-15, depending on the slenderness ratio).

To resist M_{ft} and P_f , a masonry wall cross-section compliant to a masonry standard (i.e., S304-14) is proposed. For an optimal design, the combination of total factored moment and axial load (M_{ft}, P_f), as denoted by point S_d , is made equal to the design resistance of the section (M_r, P_r), as denoted by point R_d , which is shown in Fig. 3-12a.

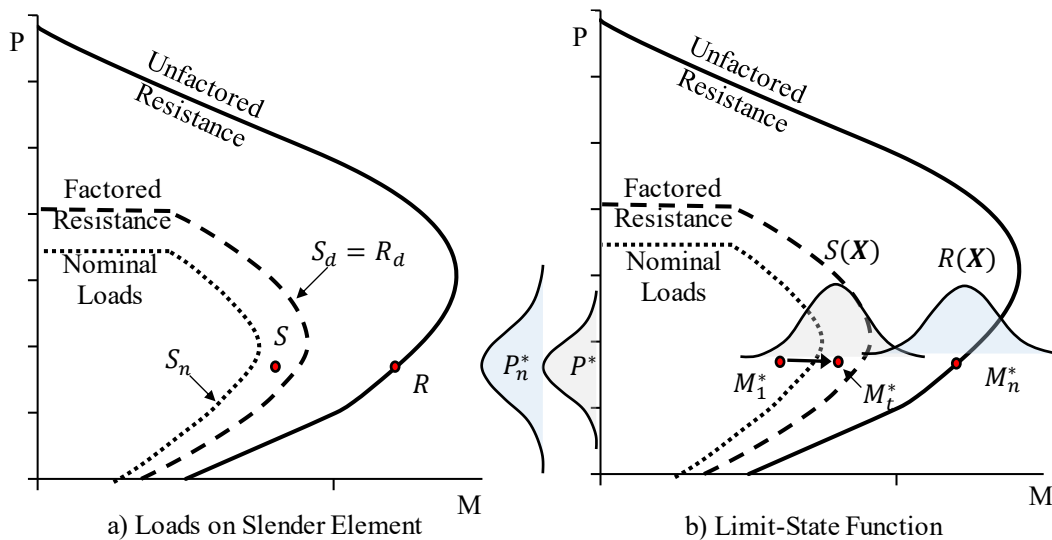


Fig. 3-12 Representation of the Limit-State for Slender Walls

Once a design is obtained with its corresponding nominal properties, reliability analysis is performed, and Eq. 3-18 is evaluated when Monte Carlo simulation is used for reliability analysis. The nominal loads and nominal strength of the cross-section need to be transformed into random variables using their specific statistical properties (this information is provided in the *Random Variables* section).

For each sample generated during Monte Carlo simulation, the resulting probable load $S(\mathbf{X})$ in terms of probable axial load (P^*) and probable total moment (M_t^*) is shown in Fig. 3-12b. The probable primary moment (M_1^*) is also illustrated as a reference. Similarly, $R(\mathbf{X})$ represents the probable moment resistance M_n^* of the cross-section, at the level of the probable axial load (P^*).

Similar to a non-slender element, Fig. 3-12b shows that the reliability of a slender element can be calculated using a reliability method, as the “distance” between the probabilistic load effect $S(\mathbf{X})$ and probabilistic resistance $R(\mathbf{X})$ in terms of the axial load and bending moment. Figure 3-12b also shows that the proposed limit state function is similar to the “fixed axial load” approach described earlier, with the limit state function depending on the comparison of the probable total moment including second-order effects (M_t^*) and the probable resistant moment (M_n^*) for a given level of probable axial load (P^*).

To summarize, the limit state function for slender elements will assess the difference between M_n^* and M_t^* for a given level of the probable axial P^* , Eq. 3-28 can be written in terms of the probable total moment (M_t^*), and the axial load, as follows.

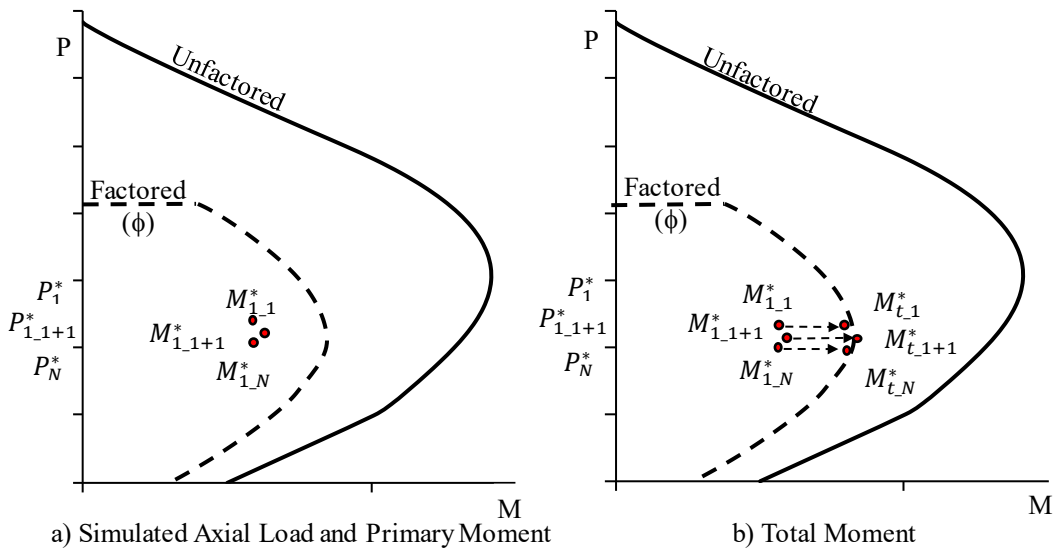
$$G(\mathbf{X}) = M_n^*(\mathbf{X}, P_n^*) - M_t^*(\mathbf{X}, P^*) \quad (3-28)$$

Reliability Analysis for Slender Walls – Summary

The procedure to calculate reliability indices on slender masonry walls is summarized in the next steps. Steps 1-6 relate to the loads, step 7 relates to the resistance, and step 8 consists of the evaluation of the limit state function.

1. Define a wall cross-section.
2. Define a wall height and an initial eccentricity for the axial load.

3. Following the design considerations of the applicable standard (i.e., CSA S304.1-14), the design strength of the cross section (R_d) is calculated, which automatically determines the maximum factored load (S_d) that the section can resist ($R_d = S_d$).
4. Using the Monte Carlo method, and the statistical properties of the random variables for the loads, N simulations are generated, including the random axial loads: $P_1^*, P_2^*, \dots, P_N^*$.
5. After the simulation of the random variables for the loads (dead, live and wind), the primary moment ($M_{1-1}^*, M_{1-2}^*, \dots, M_{1-N}^*$) is calculated (Fig. 3-13a).
6. Once the primary moment is known for each level of axial load, the moment magnifier method is used in each simulated case to calculate the total moment (M_t^*), Fig. 3-13b.
7. The moment resistance (M_n^*) of the cross-section is calculated using N samples for the material and geometry of the cross-section, Fig. 3-13c.
8. Finally, the Eq. 3-28 is used to calculate the reliability index (β).



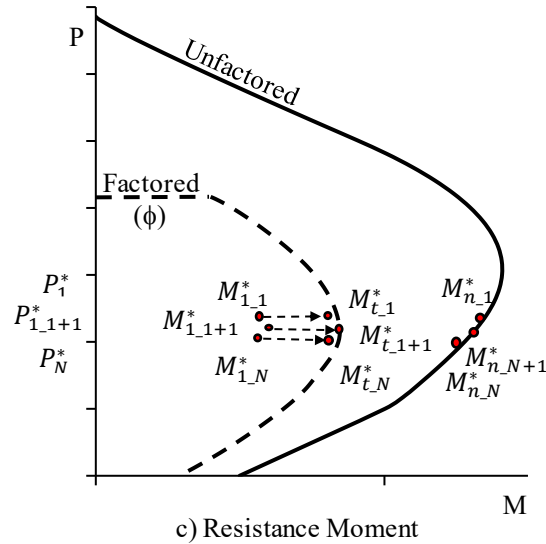


Fig. 3-13 Limit State Simulations for Slender Elements

3.3. Random Variables for Masonry Materials and Loads

The random variables considered to take into account the uncertainties in the material and geometry are the masonry compressive strength (f_m), reinforcement yield strength (f_y), reinforcement location (d), and thickness of the wall (t). The statistical properties of these variables are shown in Table 3-1. The n subscript indicates nominal values.

Compressive Strength (f_m)

The statistical properties for the compressive strength of masonry were obtained from the study conducted by Moosavi and Korany (2014). They recommended using a Gumbel distribution for grouted masonry, as shown in Table 3-1. In the table, f_{mn} represents the nominal compressive strength.

Reinforcement Yield Strength (f_y)

The statistical information for the reinforcement yield strength was taken from a study conducted by Bournonville et al. (2004). The study used the mechanical properties and weight of the steel bars produced in the United States and Canada and a normal distribution was recommended. The

statistical values are shown in Table 3-1, and f_{yn} represents the nominal reinforcement yield strength.

Reinforcement Location (d)

The statistical properties for the reinforcement location of the wall, shown in Fig. 3-1, were taken from the study presented by Ellingwood and Tallin (1985). A normal distribution was recommended, and Table 3-1 shows the statistical properties, with d_n representing the nominal distance from the extreme compression surface to the centroid of the tension steel.

Wall Thickness (t)

The statistical properties for the wall thickness were derived from an analysis conducted by Moosavi et al. (2014), where information from various concrete block producers across Canada was examined. A normal distribution was recommended, and Table 3-1 presents the statistical properties, with t_n representing the nominal width of the wall.

Table 3-1 Statistical Information for Material and Geometry

Random Variable	Mean	C.O.V.	Distribution	Reference
Masonry compressive strength (f_m)	$1.60f_{mn}$	0.236	Gumbel	Moosavi and Korany (2014)
Reinforcement yield strength (f_y)	$1.14f_{yn}$	0.070	Normal	Bournoville et al. (2004)
Reinforcement location (d) (d_n in mm)	$1.00d_n$	$4/d_n$	Normal	Ellingwood and Tallin (1985)
Wall thickness (t)	$1.00t_n$	0.010	Normal	Moosavi and Korany (2014)

Workmanship factor

The strength of masonry is highly dependent on construction practices, mason qualifications, and inspection. Some of the problems that are included in the workmanship factor are the thickness and furrowing of mortar joints, grouting procedures, wall verticality, geometrical compliance with the design values, and the quality control of construction materials. Turkstra et al. (1989) based on experimental data proposed three sets of values, which are shown in Table 3-2. This factor has been found by different researchers that has an important influence in the strength of the masonry (Stewart 1995, Fyfe et al. 2000).

Table 3-2 Workmanship Factor (Turkstra et al. 1989)

Variables	Mean	COV	Distribution
Rigorous work inspection	1.00	0.10	Normal
Moderate work inspection	0.80	0.15	Normal
Uninspected	0.70	0.20	Normal

The three levels of work inspection presented in Table 3-2 correspond to: rigorous work inspection is considered when the work is in compliance with the design and construction standards (CSA S304 and CSA 371), moderate work inspection which includes regular sites visits and records, and uninspected work.

In this study, it is assumed that the design and construction are accordance with the standards (CSA S304 and CSA 371), then *rigorous work inspection* is considered as workmanship factor in the reliability analysis, therefore the compressive strength of the masonry is affected by these statistical properties.

Loads

The statistical parameters for the loads used in this research were reported by Bartlett et al. (2003), these parameters were used to calibrate the NBCC-2005 and are summarized in Table 3-3. The

table shows the statistical values for the maximum load based on 50-year return period, the load effect modelling factors, and the point-in-time statistical values.

Table 3-3 Statistical Information for loads

Load	Bias	C.O.V.	Distribution
Dead load	1.050	0.100	Normal
Live load			
50 year maximum load	0.900	0.170	Gumbel
Point-in time load	0.273	0.674	Weibull
Transformation to load effect	1.000	0.206	Normal
Snow load			
50 year maximum depth	1.100	0.200	Gumbel
Point-in time depth	0.196	0.882	Weibull
Density	1.000	0.170	Normal
Transformation to load effect	0.600	0.420	Log-Normal
Wind load			
50 year maximum velocity			
Regina	1.039	0.081	Gumbel
Riviere du Loup	1.054	0.112	Gumbel
Halifax	1.049	0.103	Gumbel
Point-in time velocity			
Regina	0.156	0.716	Weibull
Riviere du Loup	0.064	1.149	Weibull
Halifax	0.084	1.001	Weibull
Transformation to load effect	0.680	0.220	Log-Normal

In previous studies on masonry walls that included lateral loads such as wind (Turkstra et al. 1983, Moosavi et al. 2017), the load combinations that were analyzed were relatively simple (i.e., dead plus live load, or dead plus wind load only). More complex combinations, such as the simultaneous combination of dead, live, and wind load (typically required by building codes), were not addressed. Live load and wind load are both “time-varying loads” – this means that two types of statistical properties need to be considered. One is applicable when the load is acting at its average or normal condition as the accompanying time-varying load, and the other applies when the load is acting in its extreme condition as the primary time-varying load. To address combinations that contain several time-varying loads, the Turkstra’s rule (Turkstra and Madsen,

1980) can be used. The Turkstra's rule is based on the observation that when one load component reaches an extreme value ($max(X_i)$), accompanying load components is often acting at its average value (X_{i+1}^{apt}). Here, apt is the arbitrary point-in-time probability of occurrence, and max is a maximum probability of occurrence during a suitable period of time (e.g., 50 years). It is assumed that the possibility of two or more load components acting at their extreme values simultaneously is unlikely. Equation 3-29 shows the generalized Turkstra's rule for a maximum value the load:

$$S_{max} = max \begin{cases} max(X_1) + X_2^{apt} + \dots + X_N^{apt} \\ X_1^{apt} + max(X_2) + \dots + X_N^{apt} \\ \vdots \\ X_1^{apt} + X_2^{apt} + \dots + max(X_N) \end{cases} \quad (3-29)$$

where N is the number of components in the combination.

In this research, the load combinations using the proposed types of loads and the information given in Table 3-3 are:

$$S_{max} = max \begin{cases} D + max(L) + W^{apt} \\ D + L^{apt} + max(W) \end{cases} \quad (3-30)$$

Rate of loading factor (ρ_r)

Previous studies on the statistical descriptions of the strength of concrete based on data from testing (Mirza et al. 1979, Jones and Richart 1936), showed that the strength is affected by the rate of application of the load. Jones and Richart (1936) reported a study on concrete cylinders loaded at different rates and proposed a relationship between the compressive strength of concrete and the rate of loading. The variation of the concrete strength due to the rate of loading was observed to have a relatively small dispersion, thus it was ignored in the overall coefficient of variation. Studies on the compression strength of masonry conducted by Korany and Moosavi (2011, 2017) were based on the equation proposed by Jones and Richart (1936) to estimate the rate of loading factors (ρ_r) values for the effect of dead load plus live load (0.88), dead load plus snow load (0.79), and dead load plus wind load (0.94). In this study, the effect of loading is considered by

multiplying the compressive strength of masonry (f_m) by the rate of loading factor (ρ_r). In slender walls the axial load normally is low, due to code requirements, and therefore, $\rho_r = 0.94$ will be used for the combination of dead, live and wind on slender walls.

4. NUMERICAL ANALYSIS AND RESULTS

The proposed limit state function is used in this section to calculate the reliability levels of reinforced concrete block masonry walls designed according to Canadian standards CSA S304, accounting for the uncertainties associated with material properties, design parameters and loads. Reliability indices for walls with different nominal values, such as masonry compressive strength, and steel reinforcement schemes, were calculated to illustrate the process outlined in the proposed limit state function. The reinforcement bar sizes, spacings, compressive strength, and block dimensions used in the analysis are typical of Canadian construction.

The cross-sections under study (Fig. 4-2) are proposed to investigate the reliability index for masonry walls designed with different values for the masonry compressive strength and reinforcement ratio.

The thickness of the concrete block used in this research is 190 mm since it is one of the most typically employed sizes in the industry. The walls have fully grouted cross-sections, but a similar approach is applicable for partially grouted masonry walls.

A “classic” reliability analysis is performed, in which the cross-section factored strength (R_d) is set equal to the amplified factored loads (S_d).

4.1. Compressive Strength, Workmanship, and Rate of Loading

Table 4 from CSA S304-14 provides information on the compressive strength of masonry when concrete blocks are used. This table classifies compressive strength into different categories based on factors such as the compressive strength of the units, type of mortar, ungrouted hollow units, and grouted or solid hollow units. The table is a resource for designers who lack experimental data or need to check that their design complies with safety regulations.

This research proposes walls with three levels of compressive strength, f'_m , using type S mortar, Table 4-1(adapted from Table 4 in CSA S304-14). The first one is the minimum requirement of 5.0 MPa, the second is a value of 10.0 MPa, which is one of the most typically used in the industry, and the third is the upper limit of 13.5 MPa allowed by CSA S304-14 when the compressive

strength of the block is 30 MPa or greater in grouted masonry walls. These values are taken as nominal for the reliability analysis.

The compressive strength is also affected by the workmanship factor. It is assumed in this study that the design and construction are in accordance with CSA S304, and therefore, a *rigorous work inspection* (Table 3-2) factor can be used. Another factor that affects the compressive strength is the rate of loading factor (ρ_r), taken as 0.94 for the load combination analyzed in this study.

Table 4-1 Compressive Strength Adapted from Table 4 (CSA S304-14)

Specified compressive strength of unit (average net area), MPa	Type S mortar
	Solid units or grouted hollow units, MPa
30 or more	13.5
20	10
15	7.5
10	5

4.2. Steel Reinforcement

The spacing of the steel reinforcement was assumed to be constant for the walls under analysis, and it is equal to 600 mm which is a value typically used in the industry. Two levels of reinforcement ratios are analyzed. The first level corresponds to the minimum amount of steel required by CSA S304-14 ($A_{s,min} = 0.00125A_g$, where A_g is the gross cross-sectional area of the wall), for the proposed spacing and cross-section, with a reinforcement ratio of $\rho = 0.0018$. This ratio represents the least amount of steel that can be placed in this section and in accordance with the masonry standard. The second level of reinforcement is close to that corresponding to the balanced reinforcement ratio (ρ_b), which is the maximum allowed by CSA S304-14 for walls with slenderness ratios h/t greater than 30 (Eq. 3-14). Note that reinforcement ratios greater than the balanced ratio, ρ_b , are allowed for walls with $h/t < 30$. However, reinforcement ratios greater than those corresponding to the balanced condition were not considered in this study, warranting investigation in future studies.

For the reliability analysis, the reinforcement ratios are considered deterministic. The reinforcing yield strength is considered a random variable and assumed that its nominal value is equal to 400 MPa for the analysis.

4.3. Slenderness

According to the standard, the slenderness ratio is classified into three levels, and the proposed slenderness ratios aim to cover these categories. The first category includes walls with slenderness (h/t) ratio of 10.5 (2.0 m), which are close to the boundary of being classified as non-slender walls according to CSA S304 (Eq. 3-10), then the slenderness effects can be neglected. In the second category, walls with a slenderness ratio less than 30 ($h/t \leq 30$) are analyzed, with slenderness ratios of 15.8 (3.0 m), 21.1 (4.0 m), and 26.3 (5.0 m), the slenderness effects are considered and calculated with the moment magnifier method. The third category corresponds to slenderness ratios of 31.6 (6.0 m) and 36.8 (7.0 m), where $h/t \geq 30$, as in the second category the slenderness effects are considered and calculated with the moment magnifier method, and the special requirements to calculate the total moment are also taken into account.

4.4. Eccentricity

The eccentricity of a wall refers to the distance between the centre of the wall and the point of application of the vertical load. This distance has a significant impact on the structural behaviour of a loadbearing wall. Some examples of typical eccentricities in buildings are shown in Fig. 4-1, where a loadbearing masonry wall is interacting with a steel deck roof, a concrete slab, and with a steel joist, which are typical connections found in buildings such as schools, gymnasiums and warehouses. In this research an eccentricity at the top of the wall is considered, which is the system most commonly found in real-world contexts, ranging from the minimum of $0.1t$ specified in CSA S304-14 up to $3t$.

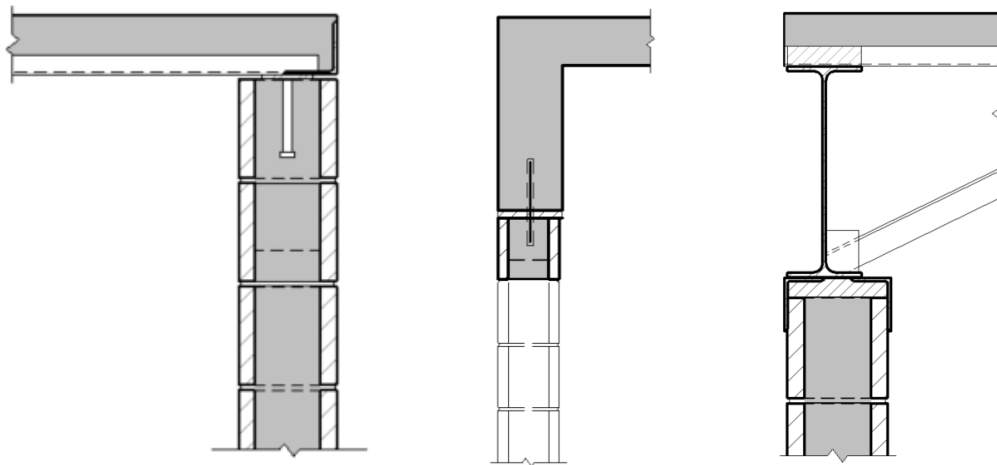


Fig. 4-1 Examples of Typical Eccentricities in Buildings

4.5. Loads

The loads considered in this study are the combination of dead load (D) plus live load (L) plus a lateral uniformly distributed load due to wind (W). The relationship between the nominal axial live load and dead load (L/D) is considered as 1.0 and 1.5. The lateral nominal wind load used in these analyses was proposed based on a calculation of the maximum design wind velocities in Western Canada, then considering that the walls correspond to a gymnasium, warehouse, or a school, and calculating the design pressure according to the Canadian code NBCC-2015. The lateral pressures were taken as 1.2 and 1.5 kPa. The three types of nominal loads (D , L , and W) were combined using the Tursktra's Rule as it was explained earlier, and the design corresponds to a factored design load combination of $1.25D$ plus $0.50L$ plus $1.4W$.

Three groups of loads are presented in this study, Group A is assumed to have $L/D = 1.0$ and a wind load of $W = 1.2kPa$, for Group B, $L/D = 1.5$ and wind load of $W = 1.0kPa$, and finally Group C, $L/D = 1.5$ and wind load of $W = 1.5kPa$.

The properties of the cross-sections and loads proposed for the reliability analysis in this research are summarized in Fig. 4-2. The n in the variables (t_n, d_n, f_{yn}, f_{mn}) denotes nominal values for the reliability analysis. The loads shown in the Fig. 4-2 (D, L, W) are also considered nominals.

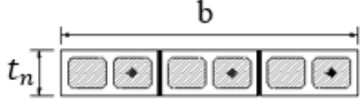

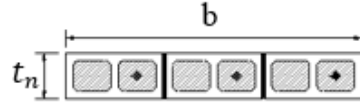
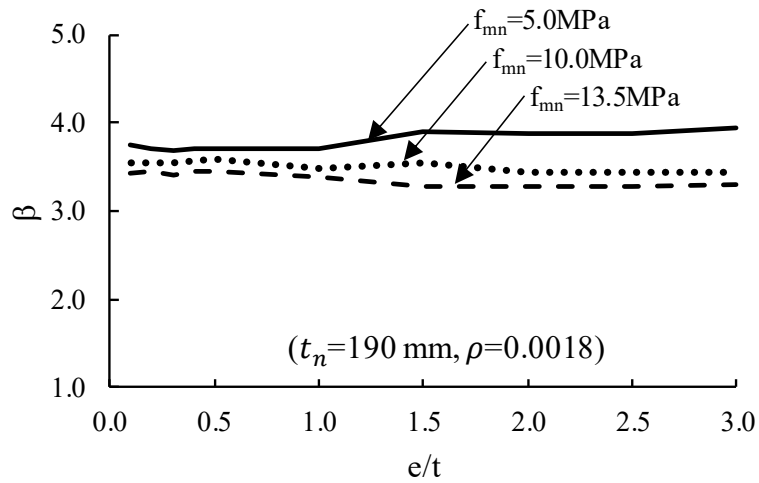
	Section	f_{mn}	Reinforcement	ρ_s	Section
Group A	 $b = 1000mm, t_n = 190mm, d_n = t_n/2$ $f_{yn} = 400MPa$ $L/D=1.0, Wind=1.2 \text{ kPa}$	5.0	1-15M@600	0.0018	W01
		10.0	1-15M@600	0.0018	W02
		13.5	1-15M@600	0.0018	W03
		5.0	1-20M@600	0.0026	W04
		10.0	1-20M@600	0.0026	W05
		13.5	1-20M@600	0.0026	W06
Group B	 $b = 1000mm, t_n = 190mm, d_n = t_n/2$ $f_{yn} = 400MPa$ $L/D=1.5, Wind=1.0 \text{ kPa}$	5.0	1-15M@600	0.0018	W07
		10.0	1-15M@600	0.0018	W08
		13.5	1-15M@600	0.0018	W09
		5.0	1-20M@600	0.0026	W10
		10.0	1-20M@600	0.0026	W11
		13.5	1-20M@600	0.0026	W12
Group C	 $b = 1000mm, t_n = 190mm, d_n = t_n/2$ $f_{yn} = 400MPa$ $L/D=1.5, Wind=1.5 \text{ kPa}$	5.0	1-15M@600	0.0018	W13
		10.0	1-15M@600	0.0018	W14
		13.5	1-15M@600	0.0018	W15
		5.0	1-20M@600	0.0026	W16
		10.0	1-20M@600	0.0026	W17
		13.5	1-20M@600	0.0026	W18

Fig. 4-2 Cross-Section Properties

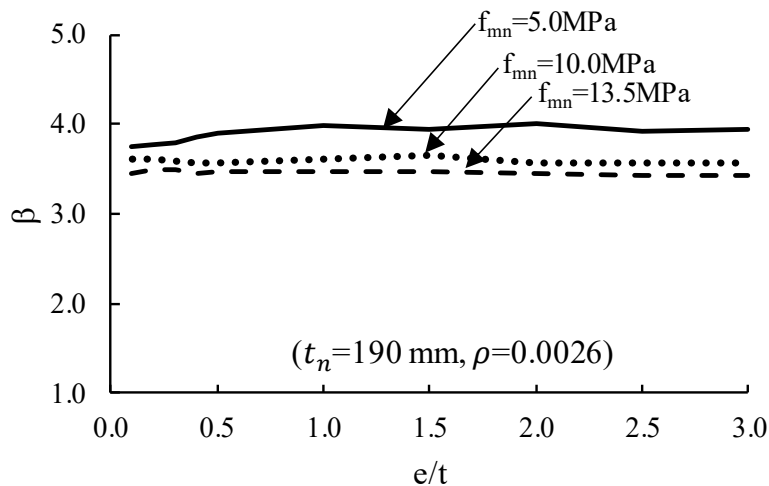
4.6. Results and Discussion

Figure 4-3 shows the reliability indices for walls with slenderness ratio equal to $h/t = 10.5$, the relationship of live to dead load is $L/D = 1.0$, and a wind load of $W = 1.2 \text{ kPa}$ which are part of the group A. The objective of these plots is to show the differences in the reliability indices when the slenderness ratio is low and the influence of the second-order effects is negligible. Figure 4-3a shows the reliability indices for walls with the minimum reinforcement ratio given by S304-14,

and different levels of compressive strength. Figure 4-3b shows the results for walls with high reinforcement ratio (close to the balanced ratio) and different levels of compressive strength.



a) β vs Initial Eccentricity



b) $h/t = 10.5, \rho = 0.0026$

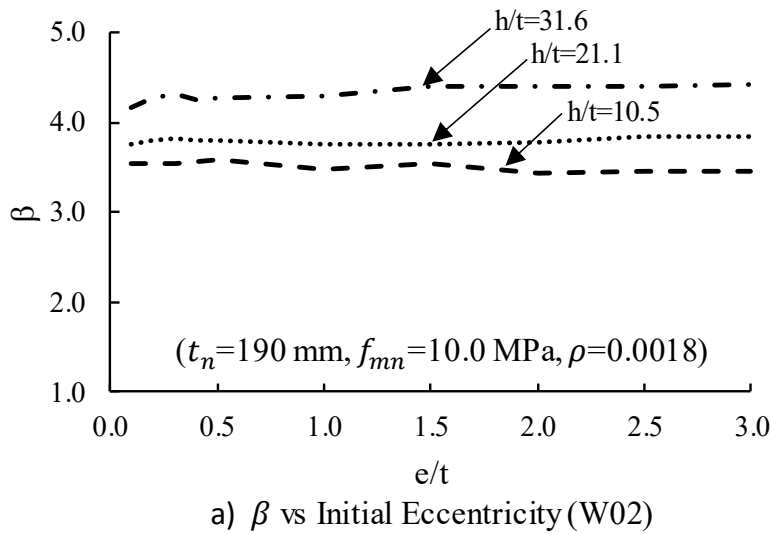
Fig. 4-3 Reliability Indices for a Wall with $h/t = 10.5$ ($L/D = 1.0, W = 1.2 \text{ kPa}$)

As it can be seen in Figs. 4-3a and 4-3b, for walls with low slenderness the reliability indices are nearly constant regardless of the eccentricity of the axial load. For the two reinforcement ratios explored, β appears not to vary significantly. However, the compressive strength of the masonry appears to have a noticeable effect on β : the reliability indices are higher when the compressive strength is low, and the reliability index is low for high compressive strengths. This is attributed

to the statistical variability compressive strength of masonry ($bias = 1.14$ and $COV = 0.07$), which is proportional to the nominal value of the compressive strength. Similar reliability indices and trends were found by Moosavi (2017) on a study of non-slender masonry walls in which second-order effects were neglected.

Walls W02 and W06 were selected to study the sensitivity of the reliability index to the slenderness ratio. Wall W06 was chosen as the “strong” wall, because it meets all the maximum requirements as per the standard, such as the highest masonry compression strength (13.5 MPa) and reinforcement ratio ($\rho=0.0026$). Wall W02 was selected to show the case of a relatively low reinforcement ratio and a practical value of masonry compressive strength (10 MPa).

The heights of the walls chosen for analysis resulted in h/t ratios of 10.5, 21.1, 31.6, and 36.8. The results for a ratio of 36.8 in W02 are not shown, since at this height of 7.0 m, a wall could not design using S304 with the compressive strength, reinforcement ratios, and geometry under study.



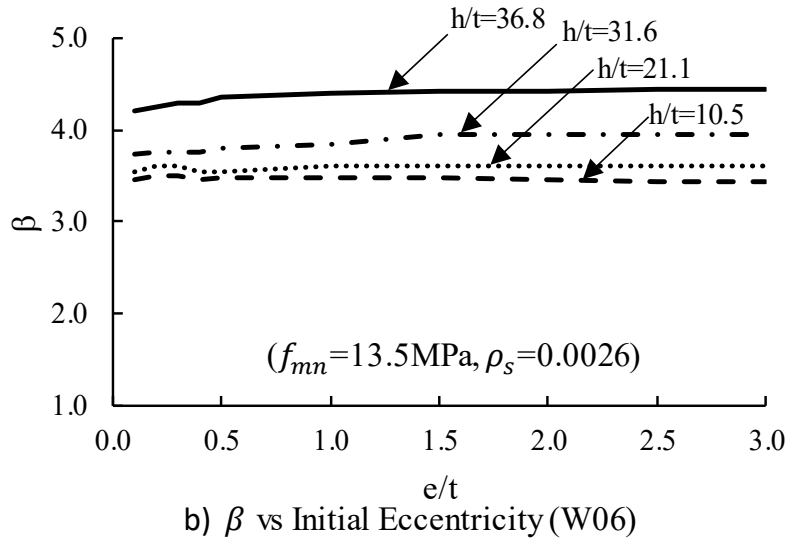
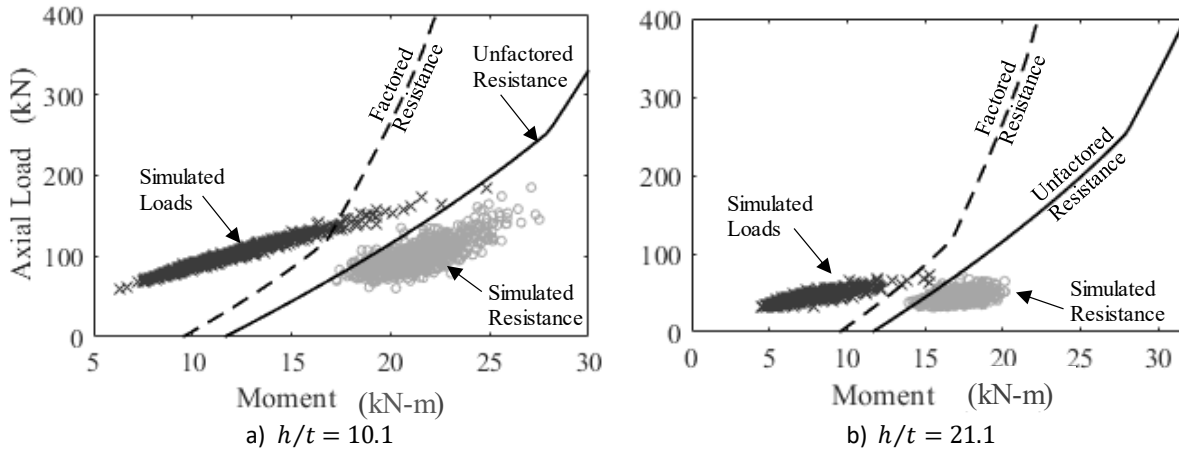


Fig. 4-4 Reliability Indices for different slenderness ratios ($L/D = 1.0, W = 1.2 \text{ kPa}$)

The results in Fig. 4-4 show that the reliability indices tend to increase as the slenderness ratio increases. Similar results were found by Ruiz and Aguilar (1994), and Ellingwood and Tallin (1985) in their investigation of slender elements under eccentrically axial load. To illustrate this effect, the Monte Carlo simulations for W02 are shown in Fig. 4-5.



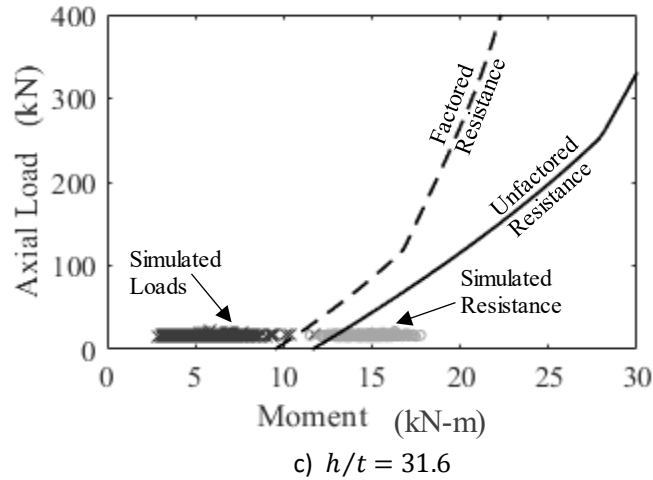


Fig. 4-5 Monte Carlo Simulations for W02

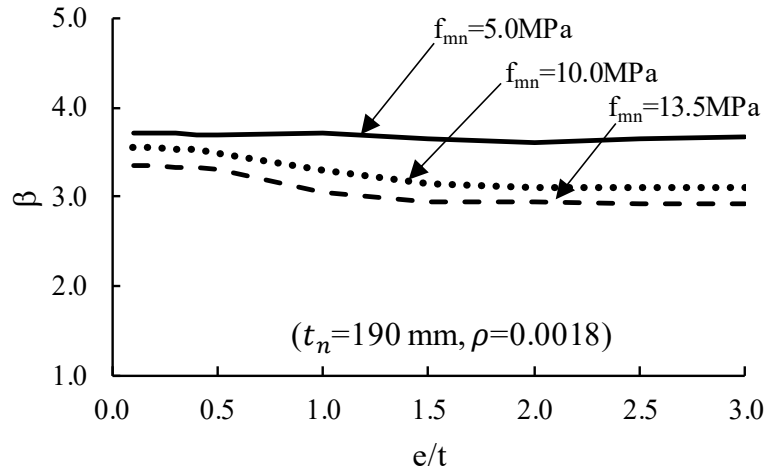
Figure 4-5 illustrates the behaviour of the simulations for loads and resistance in walls with three different slenderness ratios. It can be observed that the loads experienced by each height type decrease as the slenderness ratio increases. This is because each of the slenderness brackets in S304-14 leads to a progressive amplification of the moment when the height increases. If a wall has already been designed with a specific reinforcement (such as wall W02), any moment increment will require a reduction of the axial loads if the equality $S_d = R_d$ is to be maintained, as it is in the case of a “classic” reliability analysis. Based on the Monte Carlo simulations presented in Fig. 4-5, it can be observed that an increase in the slenderness ratio results in smaller variation of the axial load and greater dependency on the simulated moments for loads and resistances to calculate the reliability indices.

The increase in reliability indices with the slenderness ratio can be attributed to the reduction in axial loads and moments capacities resulting from the restrictions in the design of slenderness walls. When the loads are low, the response is controlled by the flexural steel in the cross-section; when the loads are high, the response is controlled by the masonry material. Since the flexural steel has less statistical variability ($bias = 1.14$ and $COV = 0.07$) than masonry ($bias = 1.60$ and $COV = 0.236$), reliability levels associated to steel-controlled behaviour will be high. Conversely, when the behaviour is masonry-controlled, the large statistical variation in the masonry materials leads to low reliability.

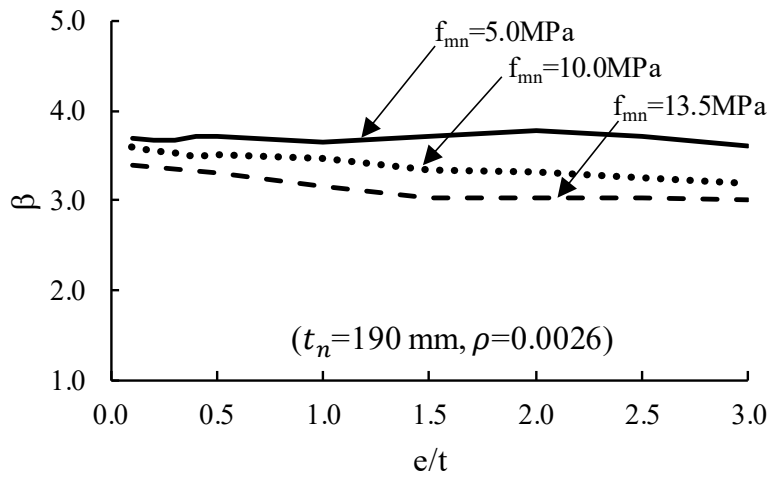
To provide context for the reliability indices obtained in the analysis presented above, for example, the target reliability index for the structural elements in a normal building (50-year design life) is defined as $\beta_T = 3.4$ for gradual failures and $\beta_T = 3.9$ for sudden failures (CSA S408, Table 2-1). In a medium-cost industrial building, a residential building or an office building the target reliability index is $\beta_T = 3.2$ according to Joint Committee on Structural Safety (JCSS), Table 2-2. For the analyzed walls, the levels of safety for walls with low slenderness ($h/t = 10.5$) have reliabilities around 3.3-3.7, while for walls with high slenderness ($h/t = 31.6$) the reliability indices are around 3.4-4.4.

From the reliability point of view, an ideal structural design could be seen as the one with consistent reliability index, regardless of the type of load or properties of the cross-section. This feature shows that the element maintains a constant level of economy and safety.

Figure 4-6 shows the reliability indices for walls with slenderness ratio equal to $h/t = 10.5$, but now the relationship of live to dead load is $L/D = 1.5$, and $W = 1.0 \text{ kPa}$. The objective of these plots is to show the differences in the reliability indices when the relationship of the live load (L) and the dead load (D) increase and the lateral wind load (W) decrease compared to the previous case (Group A).



a) β vs Initial Eccentricity

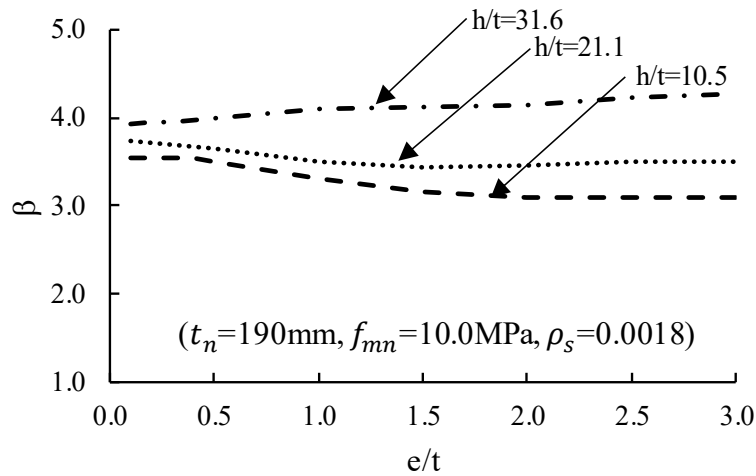


b) β vs Initial Eccentricity

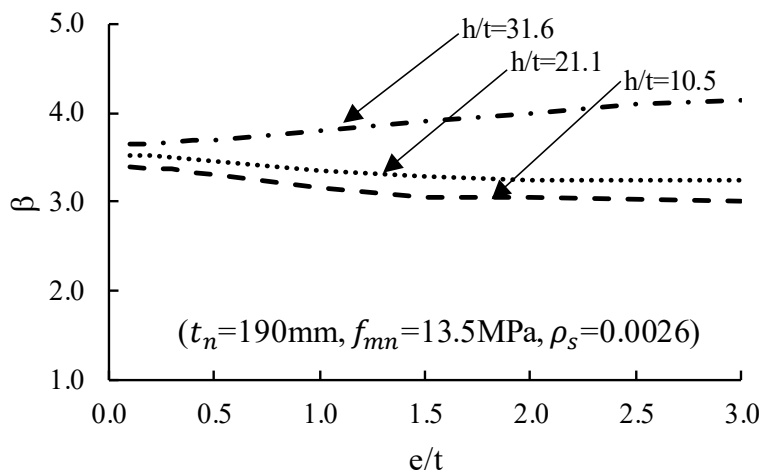
Fig. 4-6 Reliability Indices for a Wall with $h/t = 10.5$ ($L/D = 1.5, W = 1 \text{ kPa}$)

As it can be seen in Figs. 4-6a and 4-6b, Group B is showing the similar pattern of variation as Group A, for walls with low slenderness the reliability indices are nearly constant regardless of the eccentricity of the axial load for the two reinforcement ratios explored. The compressive strength of the masonry appears to have a noticeable effect on β : the reliability indices are higher when the compressive strength is low, and the reliability index is low for high compressive strengths. Regarding the variation due to the eccentricity, the reliability indices are closer for small eccentricities, but there is more variation as the eccentricities increase.

The reliability indices for various slenderness ratios are shown in Figure 4-7. The analyzed walls have the same compressive strength and reinforcement ratio.



a) β vs Initial Eccentricity (W08)



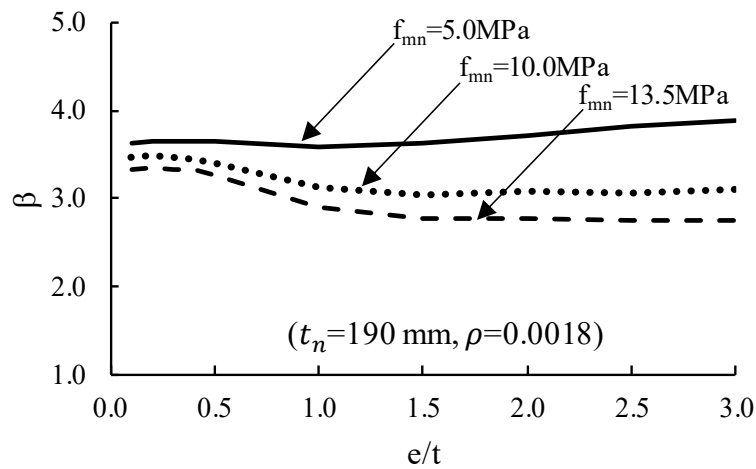
a) β vs Initial Eccentricity (W12)

Fig. 4-7 Reliability Indices for different slenderness ratios ($L/D = 1.5, W = 1 \text{ kPa}$)

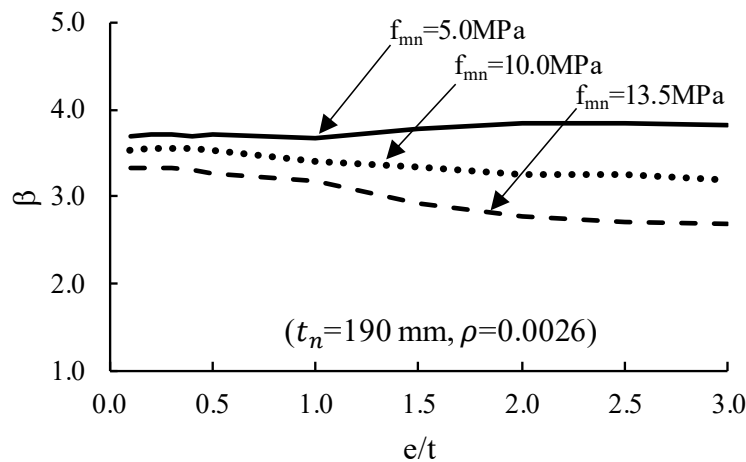
Based on the results shown in Fig. 4-7, the behaviour of the reliability indices for Group B is similar to that of Group A: as the slenderness ratio increases, the corresponding reliability indices also increase. Figure 4-7 shows that there is more variation in the reliability indices as the eccentricity increase; this is due to the effect of the bending moment. Since the relationship on the load is higher, the walls are not able to take additional moments, resulting in similar reliability

indices to low eccentricities because the compression effect is predominant. This tendency was even more pronounced compared to the results shown for the wall with low slenderness, Fig. 4-6.

Figure 4-8 shows the reliability indices for Group C: walls with the same slenderness ratio equal to $h/t = 10.5$, with a live to dead load ratio of $L/D = 1.5$, and $W = 1.5 \text{ kPa}$. This group has the highest wind load and live to dead relationship. The objective of these plots is to show the differences in the reliability indices when the relationship of the L and D increased and lateral load (W) increased from the previous cases.



a) β vs Initial Eccentricity



b) β vs Initial Eccentricity

Fig. 4-8 Reliability Indices for a Wall with $h/t = 10.5$ ($L/D = 1.5$, $W = 1.5 \text{ kPa}$)

Figure 4-8 shows the reliability indices for Group C, presenting more closer patterns to Groups B than to Group A. The reliability of walls with low compressive strength is the highest, follows by the walls with compressive strength of 10 MPa and the lowest indices were presented by walls with compression strength of 13.3 MPa, reliability indices are higher when the compressive strength is low, and the reliability indices are low for high compressive strengths. In both figures, the reliability shows a higher difference as the initial eccentricity increases.

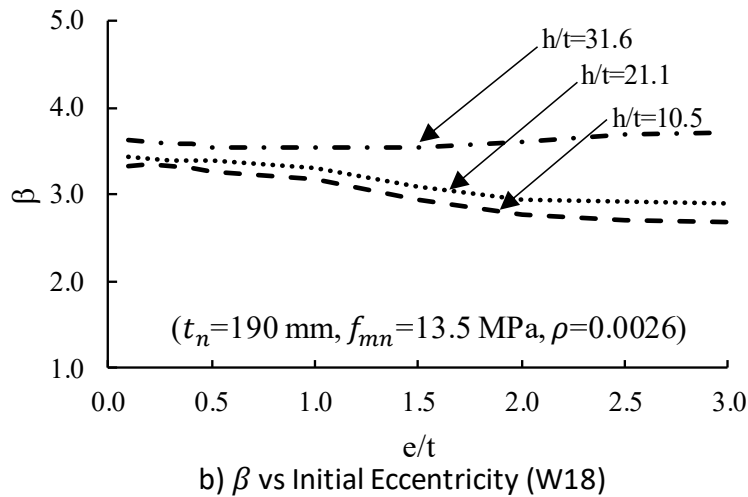
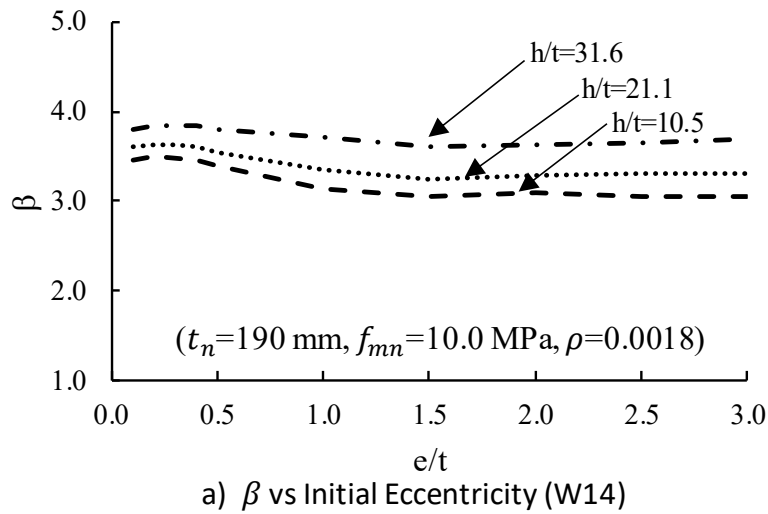


Fig. 4-9 Reliability Indices for different slenderness ratios ($L/D = 1.5, W = 1.5 \text{ kPa}$)

The results of walls with different slenderness in Fig. 4-9 show the same behaviour of the reliability indices of group A and B. As the slenderness ratio increases, the corresponding reliability indices also increase. These results align more closely with Group B, where the pattern shows an increase in reliability indices with the increasing slenderness ratio of the walls. However, it is noteworthy that there are more variations in the reliability indices when the eccentricities are large.

4.6.1. Effect of the slenderness on the reliability ratio (β)

For the analyzed walls, in Group A, the levels of safety for walls with low slenderness ($h/t = 10.5$) have reliability indices around 3.3-3.8, while for walls with high slenderness ($h/t = 31.6$) the reliability indices are around of 3.4-4.4. It was also observed that the reliability indices remained almost constants with varying the initial eccentricity.

Same pattern was observed with Group B and C. Where the highest slenderness ratio the highest reliability index. One noted difference was that as the initial eccentricity increases, the difference between the reliability indices is higher.

This increment in the reliability indices is also attributed to the uncertainties in the behaviour of slender walls.

4.6.1. Effect of the loads on the reliability ratio (β)

The load increment in the lateral force due to wind and the combined relationship of live to dead loads (L/D) have been shown to be crucial in the calculation of the reliability indices. Even though the reliability indices maintain the same pattern, the safety levels increase with higher slenderness ratios. Depending on the loads, the reliability indices could either remain constant through different eccentricities or change, with the most significant differences occurring for eccentricities around $3t$ and the smallest differences when the eccentricity is $0.1-0.5t$.

Another observation is that, as the loads with more variation increase, for example the results of Group C where the value of the live load is $L = 1.5D$, and $Wind = 1.5 kPa$, the reliability indices decrease, this is due to the increment in the uncertainties of the loads.

These results suggests that a calibration of the material reduction factors in the S304-14 masonry standard may be warranted when the slenderness is high, as the associated values of β for this case exceed those recommended in S408.

5. CONCLUSIONS AND RECOMMENDATIONS

This chapter provides a summary, conclusion, and recommendations for the analysis of the reliability levels in masonry walls based on loads, slenderness ratio, and cross-section properties.

5.1. Summary

The objective was to calculate the reliability levels of slender concrete block masonry walls. These levels were achieved by the following:

- A limit state function for non-slender and slender masonry walls was proposed and used in this research. It captures the behaviour of walls with more realistic loading conditions, such as exterior slender walls in gymnasiums or warehouses.
- For the cross-section properties, two levels of reinforcement ratios were proposed, the minimum recommended by the masonry standard CSA S304-14 for reinforced walls, but also considering the properties of the section. The second level is close to the balance reinforcement ratio and it is the maximum for walls with slenderness ratios h/t greater than 30.
- The studied eccentricities ranged from the minimum of $0.1t$ specified in the standard up to $3t$, this based on typical eccentricities of building in the masonry industry.
- Three groups of masonry walls varying in cross-section properties and load relationships were analyzed.

Group A: $L/D = 1.0$, and Wind = 1.20kPa

Group B: $L/D = 1.5$, and Wind = 1.00kPa

Group C: $L/D=1.50$, and Wind = 1.50kPa

The load combination studied in this research was dead plus live plus wind load, because this combination was not explored before, but the same limit state function can be used to expand the analysis.

5.2. Conclusions

Conclusions in this section are based on the analysis of walls described previously.

- For walls with low slenderness ratios in Group A, the reliability indices appear to be nearly constant over a wide range of load eccentricities at the top of the wall. In these types of walls, the slenderness effects are not significant, and the calculated reliability indices are similar to those found in studies of non-slender walls.
- The reliability indices are sensitive to the slenderness ratio. The reliability index increases as the slenderness ratio increases, which means that safety levels for slender walls designed as per S304-14 are higher than those corresponding to short walls. This is because slender walls are designed with lower axial loads and moments than their more robust counterparts. This is also attributed to the uncertainties in the behaviour of slender walls.
- Designs using the minimum amount of reinforcing steel, and low compressive strength of masonry have slightly larger reliability levels than those walls using higher compressive strength and reinforcement ratio in slender walls. A higher reliability level is associated with less uncertainty in the material properties. The behaviour of the masonry walls analyzed in this study was largely controlled by the compressive strength of the masonry, since there is more variation in the statistical data in the compressive strength of masonry than in the statistical information of the reinforcement steel. Consequently, higher masonry compressive strength is accompanied by more uncertainty and therefore less reliability.
- As the loads with more variation increase, the reliability indices decrease, this is due to the increment in the uncertainties of the loads.
- The design reduction factors should be evaluated in detail for a more consistent design between slender and non-slender walls. This evaluation could also work to propose levels of reliability closer to the target reliability indices recommended by the standards.
- The presented limit state function was used with the combination of dead plus live plus wind load, but it is not limited to that combination, it can be used for all type of combinations, since the limit state function is able to capture the second-order effects due to slenderness.

5.3. Recommendations and Future Research

This research was focus on the calculation of the safety levels of the slender masonry walls, and the recommendations of the masonry design standard CSA S304-14 were assumed as correct.

Future research should consider different base boundary conditions and explore the levels of safety of slender masonry walls. The same limit state can be used, but the calculation of the capacity could include different boundary conditions.

With the advancement in the testing field of this type of walls, the statistical properties could be updated, and the same procedure could be used, but with more recent information.

This study could also be extended even to interior walls, since the standards nowadays have been recommended the design of this type of walls under lateral loads.

A reliability study on walls with slenderness ratio > 30 , even when they do not comply with the standard requirements, to observe the safety levels and overdesign conditions.

Due to the variation in the reliability indices, a calibration on the reduction factor for the compressive strength of the masonry (ϕ_m) and the reduction factor for the yield strength (ϕ_s) is recommended. Some variable factors depending on the mode of failure could be proposed, similar to the factor for the compressive strength in concrete (ACI 3018).

REFERENCES

- CSA S304-14, 2014. Design of Masonry Structures. Canadian Standard Association, Mississauga, Ontario, Canada.
- CSA A371-14, 2014. Masonry Construction for Buildings. Canadian Standard Association, Mississauga, Ontario, Canada.
- CSA S408-11, 2011. Guidelines for the development of limit states design standards. Canadian Standard Association, Mississauga, Ontario, Canada.
- American Concrete Institute (ACI). (1979). Building Code Requirements for Concrete Masonry Structures ACI 531. Detroit, Mich.
- American Concrete Institute (ACI). (1989). Building Code Requirements for Structural Concrete ACI 318. Farmington Hills, MI.
- AS3700 (2018). Masonry Structures, Standards Australia, Sydney.
- Ayyub, B.M. & Haldar, A. (1984). "Practical Structural Reliability Techniques." Journal of Structural Engineering, ASCE, Vol. 110, No. 8, pp. 1707-1724.
- Bournonville, M., Dahnke, J., and Darwin, D. (2004). "Statistical Analysis of the Mechanical Properties and Weight of Reinforcing Bars." University of Kansas Report.
- Brick Institute of America, 1969. Building Code Requirements for Engineered Brick Masonry, McLean, Va., Aug.
- Chi, B., Yang, X., Wang, F., & Zhang, Z. (2019). "Structural Reliability of Reinforced Concrete Block Masonry Wall Subjected to Seismic Force." 13th North America Masonry Conference, Salt Lake City, pp. 1512-1521.
- Cornell, C.A. (1969). "A Probability-Based Structural Code." ACI Journal Proceedings, Vol. 66, pp. 974-985.
- Diniz, S.M.C. & Frangopol, D.M. (1997). "Reliability Bases for High-Strength Concrete Columns." Journal of Structural Engineering, 123, 1375-1381.

Diniz, S.M.C. & Frangopol, D.M. (1998). "Reliability Assessment of High-Strength Concrete Columns." *Journal of Engineering Mechanics*, 124, 529-536.

Drysdale, R.G. & Hamid, A.A. (2005). *Masonry Structures: Behaviour and Design*. Canadian Edition. Canadian Masonry Centre, Mississauga, Ont.

Ellingwood, B.M., Galambos, T.V., MacGregor, J.G. and Cornell, C.A. (1980). Development of a Probability-Based Load Criterion for American National Standard A58. National Bureau of Standards. Special Publication No. 577. Washington, D.C. 1980.

Bartlett, F., Hong, H., & Zhou, W. (2003). "Load Factor Calibration for the Proposed 2005 Edition of the National Building Code of Canada: Statistics of Loads & Load Effects." *Canadian Journal of Civil Engineering*, 30(2), 429-439.

Ellingwood, B.M. & Tallin, A.A. 1985. "Limit States Criteria for Masonry Construction". *Journal of Structural Engineering*, 111: 108.

Fyfe, A.G., Middleton, J., and Pande, G.N. (2000). "Numerical Evaluation of the Influence of Some Workmanship Defects on Partial Factor of Safety (γ_m) for Masonry." *Masonry International*, 13, (2), 8-53.

GB 50003 (2011). Code for design of masonry structures. China Architecture & Building Press.

GB 50011 (2010). Code for seismic design of buildings. China Architecture & Building Press.

GB 50068 (2001). Code for seismic design of buildings. China Architecture & Building Press.

Hasofer, A. M. and Lind, N. C. (1974). "An Exact and Invariant First Order Reliability Format." *Journal of Engineering Mechanics*, 100, 111-121.

Israel, M., Ellingwood, B., and Corotis, R. (1987). Reliability-Based Code Formulations for Reinforced Concrete Buildings. *Journal of Structural Engineering*. Vol. 113. No. 10, 1987, ASCE. pp. 2235-2252. Joint Committee on Structural Safety (JCSS 2001a). Probabilistic Model Code: Part I – Basis of Design.

Jones, P.G., and Richardt, F. (1936). "The Effect of Testing Speed on Strength and Elastic Properties of Concrete." *Proceedings*, pp. 380-392.

Laird, D.A., Drysdale, R.G., Stubbs, D.W., and Sturgeon, G.R. (2005). "The New CSA S304.-04 "Design of Masonry Structures"." Proceedings of the 10th Canadian Masonry Symposium, Banff, Alberta, pp. 10.

MacGregor, J.G., Breen, J.E., and Pfrang (1970). "Design of Slender Columns." ACI Journal Proceedings, Vol. 67, pp. 6-28

Mirza, S.A., and MacGregor, J.G. (1989). "Slenderness and strength reliability of reinforced concrete columns." ACI Structural Journal, 86(4), 428-434.

Mirza, S.A., Hatzinikolas, M., and MacGregor, J.G. (1979). "Statistical Description of Strength of Concrete". Journal of the Structural Division, Vol. 106, No. ST6, pp. 1021-1037.

Moosavi, S.A.H. (2017). "Structural Reliability of Non-Slender Loadbearing Concrete Masonry Members under Concentric and Eccentric Loads", Ph.D. diss. University of Alberta.

Moosavi, H., and Korany, Y. (2014). "Assessment of the Structural Reliability of Loadbearing Concrete Masonry Designed to the Canadian Standard S304.1." Canadian Journal of Civil Engineering, 41 (2).

NBCC. (2015). "National Building Code of Canada"

Nowak, A.S. & Collins, K.R. (2000). "Reliability of Structures", McGraw-Hill Higher Education, New York.

Stewart, M.G. & Lawrence, S. (2002). "Structural Reliability of Masonry Walls in Flexure." Masonry International. Vol. 5, No. 2, 2002, pp. 48-52

Stewart, M.G. & Masia, M.J. (2019). "Reliability-Based Assessment of Safety Factors for Masonry Walls in Vertical Bending." 13th North America Masonry Conference, Salt Lake City, pp. 1159-1170.

Szerszen, M.M., Szwed, A., and Nowak, A.S. (2005). "Reliability Analysis of Eccentrically Loaded Columns." ACI Structural Journal, American Concrete Institute (ACI), 102-S69, pp. 676-688.

Ruiz, S.E. & Aguilar, J.C. (1994). "Reliability of Short and Slender Reinforced-Concrete Columns", Journal of Structural Engineering, ASCE, 120(6), pp. 1850-1865.

Rosenblueth, E. & Esteva, L. (1971). "Reliability basis for some Mexican codes." Probabilistic design of reinforced-concrete building. SP31 Special Publication, American Concrete Institute (ACI), Detroit, Mich. USA.

Shoorman, M.L. (1968). Probabilistic Reliability: An Engineering Approach. McGraw Hill, New York.

Turkstra, C. J. (1970). "Theory of Structural Design Decisions." Solid Mechanics Study No. 2, University of Waterloo, Ontario, Canada.

Turkstra, C. J. & Madsen, H. (1980). "Load Combinations for Codified Structural Design." Journal of the Structures Division (ASCE) 106, No. 12, pp. 2527-2543.

Turkstra, C. & Ojinaga, J. (1980). "Towards a Canadian Limit States Masonry Design Code." In Proceedings of the 2nd Canadian Masonry Symposium, Carleton University, Ottawa, Ontario, Canada, pp. 133-141

Turkstra, C. J. (1984). "A Safety Index Analysis for Masonry Design." In Proceedings of the 4th ASCE Specialty Conference on Probabilistic Mechanics & Structural Reliability, Berkeley, USA, pp. 77-81.

Appendix A

The calculation of a P-M interaction diagram according to the CSA S304-14 is presented.

Initial data:

$$\begin{aligned} f_y &= 400 \text{ MPa} \\ t &= 190 \text{ mm} \\ d &= 95 \text{ mm} \\ b &= 1000 \text{ mm} \\ A_e &= 190000 \text{ mm}^2 \\ A_s &= 500 \text{ mm}^2 \\ f'_m &= 13.5 \\ E_s &= 200000 \text{ MPa} \\ \phi_m &= 0.6 \\ \phi_s &= 0.85 \\ \beta_1 &= 0.8 \end{aligned}$$

a) Axial load alone ($M_r=0$) (No tied)

$$P_r = 0.8[\phi_m(0.85f'_m)A_e]$$

$$P_r = 1046520$$

b) Balance case

$$\begin{aligned} c &= \frac{300t}{f_y + 600} \\ c &= 57 \text{ mm} \\ a &= \beta_1 c = 45.6 \text{ mm} \\ C_m &= 0.85\phi_m f'_m b a \end{aligned}$$

$$C_m = 313956 \text{ N}$$

$$T_r = \phi_s A_s f_y$$

$$T_r = 170000 \text{ N}$$

Then

$$P_{rb} = C_m - T_r$$

$$P_{rb} = 143956 \text{ N} = \mathbf{143.956 \text{ kN}}$$

$$M_{rb} = C_m \left(\frac{t}{2} - \frac{a}{2} \right)$$

$$M_{rb} = 22667623 \text{ N mm} = \mathbf{22.668 \text{ kN m}}$$

and the eccentricity for the balanced case is

$$e_b = \frac{M_{rb}}{P_{rb}} = 157.5 \text{ mm}$$

c) Bending alone ($P_r = 0$)

$$\rho_{max} = 0.2448 f'_m / 340 = 0.00972$$

$$\rho_{min} = 0.002$$

$$\rho = A_s / b d = 0.005263 \quad \text{ok!}$$

$$C_m = 0.85\phi_m f'_m b a = 6885 \text{ a N}$$

$$T_r = \phi_s A_s f_y$$

$$T_r = 170000 \text{ N}$$

from $C_m = T_r$

$$a = 24.7 \text{ mm}$$

$$c = 30.9 \text{ mm}$$

$$M_r = T_r \left(d - \frac{a}{2} \right)$$

$$M_r = 14051235 \text{ N mm} = \mathbf{14.051 \text{ kN m}}$$

d) More points

$$c = 140 \text{ mm}$$

$$a = \beta_1 c = 112 \text{ mm}$$

$$C_m = 0.85\phi_m f'_m b a$$

$$C_m = 771120 \text{ N}$$

$$T_r = \phi_s A_s f_y$$

$$T_r = 170000 \text{ N}$$

Then

$$P_{rb} = C_m - T_r$$

$$P_{rb} = 601120 \text{ N} = \mathbf{601.120 \text{ kN}}$$

$$M_{rb} = C_m \left(\frac{t}{2} - \frac{a}{2} \right)$$

$$M_{rb} = 30073680 \text{ N mm} = \mathbf{30.074 \text{ kN m}}$$

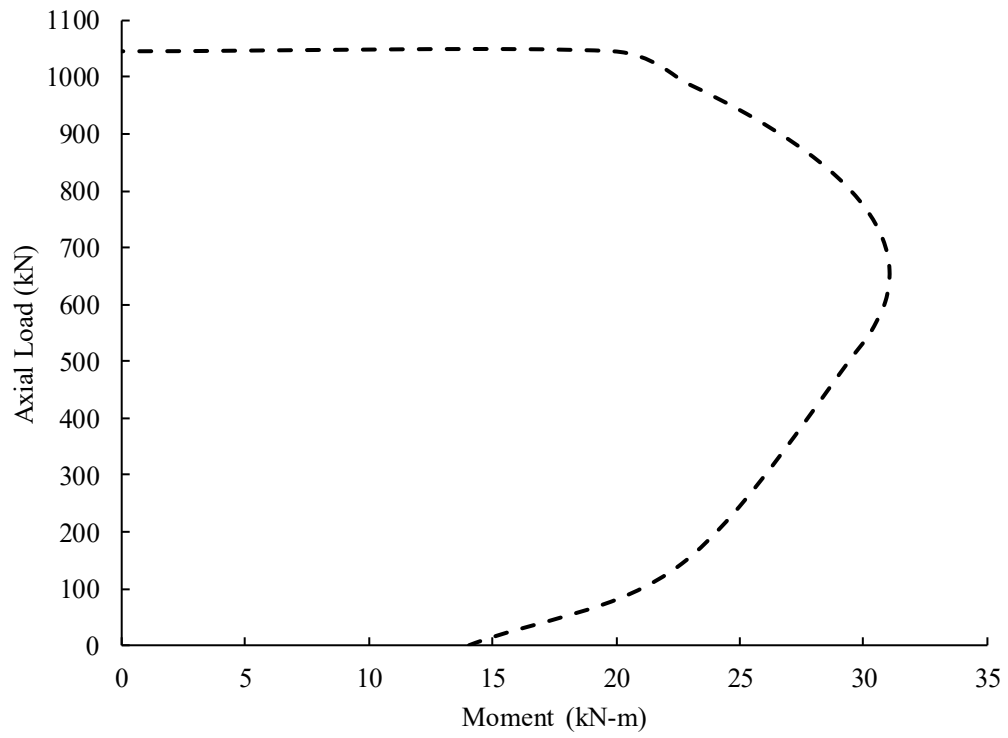


Fig. A-1. P-M Interaction Diagram

Appendix B

In this appendix the calculation of the reliability index of a non-slender and slender wall is presented. In the first example, the reliability index β for a non-slender wall using the two limit state functions is presented. In the example two, the reliability index for a slender wall is shown.

Example 1. Non-Slender Wall - Detailed Calculation

Fixed Eccentricity Limit State

The selected wall was proposed by Moosavi et al. (2017), it is a fully grouted masonry wall with 290 mm of thickness, compressive strength $f_{mn} = 17 \text{ MPa}$, under dead plus live load with a ratio of $LL_n/DL_n = 1$, and an initial eccentricity of $e_i = 0.5t$. The location of the reinforcement bars is considered at the centre of the section ($d_n = t_n/2$) with a ratio of reinforcement of $\rho = 0.0025$, and the yield strength of the reinforcement is $f_{yn} = 400 \text{ MPa}$.

The case under study is when the initial eccentricity is equal to 50% of the thickness of the wall ($e_i = 0.5t$). The fixed eccentricity limit state function is shown in Fig. B-1 where (R) is the resistance of the cross-section, S_d are the maximum design loads which are equaled to the design resistance of the section R_d and from that point, using the Eq. B-1 the nominal loads are deduced. By knowing the nominal and using the statistical properties of the loads, the probabilistic value for the load is calculated (S).

$$S_d = 1.25DL_n + 1.50LL_n \quad (\text{B-1})$$

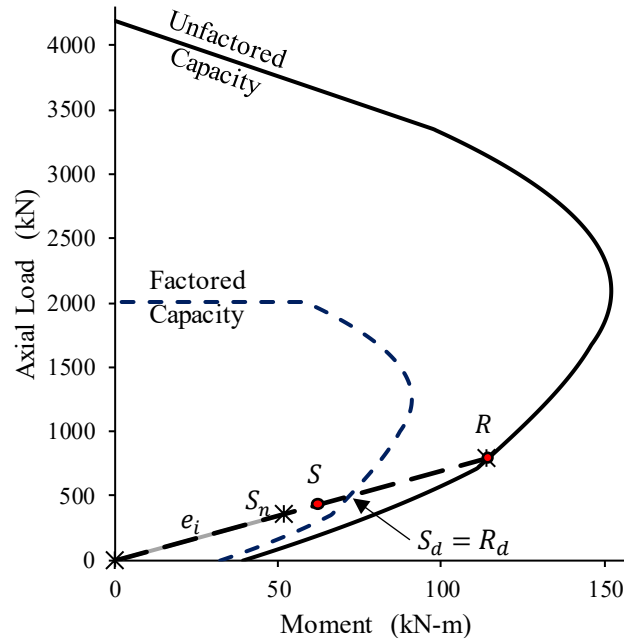


Fig. B-1 Fixed Eccentricity Limit State Function

The reliability index is calculated using the First Order Reliability Method (FORM) and the limit state function shown in Eq. B-2

$$G(\mathbf{X}) = R(\mathbf{X}) - S(\mathbf{X}) = \sqrt{M_r^2 + P_r^2} - \sqrt{(M_{DL} + M_{LL})^2 + (P_{DL} + P_{LL})^2} \quad (\text{B-2})$$

Using the statistical properties shown in Table 1 and 3 for the random variables, a workmanship as was recommended by Moosavi et al. (2017) with 0.85 mean and 0.15 COV, and a rate of loading equal to 0.88, then

$$\beta_{fe} = 3.36$$

Fixed Axial Load Limit State Function

The first step in the currently proposed method is the load simulations. In this example, the dead load (D) has a normal distribution, and the live load (L) is considered with its maximum probability of occurrence with a Gumbel distribution. Based on their probability distributions and the Monte Carlo method, a N number of simulations are generated and shown in the histogram of Fig. B-2 and B-3.

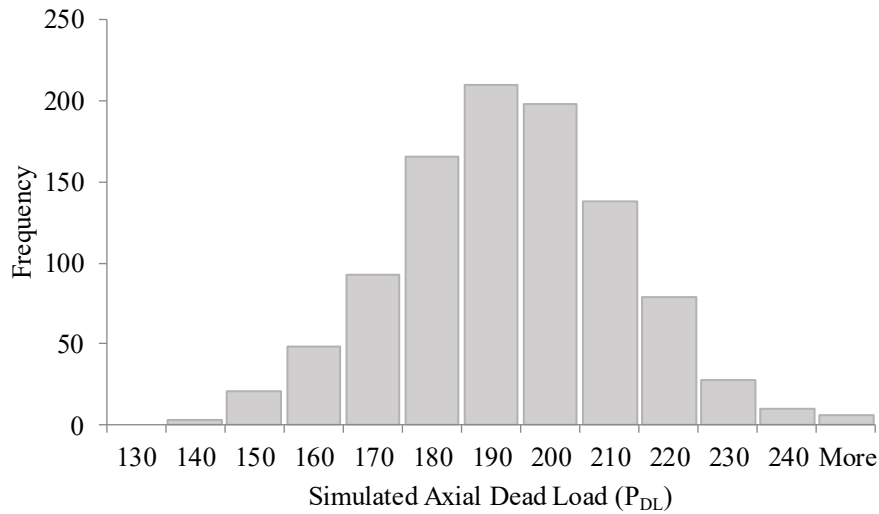


Fig. B-2 Dead Load (Normal Distribution)

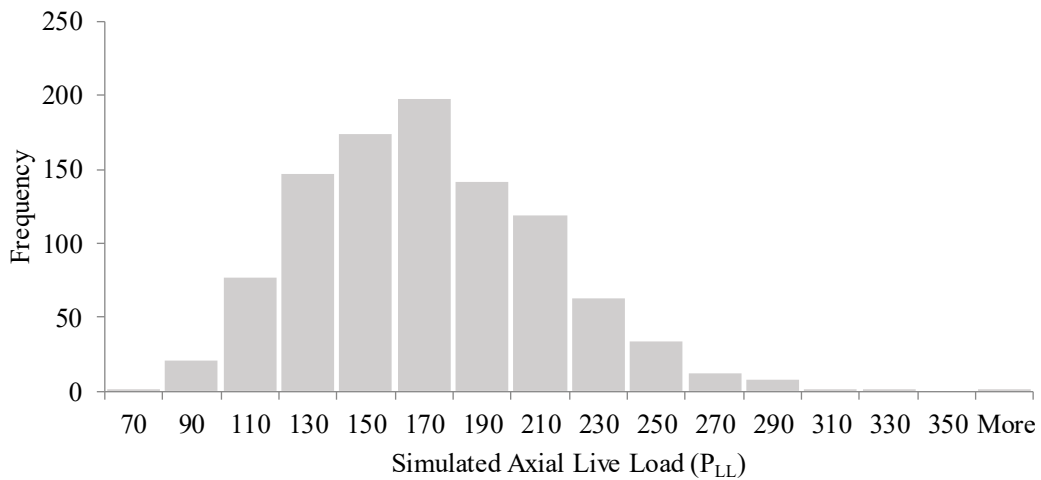


Fig. B-3 Live Load (Gumbel Distribution)

From the axial loads, the moments due to dead and live load are calculated for the initial eccentricity of this example ($e_i = 0.5t$) as $M = Pe_i$ for each of the simulated axial loads. In Fig. B-3, the loads (M, P) represent the sum of dead plus live load for the moment and axial load respectively. The simulated loads are also affected by the rate of loading (ρ_r).

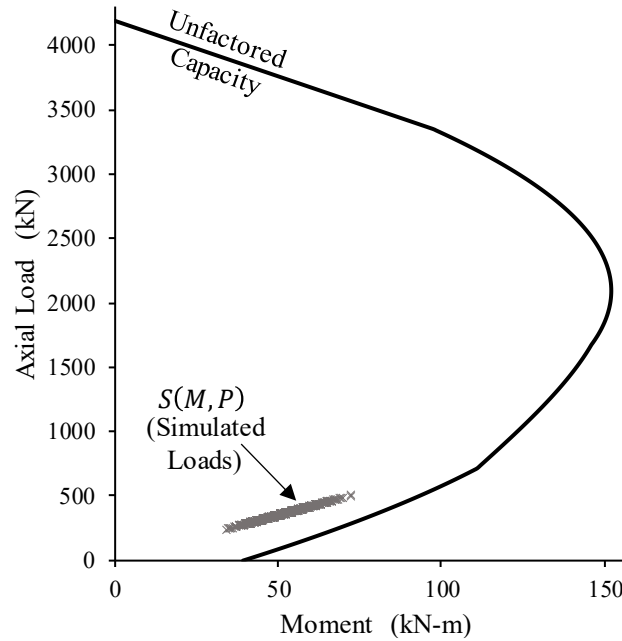


Fig. B-4 Simulated Loads (M, P)

For each simulated axial load (P) the resistance axial load and moment are calculated by the stress-strain compatibility as shown in Fig. 3-1 and by the Eq. B-3 to B-7

$$P_x = C_{m_x} - T_{s_x} \quad (\text{B-3})$$

$$C_{m_x} = \phi_m 0.85 f_{m_x} b \beta_1 c_x \quad (\text{B-4})$$

$$T_{s_x} = \phi_s A_s f_{y_x} \quad (\text{B-5})$$

$$a_x = \beta_1 c_x \quad (\text{B-6})$$

$$M_{n_x} = C_{m_x} \left(\frac{t_x}{2} - \frac{a_x}{2} \right) \quad (\text{B-7})$$

where the x represents one simulated value of a random variable. In the calculation of the probability of the resistance moment (M_n) the material factors are taken as one ($\phi_m = \phi_s = 1$), because the uncertainty is taken by the statistical properties of the random variables.

Additionally, to the axial load (P), the thickness of the block (t), the location of the steel (d), the compressive strength (f_m), and the yield strength of the steel (f_y) are also simulated by the Monte Carlo method and show them from Fig. B-5 to B-8.

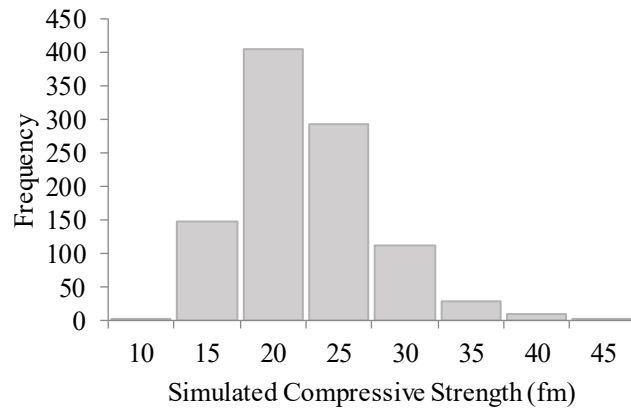


Fig. B-5 Compressive Strength (Gumbel Distribution)

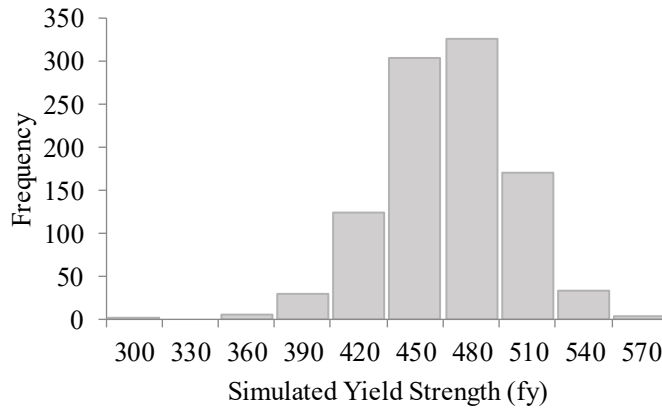


Fig. B-6 Yield Strength (Normal Distribution)

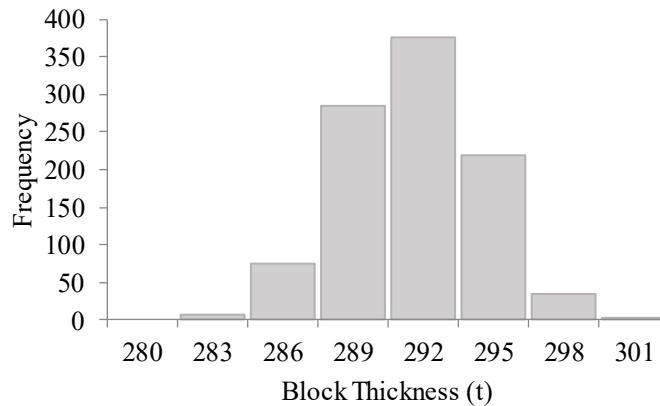


Fig. B-7 Block Thickness (Normal Distribution)

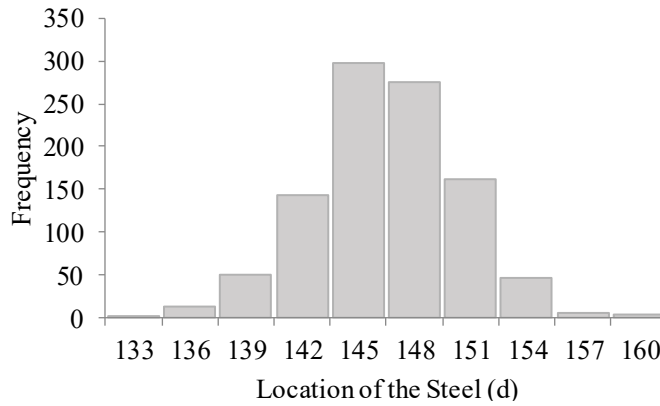


Fig. B-8 Location of the Steel (Normal Distribution)

Using Eqs. B-3 to B-7 and the simulated values, the resistance moment is calculated (M_n) and is shown in Fig. B-9. As it was mentioned in the methodology section, the compressive strength is also affected by the workmanship factor (ρ_w).

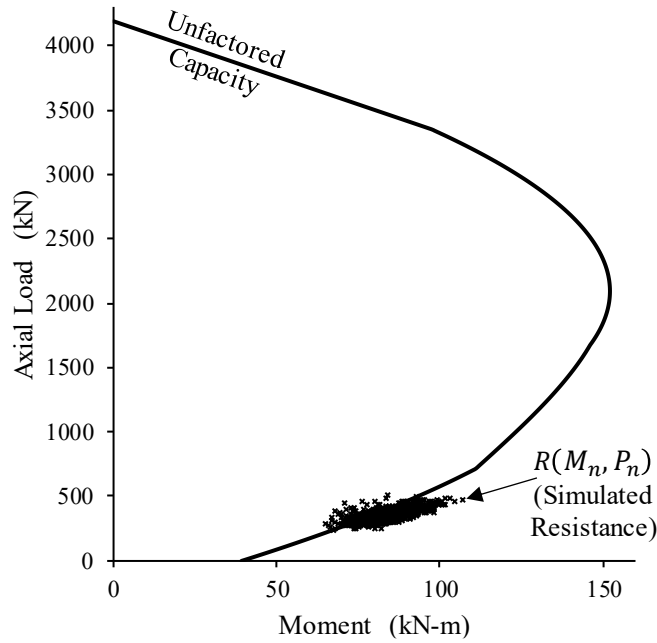


Fig. B-9 Section Resistance (M_r, P_r)

Fig. B-10 shows the loads and resistance of the wall under analysis

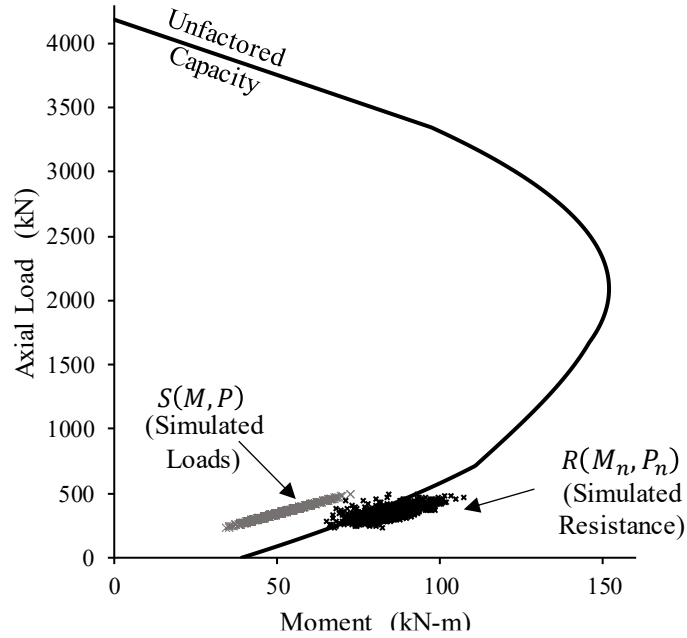


Fig. B-10 Simulated Load and Resistance

Using the proposed limit state (Eq. B-6), and the Crude Monte Carlo method

$$G(X) = M_n(X, P) - M_t(X, P) \quad (\text{B-8})$$

The probability of failure can be estimated as

$$p_f = \frac{\text{number of failures } (G(X) < 0)}{\text{total number of simulations } (N)} = 0.0004 \quad (\text{B-9})$$

and the reliability index

$$\beta = -\Phi^{-1}(p_f) = 3.35$$

Example 2. Slender Wall - Detailed Calculation

The first step for the reliability analysis is the simulation of the loads using the Monte Carlo method and the statistical properties of the Table 3-3. A normal probability distribution is used for the dead load.

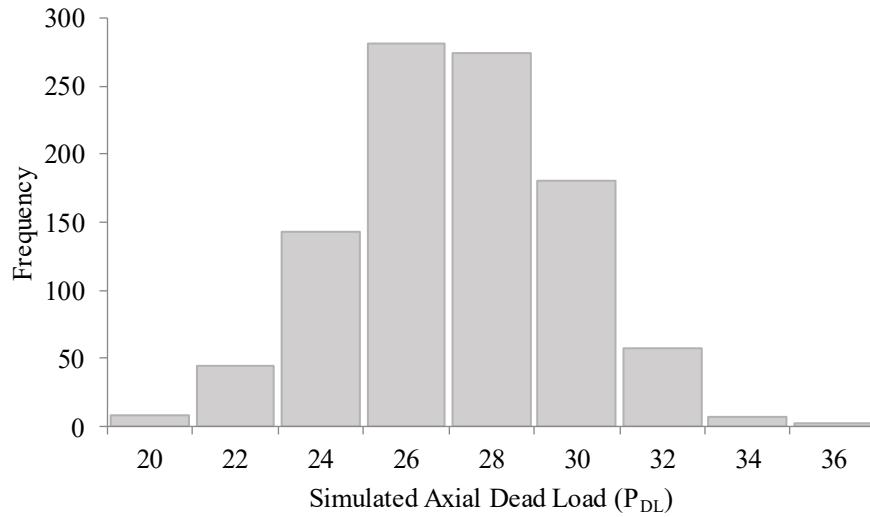


Fig. B-10 Dead Load (Normal Distribution)

In this problem, the Turkstra's rule is used, and the studied combination considers the live load as point-in-time load with a Weibull probability distribution.

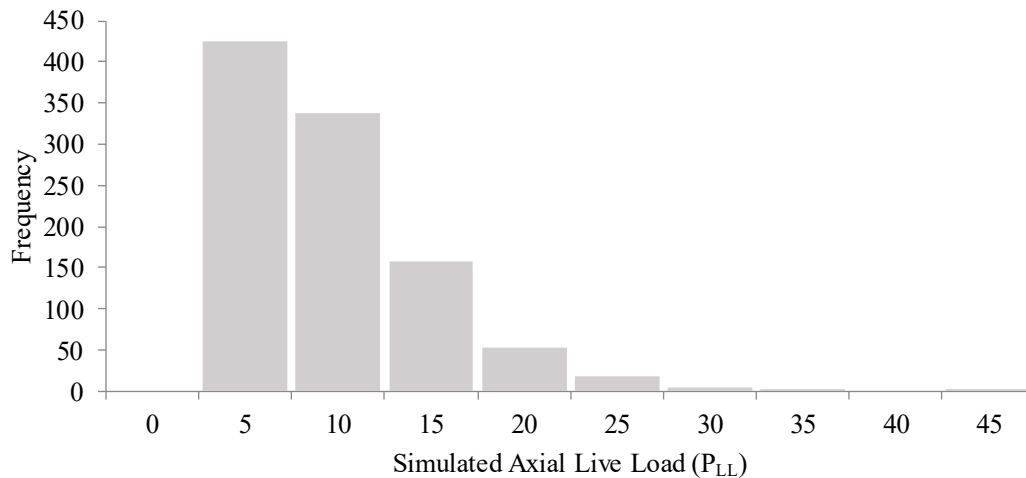


Fig. B-11 Live Load (Weibull Distribution)

The wind load is considered as 50-year maximum with a Gumbel distribution,

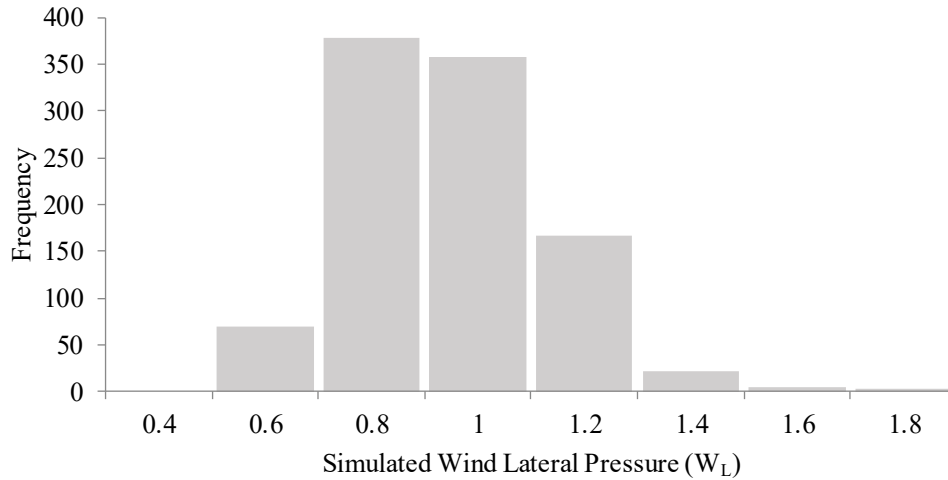


Fig. B-12 Wind Load (Gumbel Distribution)

The primary moment due to dead, live, and wind loads are calculated for each of the simulated values at the centre of the section with Eq. C-9,

$$M_{1_x} = \frac{P_{DL_x}e_i}{2} + \frac{P_{LL_x}e_i}{2} + \frac{W_x h^2}{8} \quad (C-9)$$

the primary moment (M_1) is shown in Fig. B-13.

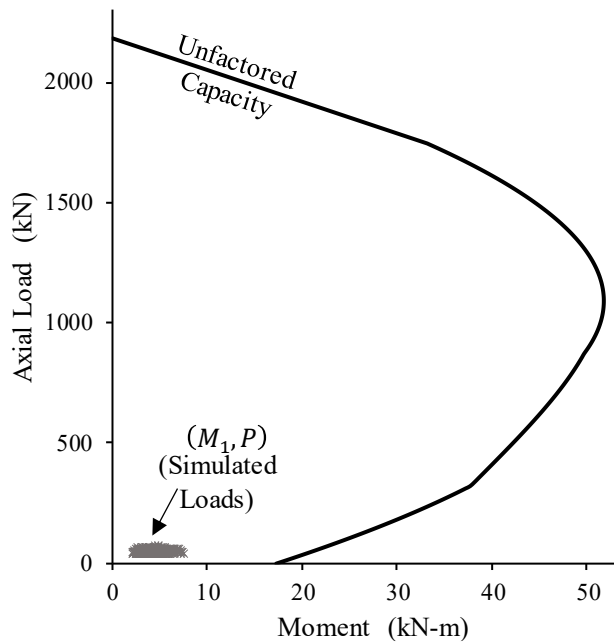


Fig. B-13 Simulated Primary Moment

The total or secondary moment (M_t) is calculated using the moment magnifier method for each simulation. In this example the wall has a slenderness ratio over 30 ($h/t > 30$), then the total moment is calculated as

$$M_t = \frac{W_x h^2}{8} + P_x(e_i/2) + (P_{sw} + P_x)\Delta_{f_x} \quad (\text{B-10})$$

In Eq. B-10, W is the uniform lateral wind on the wall, h is the height of the wall, P is the axial load, e_i is the initial eccentricity of P , P_{sw} is the tributary weight of the wall above of the design section, and Δ_f is the lateral deflection of the wall at mid-height.

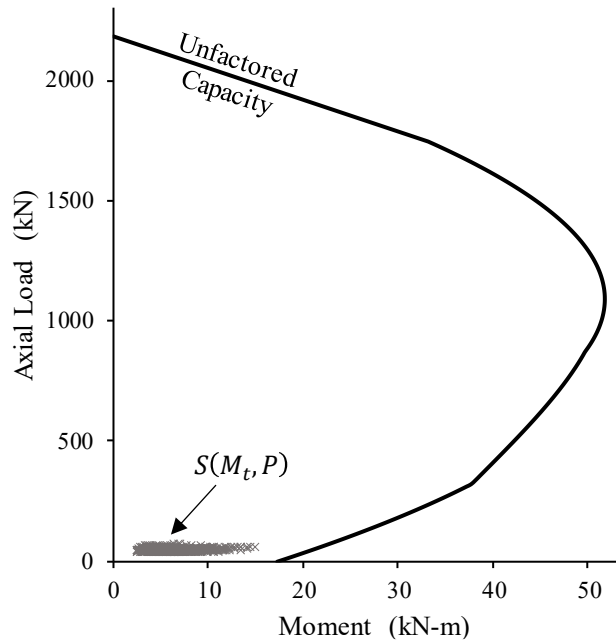


Fig. B-14 Total Moment

The resistance of the section is calculated for each of the simulated axial load by the use of stress-strain compatibility and taking the material factors as one ($\phi_m = \phi_s = 1$).

The thickness of the block (t), the location of the steel (d), the compressive strength (f_m), and the yield strength of the steel (f_y) are also simulated by the Monte Carlo method.

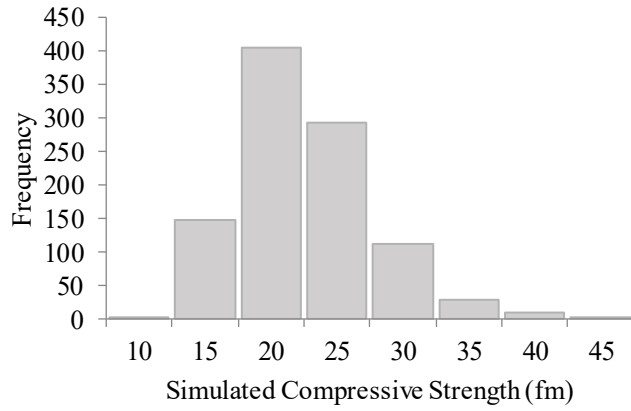


Fig. B-15 Compressive Strength (Gumbel Distribution)

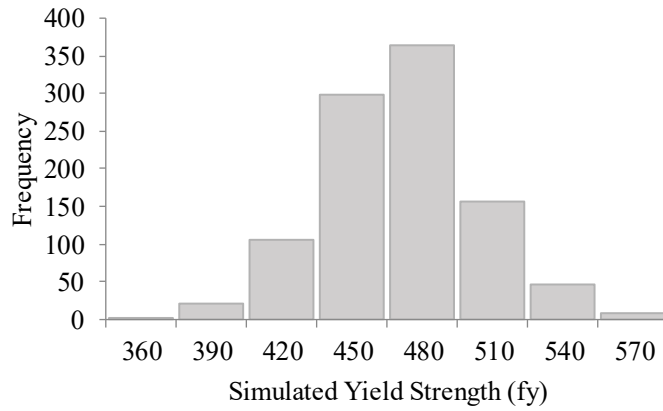


Fig. B-16 Yield Strength (Normal Distribution)



Fig. B-17 Block Thickness (Normal Distribution)

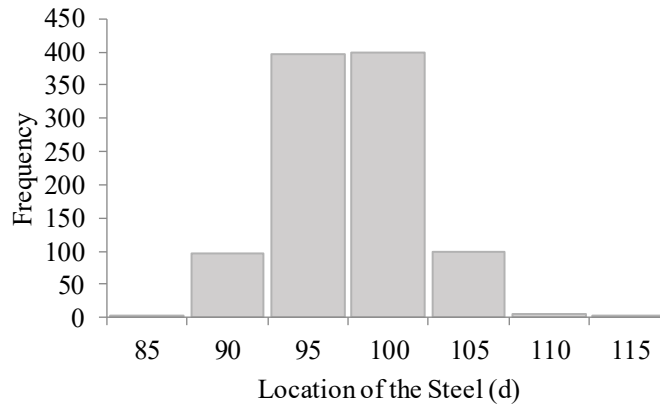


Fig. B-18 Location of the Steel (Normal Distribution)

Using Eqs. B-1 to B-5 and the simulated values, the resistance moment is calculated and is shown in Fig. B-19. To calculate the resistance of the section, the compressive strength is also affected by the workmanship factor and the rate of loading.

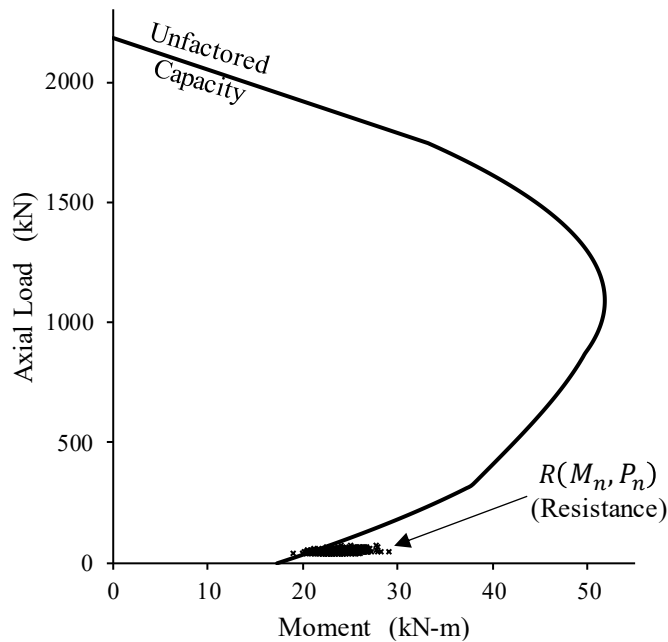


Fig. B-19 Section Resistance (M_n, P_n)

Fig. B-20 shows a summary of the loads and resistance of the wall under analysis.

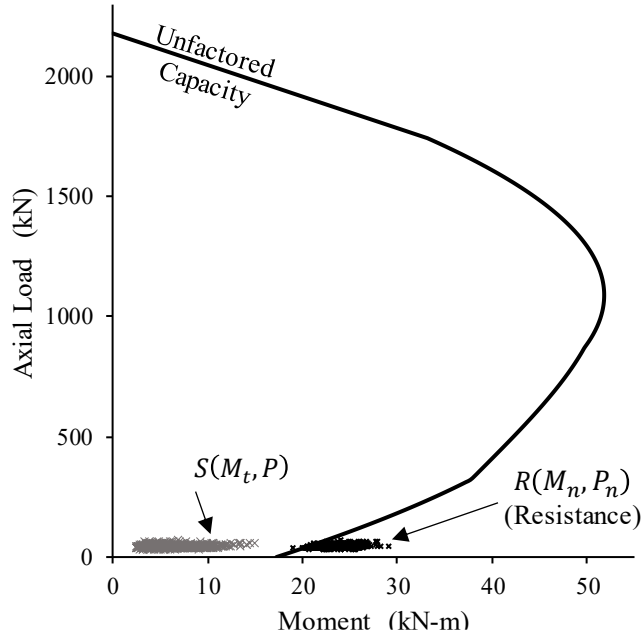


Fig. B-20 Loads and Resistance of the Wall

Using the proposed limit state (Eq. B-11), and the Crude Monte Carlo method

$$G(X) = M_n(X, P) - M_t(X, P) \quad (\text{B-11})$$

The probability of failure can be estimated as

$$p_f = \frac{\text{number of failures } (G(X) < 0)}{\text{total number of simulations } (N)} = 0.000022 \quad (\text{B-12})$$

and the reliability index

$$\beta = -\Phi^{-1}(p_f) = 4.09 \quad (\text{B-13})$$

This Crude Monte Carlo reliability method and the limit state function presented in this example were chosen to perform the analyses in this research.

During the development of this research an alternate method was also proposed and explored. This method is a combination of Monte Carlos simulations and the method of Cornell (1969). The same example 2 is used to present this method as a reference.

After the simulations in Fig. B-20, the distribution of the resultant moment of the loads and resistance moment can be observed in a histogram type plot in Fig. B-21

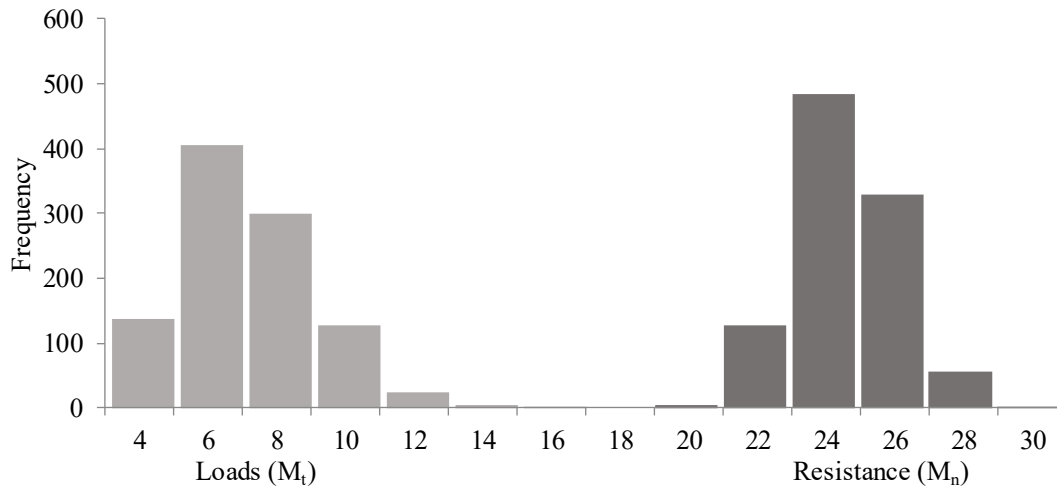


Fig. B-21 Distribution of Loads and Resistance of the Wall

The limit state of the Eq. B-11 for the calculation of the reliability index, can be simplified by using only two random variables: the total moment (M_t) that is the result of the loads on the wall considering the second order effects, and the resistance moment (M_n).

The two simplified variables are used in the method of Cornell to calculate the reliability index (β) as shown in Eq. B-14

$$\beta = \frac{\lambda_R - \lambda_S}{\sqrt{\zeta_R^2 - 2\rho_{\ln R,S}\zeta_R\zeta_S + \sigma\zeta_S^2}} \quad (\text{B-14})$$

The Eq. B-14 uses two variables with Lognormal distributions and takes into account the correlation between the resultant two random variables.

To verify the distribution of the loads and resistance the Kolmogorov-Smirnov (K-S) goodness-of-fit test is used. In this test the simulated cumulative frequency is compared to the cumulative density function (CDF) of the assumed theoretical distribution.

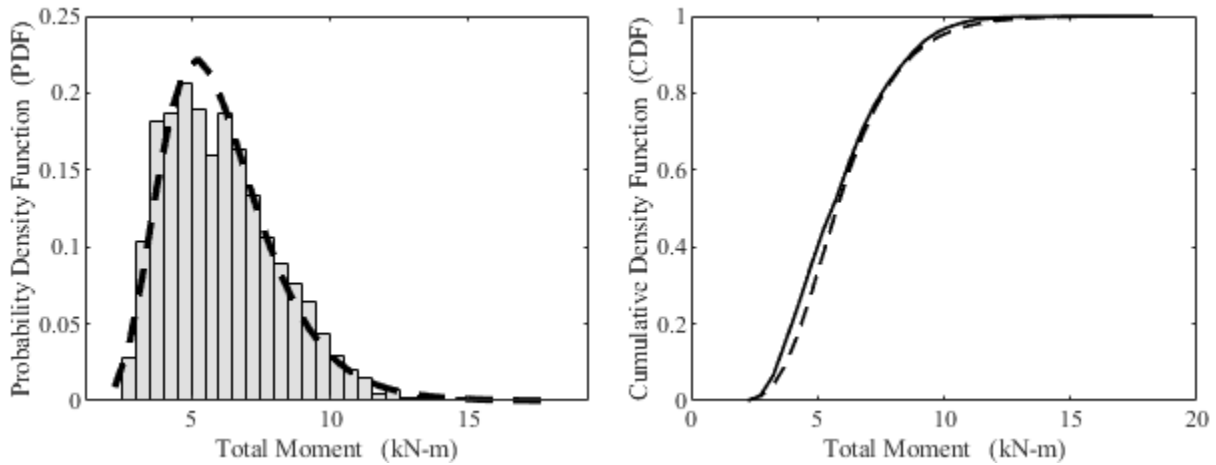


Fig. B-22 Distribution of the Total Moment

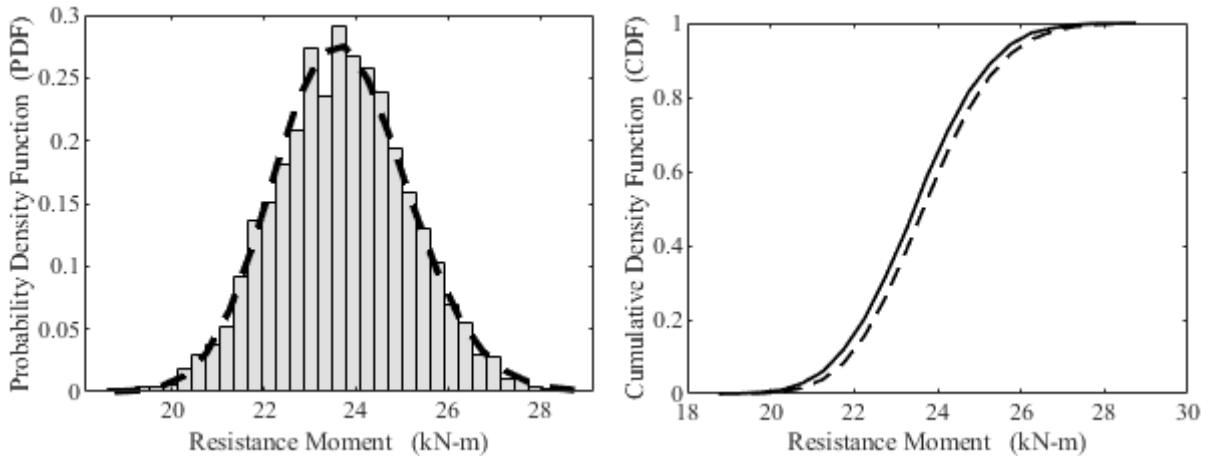


Fig. B-23 Distribution of the Resistance Moment

This test was proven for a significance level of 1%, and it was found that the distributions matched a theoretical lognormal distribution.

The correlation coefficient (ρ) between the resistance and the load for lognormal probabilities distributions is given by the Eq. B-15

$$\rho_{\ln R,S} = \frac{Cov[R,S]}{\zeta_R \zeta_S} \quad (\text{B-15})$$

Finally, the reliability index (β) is calculated using the method of Cornell for lognormal distributions and by considering the correlation between the resistance and the loads (Eq. B-16)

$$\beta = \frac{\lambda_R - \lambda_S}{\sqrt{\zeta_R^2 - 2\rho_{\ln R,S}\zeta_R\zeta_S + \zeta_S^2}} = 4.09 \quad (\text{B-16})$$

Appendix C

MATLAB Code

```
% Moment Magnifier Method
clear, clc
tic
Input - Materials, Geometry & Loads
% Wall Properties (mm)
    H=2000;
    t=190.0;
    d=t/2;
    tf=38;
% Masonry
    fm= 13.50 ;
    Em=850*fm ;
    Epsm=0.003;
% Steel
    fy=400.0;
    Es=200000;
    Epss=0.002;
% Steel Reinforcement & Width
    Space = 600.0 ;           % Reinforcement space
    as = 200.0 ;           % Total Area of the bars
% Loads
    PDL = 74.60 ; % Dead Load (kN)
    PLL = 1.50*PDL ; % Live Load (kN)
    WL = 1.0 ; % Wind Load (kN/m2=kPa)
    PSL = 0.00 ; % Snow Load (kN)

    e = 1.0*t ; % mm           % Initial Eccentricity
Loads & Eccentricity
% Effective width
beff1 = min(4*t,Space);
beff=beff1*(1000/Space)

% Effective Area of Steel
Aseff=(1000/Space)*as
% Psfender ratio
Psfender_ratio = H/t

Ae=beff*t;           % Fully grouted
Io=beff*t^3/12;
Se= Io/d;
ek=Se/Ae;

% Self-weight
    Db=2100; % Density block
```

```

    Solid=0.56; % 56%
    Block=Solid*(t/1000)*(beff/1000)*Db*9.81/1000; % kN/m2
    Dg=2350; % Desnity grout
    Grout=(1-Solid)*(t/1000)*(beff/1000)*Dg*9.81/1000; % kN/m2
SW=1;
if SW == 1
    Psw= (Block+Grout)*(H/2/1000);
else
    Psw=0;
end
Psw

% LOOP
    cont = 0;
for COMB = 5 % 1: 1 :9 ; % Combinations
    cont = cont + 1;
% Nominal
% FD = 1; FL=1; FW=1;
% Combinations
% COMB=5;
% FD = 1.40; FL=0.0; FW=0.0; % Combination 1
% FD = 1.25; FL=1.5; FW=0.0; % Combination 2
% FD = 1.25; FL=0.0; FW=1.4; % Combination 3
% FD = 1.25; FL=1.5; FW=0.4; % Combination 4
% FD = 1.25; FL=0.5; FW=1.4; % Combination 5
% FD = 0.90; FL=1.5; FW=0.0; % Combination 6
% FD = 0.90; FL=0.0; FW=1.4; % Combination 7
% FD = 0.90; FL=1.5; FW=0.4; % Combination 8
% FD = 0.90; FL=0.5; FW=1.4; % Combination 9
FD = [1.4; 1.25; 1.25; 1.25; 1.25; 0.9; 0.9; 0.9; 0.9; 1.0];
FL = [0.0; 1.50; 0.00; 1.50; 0.50; 1.5; 0.0; 1.5; 0.5; 1.0];
FW = [0.0; 0.00; 1.40; 0.40; 1.40; 0.0; 1.4; 0.4; 1.4; 1.0];
FD=FD(COMB);
FL=FL(COMB);
FW=FW(COMB);

    Pdf = PDL * FD ; % Dead Load (kN)
    Pswf = Psw*FD;
    Plf = PLL * FL ; % Live Load (kN)
    Wlf = WL * FW ; % Wind Load (kN/m2=kPa)
    Psf = PSL ; % Snow Load (kN)

% Combinations
if Wlf ~= 0
    Md1 = Pdf*e/1000/2;
    Ml1= Plf*e/1000/2;
else
    Md1 = Pdf*e/1000;
    Ml1 = Plf*e/1000;

```



```

end
Md1
M11
MWlf=Wlf*(H/1000)^2/8

Pu=Pdf+Pswf+Plf+Psf ; % kN/m Total axial load

M1=Md1+M11+MWlf ; % kN-m/m Just with axial load

Bd=Md1/M1 ; % MDL/M1 ==> *** Review this for more combinations
%Bd=Md1/20.72899

Cm=1; % Single curvature
k=1;
n=Es/Em;

Slenderness limits (EI)eff
ec=(M1/Pu)*1000 % e_current

% kd^2*(b/2)=n*Aseff*(d-kd);
kd=max(roots([beff/2 (n*Aseff) (-n*Aseff*d)]));
Icr=n*Aseff*(d-kd)^2+((beff*kd^3)/3);
EIcr=Em*Icr;
Im=(0.25*Io-(0.25*Io-Icr)*((ec-ek)/(2*ek)));
EI=Em*Im;
EIom=0.25*Em*Io;

% if EI <= Em*Icr
% EIeff=Em*Icr;
% elseif EI <= 0.25*Em*Io
% EIeff=EI;
% else
% EIeff=0.25*Em*Io;
% end
% EIeff

if EIcr <= EI ;
EIeff1 = EI ;
else
EIeff1 = EIcr ;
end
EIeff1 ;

if EIeff1 <= EIom
EIeff = EIeff1 ;
else
EIeff = EIom ;
end
EIeff ;

```

```

Phier=0.75;
Pcr=(pi()^2*Phier*EIeff)/((1+0.5*Bd)*(k*H)^2)*(1/1000);

Pu
M1
Bd
Pcr
Mt130=M1*(Cm/(1-(Pu/Pcr)))

% For walls with h/t > 30
Disp0 = (5*Wlf*H^4)/(384*EIeff)+(Pu*1000*e*H^2)/(16*EIeff);

Mth30=M1+(Pu*(Disp0/1000)*1/(1-(Pu/Pcr)))

if H/t < 30
    Mt=M1*(Cm/(1-(Pu/Pcr)));
else
    Mt=M1+(Pu*(Disp0/1000)*1/(1-(Pu/Pcr)));
end
Mt

%% Design of the wall
As=Aseff;
Phim=0.6 ;          % 0.6
Xi=1;
Phis=0.85 ;        % 0.85
B1=0.8;

% Maximum axial load
Pmax= 0.8*(Phim*(0.85*fm)*(beff*t))/1000;
Prmax= (0.85*fm)*(beff*t)/1000;

%-----
c= 0;
Pr=0;
while Pr<=Pu
    c=c+0.001 ;
    a=B1*c;

    % Resistant moment, if Pf=Pr
    % B1c=((Pu*1000)+(Phis*As*fy))/(Phim*Xi*0.85*fm*beff)

    Cm=Phim*Xi*0.85*fm*beff*a ;

    Epssr=((d-(a/B1))/(a/B1))*Epsm ;
    fs=Es*Epssr;

    if fs < 0

```

```

        fs=0;
    end

    if fy > fs
        fy = fs;
    elseif fy <= fs
        fy = fy;
    end
    fy;

    Ts=Phis*As*fy;
    Pr=(Cm-Ts)/1000;

end
c ;
Pr
Mr=Cm*(t/2-(a)/2)*(1/1000000)

error = (1-Pr/Pu)*100
%-----

% Ratio Mt/Mr
Ratio = Mt/Mr
if Ratio <= 1
    Design = 'Good'
else
    Design = 'Fail'
end

Summary (cont,:) = [COMB Pu M1 Bd Pcr Mt fm Aseff Mr c Ratio] ;

end

Summary

toc
=====
=====
close all; clear all; clc; format long
disp(datetime)
disp(mfilename)
tic
%%      Input
N = 100000 ; % Number of Monte Carlo Simulations
% Materials (MPa,mm)
fmn= 13.5 ;
fyn= 400.0;
% Geometry
tn= 190.0;

```

```

dn=tn/2 ;

tf=38;
H=4000;
% Steel Reinforcement
    Space=600.0 ;           % Reinforcement space
    as=300.0 ;             % Total Area of the bars

% Loads (N,mm)
ei=0.30*tn ;

PDn= 147.690 ; % Dead (kN)
%MDn=PDn*ec ;
% MDn=PDn*ec/2 ; % Slender
PLn= 1.50*PDn ; % Live
%MLn=PLn*ec ;
% MLn=PLn*ec/2 ; % Slender

% Rate-of-Loading factor
% DL+LL = 0.88, DL+SL=0.94, DL+WL=0.94
r_rate=0.94 ;

MWn= 1.5 ; % kPa Slender

% Considering the Second Order Effects (Yes=1, No=2)
    SOEf = 1 ;

% Considering Selfweigth (Yes=1, No=2)
    SW = 1 ;

% Mean & Standard deviation
mufm=1.60*fmn; % Gumbel
sigfm=0.236*mufm;
mufy=1.14*fyn ; % Normal
sigfy=0.07*mufy;
mut=tn ; % Normal
sigt=0.01*mut;
mud=dn ; % Normal
sigd=4 ;
ws= 1.0 ; % Normal ==> Workmanship factor (Hadi 0.85,0.15) #####**
sigws=0.10*ws ;
% Bias*nominal
muPD=1.05*PDn ; % Normal
sigPD=0.1*muPD ;
% muMD=1.05*MDn ; % Normal
% sigMD=0.1*muMD ;

%Turstra's Rule (Live(max)+W(pit) = 1, Live(pit)+W(max) = 2)
TR = 2 ;

```

```

fprintf '\n'
disp(['Number of realizations (N) = ' num2str(N)])
fprintf '\n'
disp(['Turkstra''s Rule(Live(max)+W(pit) = 1, Live(pit)+W(max) = 2)= '
num2str(TR)])
if TR==1;
    % Live (Max)
    muPL=0.9*PLn ;    % Gumbel
    sigPL=0.17*muPL ;
    % muML=0.9*MLn ;    % Gumbel
    % sigML=0.17*muML ;

    % Wind (Point-in-time)
    muWL=0.156*MWn ;    % Weibull
    sigWL=0.716*muWL ;
else TR==2;
    % Live (Point-in-time)
    muPL=0.273*PLn ;    % Weibull
    sigPL=0.674*muPL ;

    % Wind (Max)
    muWL=1.039*MWn ;    % Gumbel
    sigWL=0.081*muWL ;
end

% Transformation to load effect
leL=1.00 ; sigleL=0.206*leL ; % Normal
leW=0.68 ; sigleW=0.220*leW ; % Log-normal

% z1=fm z2=fy z3=t z4=d z5=PD z6=MD z7=PL z8=ML z9=WL z10=ws
%mu= [ mufm, mufy, mut, mud, muPD, muMD, muPL, muML, muWL, ws,
leL, leW]; % Means
%sig=[sigfm, sigfy, sigt, sigd, sigPD, sigMD, sigPL, sigML, sigWL, sigws,
sigleL, sigleW]; % Standard deviations
% % z1 z2 z3 z4 z5 z6 z7 z8 z9 z10 z11 z12
% Case=[1, 1, 1, 1, 1, 1, 3, 3, 3, 1, 1, 2];

% z1=fm z2=fy z3=t z4=d z5=PD z6=PL z7=WL z8=ws z9 z10
mu= [ mufm, mufy, mut, mud, muPD, muPL, muWL, ws, leL, leW]; %
Means
sig=[sigfm, sigfy, sigt, sigd, sigPD, sigPL, sigWL, sigws, sigleL, sigleW];
% Standard deviations
% z1=fm z2=fy z3=t z4=d z5=PD z6=PL z7=WL z8=ws z9 z10
if TR ==1;
    Case=[ 3, 1, 1, 1, 1, 3, 6, 1, 1, 2]; %
Live(max)+W(pit)
else TR==2;

```

```

        Case=[ 3, 1, 1, 1, 1, 6, 3, 1, 1, 2]; %
Live(pil)+W(max)
end

% 1 Normal
% 2 Log-normal
% 3 Gumbel
% 4 Exponetial
% 5 Uniform
% 6 Weilbull

%% precomputations
m=length(mu);
u=randn(m,N);

%%

[z]=u_2_x(u,Case,mu,sig);

fm=z(1,:);
fy=z(2,:);
t=z(3,:);
d=z(4,:);
ws=z(8,:);
leL=z(9,:);
leW=z(10,:);

PD=z(5,:);
%MD=z(6,:);
PL=z(6,:);
%ML=z(8,:);
WL=z(7,:);

%% Design with random variables

PD ;
PL=leL.*PL;
WL=leW.*WL;

% Wall Properties (mm)
H; % (Non Random variable)
t;
d;
tf;
% Masonry
fm ;
Em=850*fm;

```

```

    Epsm=0.003;
% Steel
    fy;
    Es=200000;
    Epss=0.002;
% Steel Reinforcement & Width
    Space ;           % Reinforcement space
    as ;             % Total Area of the bars
% Loads
    PD ; % Dead Load (kN)
    PL ; % Live Load (kN)
    WL ; % Wind Load (kN/m2=kPa)
    PSL = 0.00 ; % Snow Load (kN)

    e = ei ;      % mm           % Initial Eccentricity

% Effective width
beff1 = min(4*t,Space) ;
beff=beff1*(1000/Space) ;

% Effective Area of Steel
Aseff=(1000/Space)*as ;
% Psfender ratio
Psfender_ratio = H./t ;

Ae=beff.*t;           % Fully grouted
Io=beff.*t.^3/12;
Se= Io./(t/2);
ek=Se./Ae;

% Self-weight
    Db=2100; % Density block
    Solid=0.56; % 56%
    Block=Solid.*(t/1000).*(beff/1000).*Db*9.81./1000; % kN/m2
    Dg=2350; % Density grout
    Grout=(1-Solid).*(t/1000).*(beff/1000).*Dg.*9.81./1000; % kN/m2

if SW == 1
    Psw= (Block+Grout)*(H/2/1000);
else
    Psw=0;
end
Psw ;

Pdf = PD ;           % Dead Load (kN)
    Pswf = Psw ;
Plf = PL ;           % Live Load (kN)
Wlf = WL ;           % Wind Load (kN/m2=kPa)

```

```

Psf = PSL ; % Snow Load (kN)

% Combinations
if Wlf ~= 0
    Md1 = Pdf.*e/1000/2;
    M11= Plf.*e/1000/2;
else
    Md1 = Pdf.*e/1000;
    M11 = Plf.*e/1000;
end
Md1 ;
M11 ;
MWlf=Wlf.*(H/1000).^2/8 ;

Pu=Pdf+Pswf+Plf+Psf ; % kN/m Total axial load

M1=Md1+M11+MWlf ; % kN-m/m Just with axial load

Bd=Md1./M1 ; % MDL/M1 ==> *** Review this for more combinations

Cm=1; % Single curvature
k=1;
n=Es./Em ;

% Ok up to here

ec=(M1./Pu)*1000 ; % e_current

% kd^2*(b/2)=n*Aseff*(d-kd);
%kd=max(roots([beff/2 (n.*Aseff) (-n.*Aseff.*d)]))
a=beff/2 ;
b=n.*Aseff ;
c=-n.*Aseff.*d ;
kd = (-b+sqrt(b.^2-4*a.*c))./(2*a) ; % x1
%x2 = (-b-sqrt(b.^2-4*a.*c))./(2*a)

Icr = n.*Aseff.*(d-kd).^2+((beff.*kd.^3)./3);
EIcr = Em.*Icr;
Im=(0.25*Io-(0.25.*Io-Icr).*((ec-ek)./(2*ek)));
EI = Em.*Im;
EIom = 0.25*Em.*Io;

for i=1:N ;
    if EIcr(i) <= EI(i) ;
        IEff1(i) = EI(i) ;
    else
        IEff1(i) = EIcr(i) ;
    end
end

```



```

    EIEff1 ;

    if EIEff1(i) <= EIom(i)
        EIEff(i) = EIEff1(i) ;
    else
        EIEff(i) = EIom(i) ;
    end
    EIEff ;
end
EIEff ;

Phier=0.75;
%Phier=1.0;
Pcr=(pi()^2*Phier*EIEff)/((1+0.5*Bd).*(k.*H).^2).*(1/1000) ;

Pu ;
M1 ;
Bd ;
Pcr ;
%Mt=M1.*(Cm./(1-(Pu./Pcr)))
MMM=(Cm./(1-(Pu./Pcr)));

for k=1:N;
FA=(MMM(k));
    if FA > 0
        FMMM(k)=FA;
    else
        FMMM(k)=1;
    end
end
FMMM ;

if SOEf==1 ;
    Mt=M1.*FMMM ;
else SOEf==2 ;
    Mt=M1 ;
end

% Mt=M1.*FMMM ;

Pn = Pu*1000 ;
Mn = Mt*1e6 ;

%% Calculation of Mr

```

```

As=Aseff;

for k=1:N ;

    fm(k)=ws(k)*fm(k)*r_rate;
    Pu(k);

    Phim= 1.0 ; % 0.6    % (*)
    Phis= 1.0 ; % 0.85  % (*)

    % Masonry Properties
    euo = 0.014;
    em = 0.003;

    Epsm=em;

    % Steel Properties
    Xi = 1.0 ;
    B1=0.8;

    c= 0;
    Pr=0;
    while Pr<=Pu (k)
        c=c+0.001 ;
        a(k)=B1*c;
        Cm(k)= Phim*Xi*0.85*fm(k).*beff(k).*a(k) ;
        EpsSr(k)=((d(k)-(a(k)/B1))/(a(k)/B1)).*Epsm ;
        fs(k)=Es*EpsSr(k);

        if fs(k) < 0
            fs(k)=0;
        end

        if fy(k) > fs(k)
            fy(k) = fs(k);
        elseif fy(k) <= fs (k)
            fy(k) = fy(k);
        end
        fy(k);
        Ts(k)=Phis*As*fy(k);
        Pr (k)=(Cm(k)-Ts(k))/1000;
    end
    % c ;
    % a ;
    % fy ;
    % Cm ;
    % Ts ;

    Pnr (k) = Pr (k) ;

```

```

Mr(k)=Cm(k).*(t(k)/2-a(k)/2) ; % *(1/1000000)

error(k) = (1-Pr(k)./Pu(k))*100 ; % (%)

end

Pnr ;
Mr ;

%% Limit-State
% Pn=(PD);
% Mn=(MD+leW.*W);

% if TR ==1;
%   Mr = 31370.0*ws.*fm.*(0.5*t - 19.43); % Live(max)+W(pit)
% else TR==2;
%   Mr = 30120.0*ws.*fm.*(0.5*t - 18.65); % Live(pil)+W(max)
% end

% Rx=(Pnr.^2 + Mr.^2).^0.5;
% Sx=(Pn.^2 + Mn.^2).^0.5;

    Rx= Mr ;
    Sx= Mn ;

Gx= Rx - Sx ;

%% Probability of Failure
indicator = Gx <= 0;
cov_mcs=sqrt(var(indicator)./N)./mean(indicator);
pf_MCS = mean(indicator) ;
B_MCS=(-norminv(mean(indicator))) ;
fprintf '\n'
disp(['Beta_MCS = ',num2str(B_MCS), '    pf_MCS = ',num2str(pf_MCS)])
% disp(['cov_MCS = ',num2str(cov_mcs)])
fprintf '\n'

% Error estimation
    pf=mean(indicator);
    Error=sqrt((1-pf)/(N*pf))*200;
    disp(['Error = ', num2str(Error) ])
    fprintf '\n'

%% Cornell Index
    Cornell_i=(mean(Rx)-mean(Sx))/(sqrt(std(Rx)^2+std(Sx)^2));
    disp(['Beta_Cornell = ', num2str(Cornell_i)])
    fprintf '\n'

```

```

%% Plot (Yes=1,No=2)
PM = 1 ;
if PM == 1 ;

    load('PM_Diagram_Slender01.mat')
    % plot(Mn/1e6,Pn/1000,'r.',Mr/1e6,Pr/1000,'b.',PMDUF(:,1),PMDUF(:,2),'b--',
    ',PMDF(:,1),PMDF(:,2),'b')

    %Pfixed=mean(Pn)*(ones(1,N));
    subplot(2,1,2)
    histogram(Mr/1e6);
    hold on
    histogram(Mn/1e6);
    xlabel('Moment (kN/m)')
    ylabel('Simulations (n)')
    subplot(2,1,1)
    %figure

%plot(Mn/1e6,Pfixed/1000,'r.',Mr/1e6,Pfixed/1000,'b.',PMDUF(:,1),PMDUF(:,2),'
b--',PMDF(:,1),PMDF(:,2),'b')
    plot(Mn/1e6,Pn/1000,'r.',Mr/1e6,Pnr,'b.',PMDUF(:,1),PMDUF(:,2),'b--',
',PMDF(:,1),PMDF(:,2),'b')

    % grid
    xlabel('Moment (kN/m)')
    ylabel('Axial Load (kN)')

else PM == 2 ;
    fprintf ' EXIT!!! \n'
end;

% X1=Mn/1e6;Y1=Pn/1000;
% X2=Mr/1e6; Y2=Pr/1000;
% X3=PMDUF(:,1); Y3=PMDUF(:,2);
% X4=PMDF(:,1); Y4=PMDF(:,2);
% createfigure(X1, Y1, X2, Y2, X3, Y3, X4, Y4)

Summ=[Pnr; M1; t; ws; fm; fy; Mr]';

save('Betas010.txt','B_MCS','Cornell_i','-ascii')

toc

```